uOttawa

L'Université canadienne
Canada's university

FACULTÉ DES ÉTUDES SUPÉRIEURES ET POSTOCTORALES

uOttawa

L'Université canadienne
Canada's university

FACULTY OF GRADUATE AND POSDOCTORAL STUDIES

Jamei Eng

AUTEUR DE LA THÈSE / AUTHOR OF THESIS

M.Sc. (Biochemistry)

GRADE / DEGREE

Department of Biochemistry

FACULTÉ, ÉCOLE, DÉPARTEMENT / FACULTY, SCHOOL, DEPARTMENT

Localization of Anthracyclines in Drug Resistant Human MCF-7 Breast Cancer Cells

TITRE DE LA THÈSE / TITLE OF THESIS

Amadeo Parissenti

DIRECTEUR (DIRECTRICE) DE LA THÈSE / THESIS SUPERVISOR

Ian Lorimer

CO-DIRECTEUR (CO-DIRECTRICE) DE LA THÈSE / THESIS CO-SUPERVISOR

EXAMINATEURS (EXAMINATRICES) DE LA THÈSE / THESIS EXAMINERS

Jim Dimitroulakos

Michael McBurney

Gary W. Slater

Le Doyen de la Faculté des études supérieures et postdoctorales / Dean of the Faculty of Graduate and Postdoctoral Studies

LOCALIZATION OF ANTHRACYCLINES IN DRUG RESISTANT HUMAN MCF-7 BREAST CANCER CELLS

Jamei Raena Eng

Thesis submitted to the
Faculty of Graduate and Postdoctoral Studies
In partial fulfillment of the requirements
For the Masters of Science degree in Biochemistry

Department of Biochemistry, Microbiology, and Immunology
Faculty of Medicine
University of Ottawa

Your file Votre référence
ISBN: 978-0-494-49198-0
Our file Notre référence
ISBN: 978-0-494-49198-0

ABSTRACT

Multidrug resistance (MDR) commonly occurs during the treatment of cancer. Current research has focused mostly on the role of drug transporters, as the main mechanism of MDR; however, few have demonstrated a definite link between the expression or function of drug transporters and MDR in cancer patients.

Anthracyclines such as doxorubicin and epirubicin, autofluoresce and can be monitored by confocal microscopy. Two of the four resistant cell lines generated in our lab: the MCF-7_{EPI} cells and to some extent MCF-7_{DOX} cells, exhibit a localization defect, whereby epirubicin is localized primarily in the cytoplasm rather than the nucleus. This drug localization defect temporally correlated with the onset of drug-resistance during selection for drug resistance in these cell lines. Consistent with the possible sequestration of drugs into acidic vesicles, acridine orange staining has revealed the presence of aggregates of acidified vesicles in the perinuclear region of MCF-7EPI cells. However, co-localization experiments using a number of intracellular organelle markers determined that epirubicin was localized to lysosomes and not consistently to acidic vesicles. An inhibitor of vacuolar H^+ ATPase, was unable to restore the localization of epirubicin to the nucleus. Immunofluorescence using an ABCB1 antibody revealed the localization of ABCB1 predominantly in the plasma membrane and to some extent in the perinuclear region of MCF-7EPI cells. Nevertheless, inhibitors of this transporter failed to restore localization of epirubicin to the nucleus. Taken together, these findings strongly suggest that the acquisition of epirubicin resistance in breast tumour cells may involve the P-glycoprotein independent sequestration of drug into lysosomes. These lysosomes need not be acidic, nor does the removal of acid vesicles by inhibition of vacuolar H+ ATPases block the sequestration of drug into lysosomes.

DEDICATION

To my dear friends and family,
All of whom have made this journey a special one.

ACKNOWLEDGEMENTS

First and foremost, I would like to take this opportunity to thank Dr. Amadeo Parissenti, my supervisor for giving me the opportunity to conduct research in one of the most important fields of research, as well as allowing me the opportunity to work in such an engaging and enriching environment with many of the most up to date technologies. These past few years have taught me a lot about the world of research, and have given me an experience that I could not have acquired anywhere else.

For listening to my endless queries and assistance in troubleshooting my experiments, I would like to thank Dr. Robert Lafrenie for his time and patience. I would like to especially thank Jason Sprowl, Zachary Veitch and Kerry Reed for being my source of insight and entertaining conversation during these past few years. I would also like to acknowledge Stacey Santi and Monique Laberge for their contributions to my work. To the rest of our research group thank you for all the help they have given me, you have made my masters experience most memorable.

Thank you to my two brothers, Nelson and Kellton, for being there to cheer me up after those long days and weekends. Last but not least, I would like to thank my parents, James and Frances Eng who gave me so much love and support throughout my thesis.

"Time never stops, so we should always move forward..."

TABLE OF CONTENTS

LIST OF ABBREVIATIONS

ABCB1	-	ATP binding cassette
ABCC1	-	ATP binding cassette
ABCC2	-	ATP binding cassette
ABCC3	-	ATP binding cassette
AKR1C1	-	aldoketo reductase
AKR1C2	-	aldoketo reductase
AKR1C3	-	aldoketo reductase
AKR1C4	-	aldoketo reductase
AML	-	am myeloid leukemia
ATCC	-	American Type Culture Collection
ATP	-	adenosine triphosphate
CBR	-	carbonyl reductase
DDH	-	dihydro dehydrogenase
DNA	-	deoxyribonucleic acid
EDTA	-	ethylenediamine tetraacetic acid
ER	-	endoplasmic reticulum
FBS	-	fetal bovine serum
GST	-	glutathione s-transferase
GSH	-	glutathione
GTP	-	guanosine triphosphate
IC_{50}	-	inhibitory concentration
LRP	-	lung resistance protein
$MCF\text{-}7_{WT}$	-	co-cultured drug sensitive breast cancer cell line
$MCF\text{-}7_{TAX}$	-	paclitaxel resistant cell line
$MCF\text{-}7_{DOX}$	-	doxorubicin resistant cell line
$MCF\text{-}7_{EPI}$	-	epirubicin resistant cell line
MDR	-	multi-drug resistance
MRP1	-	multi-drug resistance protein
MVP	-	major vault protein
NADPH	-	nicotinamide adenine diphosphate hydrogen
PBS	-	phosphate buffered saline
RNA	-	ribonucleic acid
ROS	-	reactive oxygene species
Q-PCR	-	quantitative polymerase chain reaction
TBS	-	tris buffered saline
Topo II	-	topoisomerase II
VPS4A	-	vault protein

LIST OF FIGURES AND ILLUSTRATIONS

LIST OF TABLES

1.0 INTRODUCTION

Cancer is known as a genetic disorder that occurs at the cellular level and often involves the mutation of a number of different genes. Generally, the genes being mutated are involved in apoptosis or cell cycle regulation, resulting in rapid proliferation of cells (Klug and Cummings, 2002).

The most common cancer that occurs in women is breast cancer. Over 20, 000 cases of breast cancer are expected in Canada for 2007. Despite recent advances in early detection and treatment, breast cancer is still considered to be the second most fatal cancer after lung cancer for Canadian women (Canadian Cancer Society *et al.*, 2007). Current treatment methods include surgical removal of the tumour, chemotherapy and/or radiation. Further advances are necessary to improve the effectiveness of these treatment methods.

1.1 Chemotherapeutic Agents

In the treatment of metastatic breast cancer, the use of chemotherapy agents after surgery or in combination with radiation therapy is standard (Hudis, 2003). Two commonly used classes of chemotherapy agents are the anthracyclines and taxanes. These classes of drug are known to be predominantly hydrophobic in nature, allowing them to easily diffuse across cell membranes without the need of drug specific carriers or channels.

By researching the many molecular and genetic changes that occur when normal cells transform into malignant cells, a variety of anti-cancer agents have been developed which exploit these changes in order to selectively kill rapidly dividing cells while minimizing damage to surrounding healthy tissue (Mayer, 1998). Some of these genetic modifications present in transformed cells include activation of protooncogenes such as ras, or acquisition

of mutations in p53. These changes affect a number of biological processes such as signal transduction, transcription, cell growth, apoptosis and tumour suppression (Mayer, 1998).

Many of the standard and commonly used anti-cancer agents such as the taxanes and anthracyclines do not exhibit a high degree of specificity but to some extent target cancer cells due to their high proliferation rates. However, as a result of this lack in specificity, healthy cells are also affected during chemotherapy, which helps to explain one of the most common side effects of treatment, namely loss of hair during treatment. It is well known that cells within hair follicles, like tumour cells, consist of rapidly dividing cells (Paus and Cotsarelis, 1999). Other general side effects of chemotherapy treatment include neutropenia (killing of neutrophils) (Kondo *et al.*, 1999) nausea, vomiting, lack of energy, and changes in olfaction and taste (Lindley *et al.*, 1999).

1.1.1 Taxanes

Paclitaxel (Taxol®), a taxane, (Figure. 1.0) was first isolated from the bark of a yew tree, *Taxus brevifolia* (Wani *et al.*, 1971) . Paclitaxel blocks cell division by binding to tubulin and stabilizing tubulin microtubules during mitosis. Once formed, microtubules in the presence of paclitaxel are stable enough to resist depolymerization by dilution, low temperatures and Ca^{2+} (Schiff *et al.*, 1979). The interaction between paclitaxel and cytoplasmic microtubules occurs via hydrophobic interactions with the H6 and H7 helices of the β-subunit of tubulin, a component of microtubules (Snyder *et al.*, 2001). Photoincorporation studies showed that paclitaxel interacts with β-tubulin via the C-2, C-3', C-7 and C-13 positions of paclitaxel (Rao *et al.*, 1994). In addition, *in vitro* studies have shown that paclitaxel is able to stabilize microtubules without the usual requirement of

Figure 1.0: Structure of paclitaxel.

First isolated from the bark of a yew tree, *Taxus brevifolia*, paclitaxel blocks cell division by binding to tubulin and stabilizing tubulin microtubules during mitosis. (www.rxlist.com/cgi/generic/paclitaxel.htm)

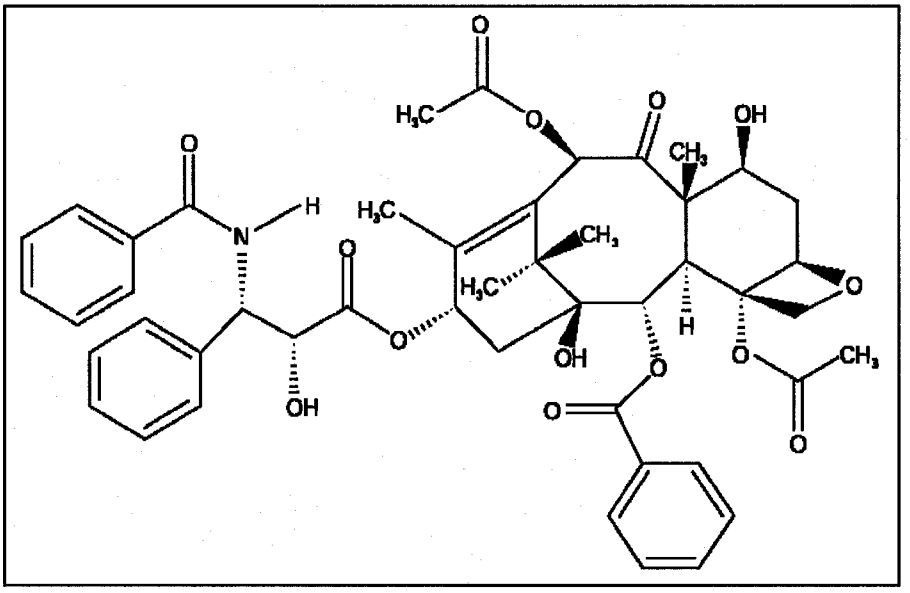
O
H3C
O
O
OH
CH3
O
N
H
H3C
CH3
O
H3C
O
H
OH
O
O
CH3
OH
O
O

guanosine triphosphate (GTP) (Parness and Horwitz, 1981). Paclitaxel also increases the rate of microtubule assembly by binding to microtubule polymers (Manfredi *et al.*, 1982). Since tumour cells are known to have higher rates of cell division, they are more sensitive to paclitaxel's effect than wild type cells (Blagosklonny and Fojo, 1999). In addition to the stabilization of microtubules, paclitaxel also affects intracellular trafficking of essential cell contents such as proteins (Sonee *et al.*, 1998) as well as DNA repair mechanisms (Wang *et al.*, 2005) resulting in cell cycle arrest at the G2/M phase (Das *et al.*, 2000). Furthermore, as the tumour cells fail to overcome the blockage in the cell cycle, they succumb to apoptosis possibly by induction of the p53, a protein which is commonly associated with DNA repair and apoptosis (Ganasia-Leymarie *et al.*, 2003).

1.1.2 Anthracyclines

First isolated as a fermentation product from *Streptomyces peucetius* var. *casius*, doxorubicin (Doxorubicin® - Pfizer, DOX) (Figure 1.1) belongs in the class of drugs known as anthracyclines (Arcamone *et al.*, 2000). The clinical use of this drug has been limited due to its cardiotoxicity and induction of "irreversible congestive heart failure". Although it is most commonly believed that oxidative stress is the source of cardiotoxicity (Zhou *et al.*, 2001); the precise mechanism by which doxorubicin causes cardiotoxicity is still under investigation. However, it is known that doxorubicin ultimately causes the death of cardiac myocyte cells (Minotti *et al.*, 2004). Deaths resulting from anthracycline induced heart failure are estimated at 20% (Horenstein *et al.*, 2000).

Epirubicin (Pharmorubicin® - Pfizer, EPI) (Figure 1.2), another anthracycline, was first synthesized in 1975 by Arcamone and colleagues (Arcamone *et al.*, 1975). As an analog

Figure 1.1: Structure of doxorubicin.

A fermentation product from *Streptomyces peucetius* var. *casius*, doxorubicin binds with DNA and topoisomerase II, causing complications in DNA replication. (Minotti, G., Licata, S. et. Al. 2000)

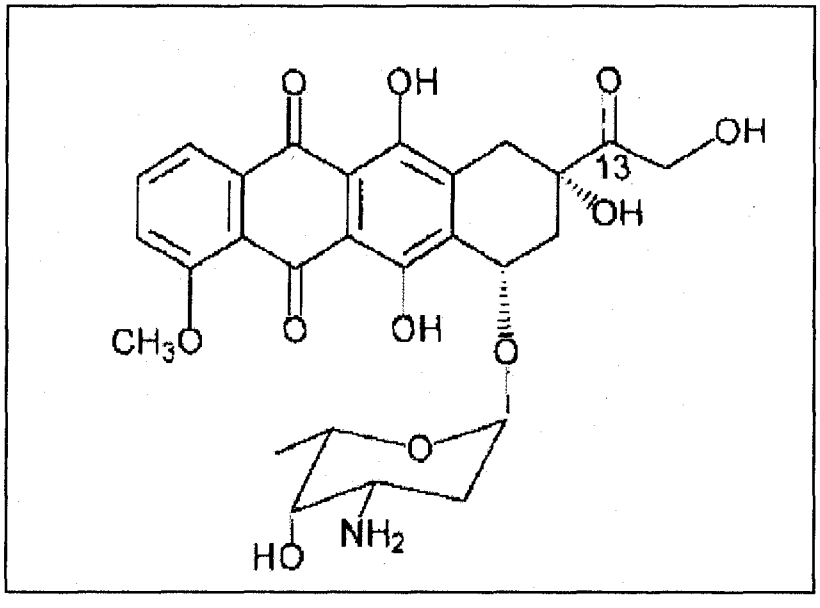
O
OH
O
OH
13
OH
CH3O
O
OH
O
O
HO
NH2

Figure 1.2: Structure of epirubicin.

An analog of doxorubicin, epirubicin is thought to have a similar mechanism of action. The only structural difference between epirubicin and doxorubicin is the epimerization of the hydroxyl group on the fourth carbon in the daunosamine backbone from an axial to equatorial position. (Minotti, G., Licata, S. et. Al. 2000)

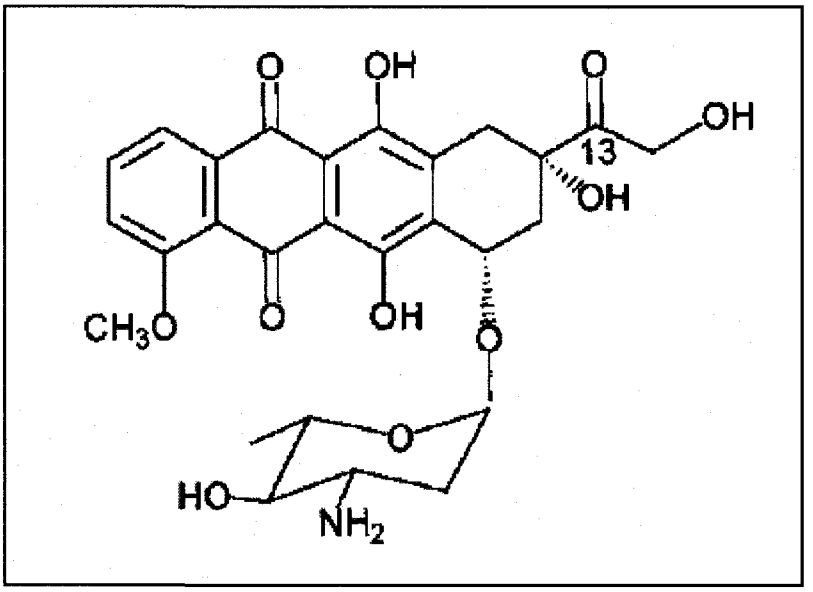
O
OH
O
OH
13
OH
CH3O
O
OH
O
O
HO
NH2

of doxorubicin, it is believed to have similar anti-tumour mechanisms. The only structural difference between epirubicin and doxorubicin is the epimerization of the hydroxyl group on the fourth carbon in the daunosamine backbone from an axial to equatorial position. Clinically, epirubicin exhibits less cardiotoxicity than doxorubicin, and it is thought that this minor dissimilarity in structure may be responsible for the more efficient removal of epirubicin's glucoronidated form before accumulating to toxic concentrations (Weisz, 2003). Culmulative doses that are related to the development of congestive heart failure for epirubicin are approximately twice as high as that of doxorubicin (Fumoleau *et al.*, 2006).

Doxorubicin has been used extensively to treat a broad range of tumours, including breast cancer, stomach cancer, acute leukemia, lymphomas, multiple myleomas, sarcomas and bone cancer (DeVita *et al.*, 1993). Typical doses for a bolus administration range between 15 and 90 mg/m^2, to give initial plasma levels near 5 μM (Brenner *et al.*, 1985;Greene *et al.*, 1983), and eventually these levels fall to about 1-2 μM (Gewirtz, 1999). Doxorubicin first enters a cell by simple diffusion; however, it is the presence of proteosomes in transformed cells that help shuttle the drug to its proper destination within the cell (Kiyomiya *et al.*, 2001a). In particular, the 20S proteosome is responsible for the high affinity binding of doxorubicin and the subsequent transport of the drug into the nucleus through the nuclear pores. Once inside the nucleus, doxorubicin dissociates from the proteosome to preferentially bind to DNA (Kiyomiya *et al.*, 2001b).

Due to the variety of effects of doxorubicin on cells, it is uncertain whether certain mechanisms predominate in killing tumour cells (Cullinane *et al.*, 2000). One of the most common theories is that the main cellular target of doxorubicin is DNA, resulting in DNA adducts and protein-associated DNA strand breakage. As with most anthracyclines, the

planar structure of the aromatic rings of doxorubicin easily allow for the compound to fit in between the nucleotide bases in a strand of DNA. DNA intercalation of doxorubicin prevents the two strands from separating, resulting in impairment of DNA replication and transcription due to the decreased attachment and efficacy of DNA and RNA polymerases (Parissenti *et al.*, 2007). Doxorubicin also inhibits topoisomerase II, which also leads to DNA strand breaks (Cullinane *et al.*, 2000). Stabilization of the DNA-Topo II intermediary complexes occur through the interaction of the Topo II catalytic cleft with the danuosamine sugar moiety (Tewey *et al.*, 1984). Since the quinone ring in doxorubicin readily undergoes reduction, another known effect of doxorubicin is the induction of oxidative stress. The quinone regenerates via the reduction of oxygen and the production of reactive oxygen species (ROS) such as hydrogen peroxide or superoxide anions. These processes are mediated via NAD(P)H-oxidoreductases (Minotti *et al.*, 1999;Vasquez-Vivar *et al.*, 1997). ROS products damage the cells by propagating the formation of DNA adducts, thymine dimers, and lipid peroxidation (Singal and Pierce, 1986). Finally, doxorubicin also activates the Fas pathway and induces p53-dependent cell death (Wu *et al.*, 2000).

1.2 Multidrug Resistance

Anthracyclines such as doxorubicin are commonly used in first line treatment of breast cancer, since they are considered to be one of the most effective anti-tumour agents for this neoplasm. Taxanes are also being increasingly used in first line chemotherapy (Bonneterre *et al.*, 2005;Pivot *et al.*, 1999;Trudeau *et al.*, 2005). Regardless of the anti-tumour agent being used, drug efficacy will vary from patient to patient. Unfortunately, tumours initially treated with anthracyclines can often develop resistance to this class of

drugs and become refractory to further treatment with an anthracycline and possibly other structurally-unrelated agents. This resistance can be either "intrinsic" or "acquired". Resistance is believed to be intrinsic if it is found to occur prior to the first round of chemotherapy. In acquired resistance, resistance occurs only after exposure to one or more chemotherapy agents (Biedler, 1992). Furthermore, when an individual becomes resistant to a particular chemotherapy agent, he or she may also simultaneously acquire resistance to a variety of structurally unrelated drugs. This phenomenon multidrug resistance or (MDR) is believed to be the cause of treatment failure in approximately 90% of metastatic cancer patients (Longley and Johnston, 2005). In order to improve the success of future chemotherapy treatments, we must obtain a better understanding of the mechanisms involved in multidrug resistance and how to circumvent them.

Despite 20 years of research directed towards understanding mechanisms which could lead to the development of multidrug resistance in cancer patients, preventing or reversing clinical MDR has not yet been achieved and its complexity is now being realized (Gottesman *et al.*, 2006). Furthermore, it is now more widely accepted that there are likely a myriad of cellular mechanisms that contribute or give rise to drug resistance (Figure 1.3). Some mechanisms contributing to drug resistance *in vitro* include altered drug influx or efflux, inactivation of drug, alterations in the amount drug targets, repair of drug-induced damage to DNA , and upregulation of genes or proteins involved in cell survival (Longley and Johnston, 2005).

Figure 1.3: General mechanisms of resistance.

The accompanying image shows the large variety or resistance mechanisms commonly studied in multidrug resistance. These mechanisms include extrusion from the cell from plasma membrane multidrug resistant pumps like ABCB1, metabolism of chemotherapeutic agents to an inactive forms, drug binding and sequestration, or by alteration of the chemotherapeutic targets (eg. Tubulin or topoisomerase II).

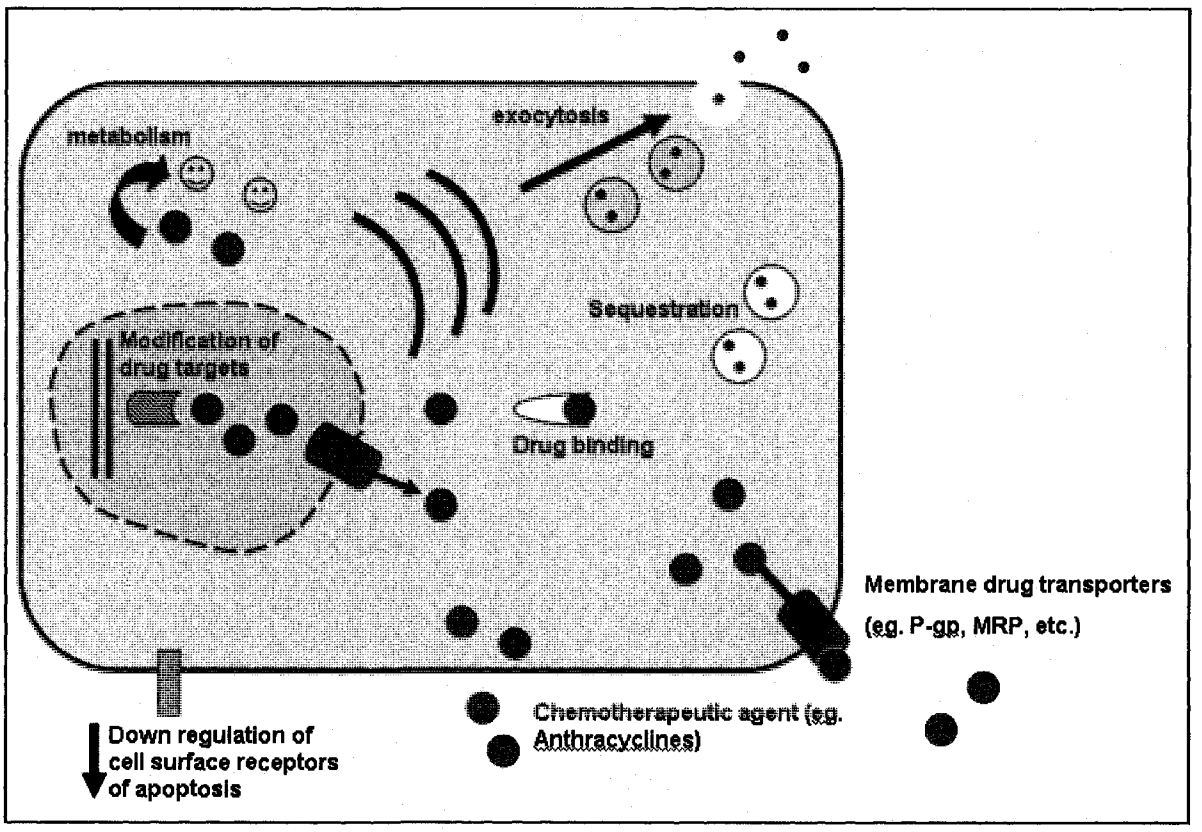
metabolism
exocytosis
Sequestration
Modification of drug targets
Drug binding
Membrane drug transporters
(eg. P-gp, MRP, etc.)
Chemotherapeutic agent (eg. Anthracyclines)
Down regulation of cell surface receptors of apoptosis

1.2.1 Drug Efflux and Cellular Transport Proteins

One of the most explored and main classes of drug transporters involved in multidrug resistance are the ATP-Binding Cassette (ABC) family of transporters. The first ABC transporter to be associated with the development of MDR was the 170kDa (Richert *et al.*, 1988) transmembrane protein ABCB1 (known before as P-glycoprotein), the gene product of MDR1. In normal tissue, ABCB1 is expressed in the liver, kidney, adult adrenal tissue, pancreas, colon and jejunum (Endicott and Ling, 1989). Ueda and colleagues were among the first to correlate the expression of the MDR1 gene with various degrees of drug resistance in multi-drug resistant human KB cells (Ueda *et al.*, 1986). ABCB1 has been shown to be involved in the transport of a variety of structurally unrelated anti-cancer agents such as vinblastine, epirubicin, paclitaxel, etoposide, and topotecan (Zhu, 1999).

Another well characterized ABC transporter linked to drug resistance and poor prognosis in breast cancer is ABCC1 (also known as MRP1) (Nooter *et al.*, 1997). In this "C" subfamily of ABC transporters are ABCC2 (MRP2) and ABCC3 (MRP3) both of which have increased expression in various drug-selected cell lines (Kool *et al.*, 1997). However, the contribution of these proteins in drug resistance is still unclear. MRP1 has been shown to transport mostly conjugated substrates, for example glutathione- and sulfate-conjugated drugs (Bakos and Homolya, 2007). The overexpression of this gene has been associated with resistance to a number of classes of chemotherapeutic agents *in vitro* including the anthracyclines (Borst *et al.*, 2000).

Although not included in the ABC family of transporters, another transporter implicated in MDR is LRP. This major vault protein (MVP), is expressed in many primary breast cancers (Pohl *et al.*, 1999) and has been reported to be involved in the redistribution of intracellular drug in cancer cells (Kitazono *et al.*, 1999). Moreover, some clinical studies have shown that LRP expression levels affect the prognosis of some cancers including ovarian cancer and acute myeloid lymphoma (AML) (List *et al.*, 1996;Scheffer *et al.*, 2000)

1.2.2 Metabolism of Chemotherapeutic Agents

In addition to drug efflux and transport, drug metabolism has also been examined as a possible contributor to MDR. One enzyme, proposed to be involved in drug resistance, is the dimeric enzyme glutathione S-transferase (GST). GSTs add glutathione residues to a wide variety of drug substrates. Gaudiano and colleagues reported high levels of glutathione S-transferase activity in doxorubicin-resistant MCF-7 cells. The glutathione-conjugated drug substrates such as doxorubicin-GSH were found to be less toxic than their original counterparts (Gaudiano *et al.*, 2000). Furthermore, using confocal microscopy, it was observed that doxorubicin and its glutathione conjugate (ADRIGLU), had different subcellular locations, which varied depending on the cell line used. In MCF-7 cells, doxorubicin was found to be solely within the nucleus, whereas the glutathione conjugate form of doxorubicin was found to be co-localized with the golgi apparatus (Serafino *et al.*, 1998). Moreover, when doxorubicin and its glutathione conjugate were added to doxorubicin-resistant MCF-7 cells, they were both localized within the golgi apparatus. Consequently, it has been suggested that glutathione conjugated drugs remain in the cytoplasm and that glutathione conjugation may contribute to resistance by sequestering

drugs in the cytoplasm. While elevated levels of glutathione have been found to be associated with multidrug resistance (Serafino *et al.*, 1998), the role of GST in clinical drug resistance is still not yet understood. One such example was the study performed by Gaudiano using GST P1-1, a human placental GST, which showed that despite the reproducible differences in localization of doxorubicin and its conjugated form in sensitive and resistance cell lines, glutathione conjugation to doxorubicin does not effectively occur in the resistant MCF-7/DOX cell line under typical physiological conditions (Gaudiano *et al.*, 2000).

Another class of drug metabolizing enzyme proposed to be involved in drug resistance are the carbonyl reductases. Carbonyl reductases (CBR) catalyze the reduction of a variety of xenobiotic carbonyl compounds including anthracyclines (Bachur and Huffman, 1971;Takanashi and Bachur, 1975). Ubiquitous in nature, CBRs are typically found in the cytosol and are NADPH dependent. In anthracyclines, such as daunorubicin and doxorubicin, it is the aliphatic keto side chain which is reduced by CBRs (Felsted and Bachur, 1982). One example of these CBRs is dihydrodiol dehydrogenase (DDH), or aldoketoreductase. Recently, it was determined that overexpression of the 1C2 aldoketoreductase caused resistance to cisplatin and carboplatin in ovarian carcinoma cells (Deng *et al.*, 2002). Furthermore, it has been demonstrated that the increased expression of carbonyl reductase is associated with doxorubicin resistance in stomach cancer cells (Ax *et al.*, 2000). To date, four isoforms of the 1C aldoketoreductases have been identified and characterized including AKR1C1, AKR1C2, AKR1C3 and AKR1C4 (Burczynski *et al.*, 1998). In clinical studies, it has been found that high levels of DDH expression correlates with poor prognosis in non-small-cell lung cancer patients (Hsu *et al.*, 2001).

1.2.3 Sequestration and Efflux of Chemotherapeutic Agents

Since the target of anthracyclines is typically DNA and topoisomerases, (both of which are located in the nucleus) another mechanism which may play an important role in clinical drug resistance is the sequestration of drugs. By sequestering anthracyclines into intracellular organelles, it is possible that cell survival will occur as the drugs are no longer able to reach their target of action. Although it has been previously thought that ABCB1 played a central role in drug resistance, it has been found that some resistant cells which express this protein only express a small change in intracellular drug accumulation (Siegfried *et al.*, 1983). Recently, the focus has changed to determine where intracellular anthracycline localizes within drug-resistant cells. Due to the inherent ability of anthracyclines to fluoresce, many studies now use confocal and fluorescence microscopy to track anthracycline localization in drug-sensitive and drug-resistant cancer cell lines.

In a study performed by Schuurhuis and colleagues, two independent selections for doxorubicin resistant cell lines were conducted via exposure to increasing concentrations of doxorubicin (50-160 nM). In one selection, cells lacked ABCB1 expression, while in the other selection ABCB1 was highly expressed. Defects in doxorubicin accumulation were most evident in cell lines that expressed higher levels of ABCB1. Moreover, they found that the nuclear/cytoplasmic (N/C) fluorescence ratio was inversely proportional to the magnitude of doxorubicin resistance cells. However, when they compared doxorubicin resistant human non-small cell lung cancer cell lines with and without ABCB1 expression, they found that both cell lines showed a decrease in their N/C ratios when quantifying the fluorescence emitted by doxorubicin (Schuurhuis *et al.*, 1991). Most interesting however, was the observation that in cells lacking ABCB1 expression, the values for the N/C ratios were lower

(Schuurhuis *et al.*, 1991). As a result, it has been suggested that the alteration in intracellular doxorubicin could be an ABCB1 independent mechanism of resistance.

Changes in intracellular anthracycline distribution have already been reported in a number of drug-resistant cell lines, such as myeloma (Broxterman *et al.*, 1990), lung carcinoma (Keizer *et al.*, 1989), epidermoid carcinoma (Willingham *et al.*, 1986), ovarian carcinoma (Schuurhuis *et al.*, 1993), leukemic lymphoblastic (Bobichon *et al.*, 1996), bladder cancer (Featherstone *et al.*, 2005), and breast cancer cells (Bour-Dill *et al.*, 2000).

A study conducted by Altan and colleagues demonstrated that in MCF-7 (NCI-ADR), cells, doxorubicin was found to be absent in nuclei. After using a series of pH sensitive intracellular markers, they also observed that acidified vesicles were present within the cytoplasm of MCF-7ADR cells. Moreover, using intracellular organelle markers, they found that doxorubicin co-localized with the lysosomes, trans-golgi network, and recycling endosomes (Altan *et al.*, 1998) in these cells. It is known that these compartments are also highly acidified.

Thus, one theory to account for the drug localization defect is the sequestration of anthracyclines into acidic organelles (Altan *et al.*, 1998). In eukaryotic cells, the pH decreases along the endocytic pathway which consists of the early endosomes, late endosomes, and lysosomes (Weisz, 2003). The trans-Golgi network (TGN) is also been reported to be moderately acidified (Seksek *et al.*, 1995). Acidification of organelles is achieved by adjusting the balance of proton pumps, counterion conductance, and proton leakage (Weisz, 2003). Normal cells have normal acidification in these compartments, whereas in transformed cells it has been reported that the cytoplasm and organelles are slightly more alkaline. However, in anthracycline-resistant cells the normal acidification

pattern appears to be restored (WARBURG, 1956). The mechanism by which the pH gradient between the cytoplasm and organelles is restored is still under debate. Studies suggest that disruption of the pH gradient can be achieved by changes in the activity of vacuolar H^+ ATPase by using inhibitors (Altan *et al.*, 1998). Other studies suggest that ABCB1 expression in these vacuoles contribute to the regulation of pH (Thiebaut *et al.*, 1990) or is aiding the transport of anthracyclines into acidic vesicles directly (Rajagopal and Simon, 2003).

Anthracyclines, by nature are weak bases, and due to this characteristic, they become protonated upon entry into an acidified organelle. After being protonated, the compounds are no longer membrane permeable and are consequently sequestered into these acidified organelles (Altan *et al.*, 1998). The above theory is known as the protonation, sequestration and secretion (PSS) model (Schindler *et al.*, 1996). When comparing anthracycline resistant and sensitive cell lines, it was observed that the pH of cytoplasmic organelles is lower in resistant cells (Altan *et al.*, 1998). Based on this theory, protonated anthracyclines that are sequestered in vesicles are eventually removed via recycling endosomes or by exocytosis.

In addition to plasma membrane and vacuolar ABCB1, this protein has also been isolated from the nuclear envelope of anthracycline resistant cells. These findings suggest another possible type of localization defect of anthracyclines in which nuclear extrusion of anthracyclines is achieved via nuclear envelope ABCB1 (Calcabrini *et al.*, 2000). Other theories of how sequestration is achieved is the conjugation of anthracyclines to glutathione (the conjugated compound is also fluorescent) which ultimately then prevents the anthracylines from entering the nucleus (Serafino *et al.*, 1998) More recently, intracellular ABCB1 (Molinari *et al.*, 2002) and MRP1, have been suggested to play a role, by actively

pumping cytosolic drug into vesicles without the requirement of a pH gradient (Rajagopal and Simon, 2003).

1.3 The Human Breast Cancer Cell Line MCF-7 and Resistant MCF-7 Cell lines

Cell lines have been used extensively as an easily renewable source of tumour cells as models to study the origins of cancer. For the purpose of our studies, the MCF-7 human breast adenocarcinoma cell line will be used as one model for breast cancer. The MCF-7 cells used in this study originated from a pleural effusion of a patient treated at the Michigan Cancer Foundation (Soule *et al.*, 1973). These cells are estrogen receptor positive, fibroblastic in nature and capable of high cell to cell adhesion (http://www.atcc.org/common/catalog/numSearch/numResults.cfm?collection=ce&atccNum=HTB-22). MCF-7 cells are considered to be an invasive ductal type of carcinoma (Lacroix and Leclercq, 2004) and lack caspase-3 due to a mutation resulting in a deletion in exon 3 (Janicke *et al.*, 1998).

In order to increase our understanding of the mechanisms involved in drug resistance, our laboratory has previously generated 4 drug-resistant cell lines through the stepwise selection of MCF-7 cells using one of 4 chemotherapy agents using various increasing concentrations of chemotherapeutics. The surviving fraction from each treatment is considered a "dose n", whereby n represents the number of the treatment (eg. Dose 10, refers to cells that survived the 10^{th} treatment in the generation of resistant cell lines). In total, 12 doses were selected by treatment to each drug (see materials and methods for cell line nomenclature). These cell lines have been characterized for drug sensitivity via clonogenic

assays and the threshold IC_{50} concentration for resistance was found at dose 9 for each for each of the drug treated cell line selections (Figure 1.4).

Advantages of using the MCF-7 and its corresponding resistant cell lines allow us to temporally correlate changes in gene expression or potential mechanisms of resistance with the onset of resistance. Moreover, the resistant cell lines were generated using concentrations well within the range achieved in clinical settings, and as such any mechanisms of resistance observed are more likely to occur in patients. Interestingly, although two anthracycline resistant cell lines were created, QPCR studies (Figure 1.5) show that only the epirubicin-resistant cell line expressed the MDR1 gene, which encodes for the well known ABCB1 drug pump, providing the ability to determine if mechanisms of resistance observed are ABCB1 dependent.

There are limitations, however, to using these cell lines to study drug resistance. Firstly, as the MCF-7 cell line lacks caspase-3 expression, it is more difficult to study cell death. Moreover, it is important to know that these are *in vitro* studies, using a monolayer of cells, and this does not accurately portray a 3-dimensional tumour in which not all cells would be exposed to the same concentration of drugs, and it must also be taken into account that drug delivery via blood vessels also varies. Due to these factors, it is very difficult to determine the concentration of drug each cancer cell is exposed to (Jain, 1990;Jain, 1997).

Figure 1.4: Comparison of Epirubicin sensitivity across cell lines.

Clonogenic assays. The divergence of the resistant cell lines from the co-cultured control can be observed beginning at dose 9 selection, whereby the resistant cell lines become less sensitive to epirubicin and this phenomenon persists in the resistant cell lines from later selections (eg. Selection dose 10 and 12). (Veitch, Z, 2006, Unpublished data)

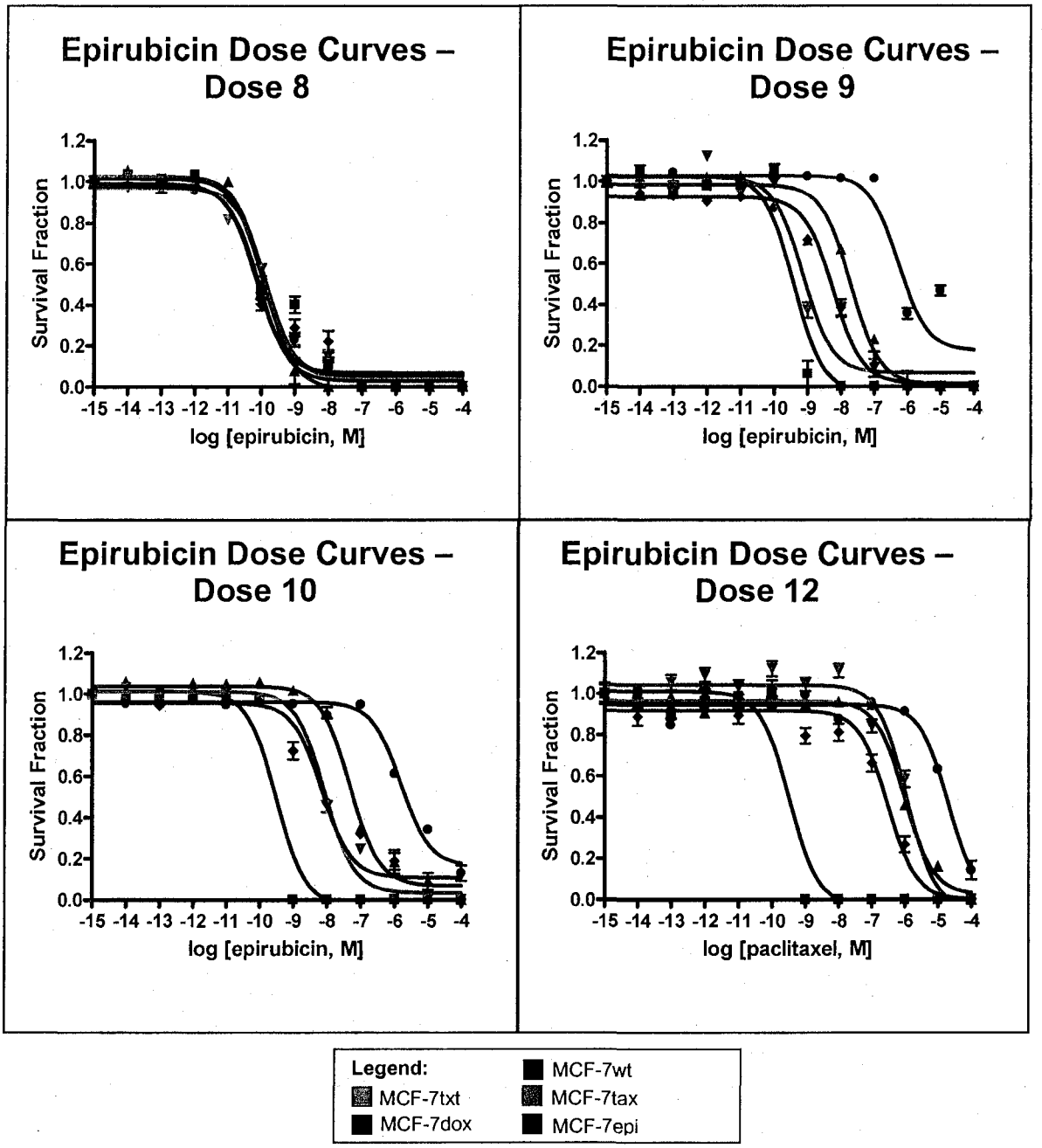
Epirubicin Dose Curves – Dose 8
Survival Fraction
1.2
1.0
0.8
0.6
0.4
0.2
0.0
-15 -14 -13 -12 -11 -10 -9 -8 -7 -6 -5 -4
log [epirubicin, M]
Epirubicin Dose Curves – Dose 9
Survival Fraction
1.2
1.0
0.8
0.6
0.4
0.2
0.0
-15 -14 -13 -12 -11 -10 -9 -8 -7 -6 -5 -4
log [epirubicin, M]
Epirubicin Dose Curves – Dose 10
Survival Fraction
1.2
1.0
0.8
0.6
0.4
0.2
0.0
-15 -14 -13 -12 -11 -10 -9 -8 -7 -6 -5 -4
log [epirubicin, M]
Epirubicin Dose Curves – Dose 12
Survival Fraction
1.2
1.0
0.8
0.6
0.4
0.2
0.0
-15 -14 -13 -12 -11 -10 -9 -8 -7 -6 -5 -4
log [paclitaxel, M]
Legend:
MCF-7wt
MCF-7txt
MCF-7tax
MCF-7dox
MCF-7epi

Figure 1.5: Expression profiles of the expression of ABC transporters and LRP in resistant cell lines.

Q-PCR data comparing the levels of expression of ABC transporters known to be involved in resistance. The most highly expressed transporter was the ABCB1 transporter in MCF-7_{EPI} cells selected to dose 10. The expression of LRP was also investigated but was found to be only slightly upregulated in expression. (Laberge, M. 2006, Unpublished data).

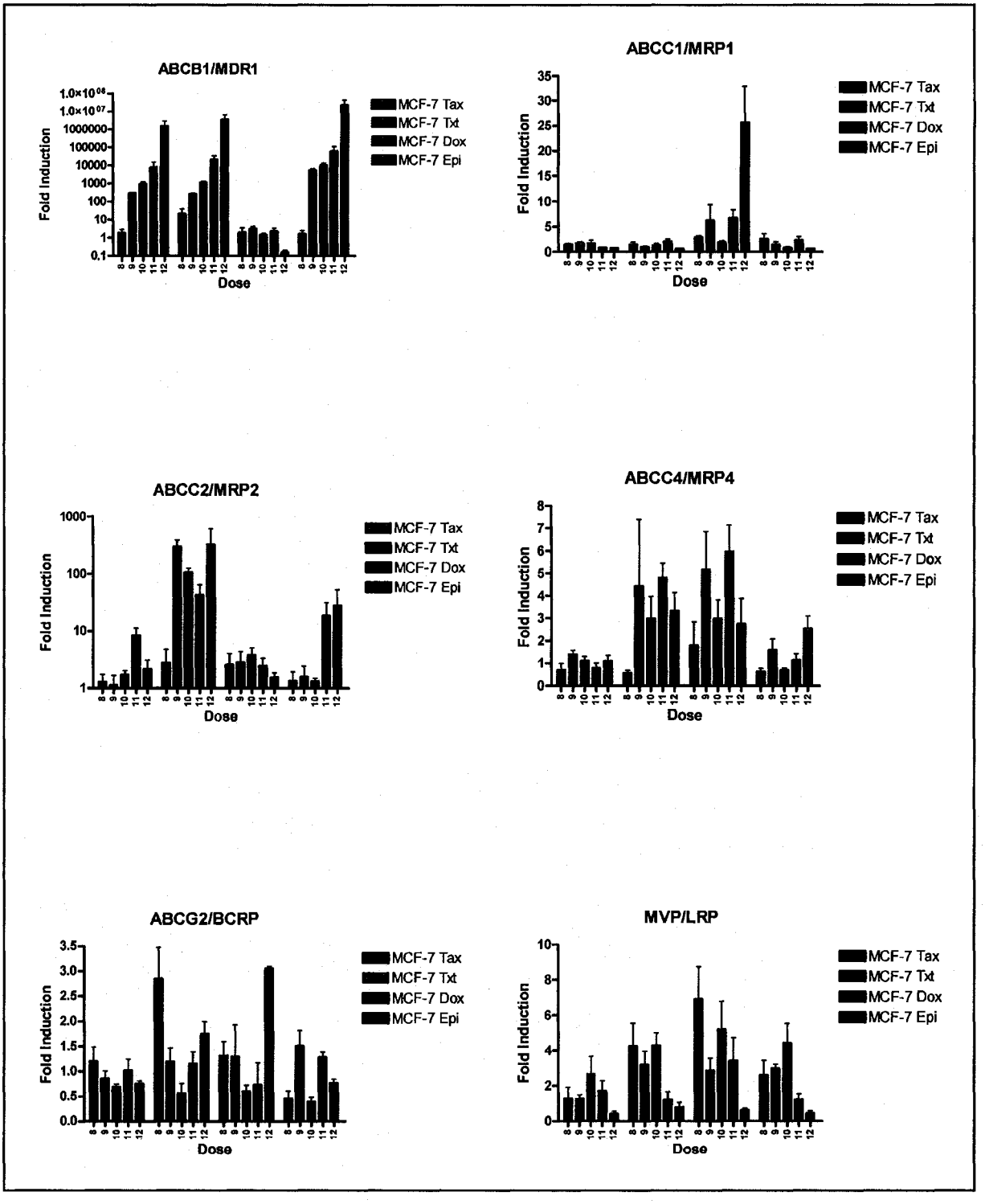
ABCB1/MDR1
Fold Induction
Dose
MCF-7 Tax
MCF-7 Txt
MCF-7 Dox
MCF-7 Epi
ABCC1/MRP1
ABCC2/MRP2
ABCC4/MRP4
ABCG2/BCRP
MVP/LRP

1.4 Monitoring Drug Localization by Confocal Fluorescence Microscopy

The first confocal microscope was invented by Marvin Minsky in the mid 1950s in an attempt to visualize and capture images of biological events as they occur in living systems (Minsky, 1988). Before confocal microscopy was available, widefield optical fluorescence microscopes were used. Problems arose in image processing as secondary fluorescence is emitted from the specimen, which interferes with the resolution of objects within the objective focal plane (Wilson, 1989). Furthermore, when the specimen thickness exceeded 2 μM, the interfering fluorescence becomes more significant. Although the confocal microscope has provided a slight improvement in the axial and lateral optical resolutions, it is more successful in filtering out extraneous fluorescence from the plane of focus (Lichtmann, 1994;Swedlow *et al.*, 2002;White *et al.*, 1987) which will be discussed later in more detail. Despite these features, the confocal microscope still cannot even remotely produce the high resolution images that the scanning electron microscope is capable of.

A diagram illustrating the components of a typical confocal microscope can be seen in figure 1.6. When coherent light is emitted by an excitation source or laser system, it passes through a tiny pinhole known as the light source pinhole and then hits a dichromatic mirror, which reflects the laser light for scanning and excitation across the focal plane of the specimen. Secondary fluorescence emitted from the specimen, passes through the dichromatic mirror and is sent to the detector after passing through a second pinhole called the detector pinhole. The fluorescence that goes through the pinhole is an electrical signal that is converted into the pixels of an image by an analog to digital converter usually located in the scanning unit (Stelzer, 2000).

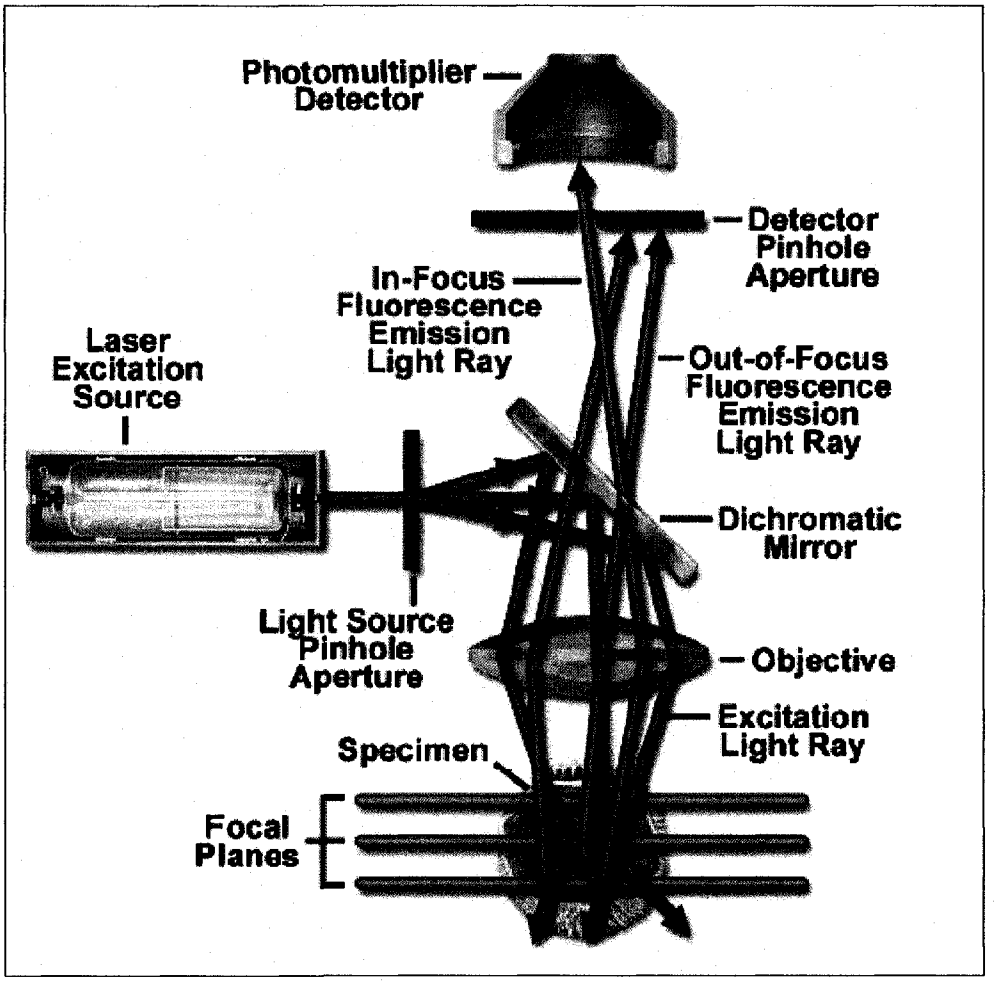
Photomultiplier Detector
Detector Pinhole Aperture
In-Focus Fluorescence Emission Light Ray
Laser Excitation Source
Out-of-Focus Fluorescence Emission Light Ray
Dichromatic Mirror
Light Source Pinhole Aperture
Objective
Excitation Light Ray
Specimen
Focal Planes

There are a number of advantages to using a confocal microscopy in monitoring the localization of anthracyclines in tumour cells compared to conventional widefield optical microscopes such as the ability to control field depth and improved image quality due to the reduction in background signals from above and below the plane of focus. The reason why this difference exists between traditional widefield microscopes and confocal microscopes lies in the emission that is directed back through the eyepiece or detector. In traditional widefield microscopes, which illuminate a larger volume of the specimen, a significant quantity of fluorescence is directed back to the microscope through the aperture, resulting in decreased image resolution due to increased levels of background fluorescence. However in confocal microscopy, the laser is first expanded and then refocused to a very small point, which then illuminates the focal plane. The diameter of this small point can range from 0.25 to 0.8 μM and the depth can vary from 0.5 to 1.5 μM (Wright and Wright, 2002). Furthermore, confocal microscopy is most well known for its ability to produce a series of very thin optional sections 0.5 to 1.5 μM in specimens as thick as 50 μM or more. The confocal microscope is able to achieve this via a stepper motor which adjusts the fine focus to sequentially acquire images at each interval, ultimately creating a three-dimensional image (Sandison and Webb, 1994). The ease by which high quality images can be taken has made confocal microscopy, an increasingly popular choice for a number of biological applications. The confocal microscope can also easily change the size of the area scanned by the laser without switching to a different objective through the use of the zoom factor. The resultant image after increasing the zoom factor is displayed on the connected computer screen with increased spatial resolution and magnification (Centonze and Pawley, 1995). Finally, confocal microscopy often has accompanying software in order to immediately process and

Figure 1.6: Schematic representation of a typical confocal microscope.

General mechanism of the typical confocal microscope: Laser light is emitted from a source through a pinhole, then hits the dichromatic mirror, concentrated to a point by the objective to scan the specimen of interest, which is then reflected back through the detector after passing through the detector pinhole, which is responsible for producing higher resolution images with fewer background fluorescence compared to a typical fluorescence microscope (Claxton, N et. al. Laser Scanning Confocal Microscopy).

analyze images for information concerning cell length, volume, depth, and opacity as well as to interactively alter images to examine structures at different levels in the specimen (Conchello *et al.*, 2005).

Confocal microscopy is most useful in providing qualitative rather than quantitative data. Moreover, due to the high magnification of the objectives, the sample size examined is small and limited. Other disadvantages to using laser confocal microscopy include loss of fluorescence signals due to photobleaching. The above concerns are addressed by repeating experiments and controlling for laser settings between experiments. Moreover, quantitative results can be obtained by using software designed to quantify total fluorescence units in a selected area of a specimen observed using confocal microscopy.

1.5 Rationale and Objectives

The conclusions of the compelling study by Altan and colleagues must be tempered by a subsequent disclosure by another investigator that MCF-7ADR cells are genetically unrelated to MCF-7 cells and are of ovarian origin (Scudiero *et al.*, 1998). Thus, it is unclear whether MCF-7 cells selected for resistance to doxorubicin would, in fact, exhibit nuclear drug exclusion with a large amount of drug being associated with acidic vesicles. It is also unclear whether changes in drug localization are temporally correlated with the acquisition of drug resistance and whether drug transporters such as ABCB1 and proton transporters (involved in vesicle acidification) play central roles in this process. Answering these questions could contribute valuable information for future clinical studies on the identification and circumvention of drug resistance in breast cancer patients.

Thus, the objectives of this study were as follows:

1. to characterize the localization of the anthracyclines, doxorubicin and epirubicin as they accumulate in drug-sensitive and drug-resistant human MCF-7 cells;
2. to determine the temporal relationship between the onset of drug localization changes and the acquisition of drug resistance
3. should localization changes occur, to determine whether epirubicin is sequestered in acidic vesicles and whether these vesicles are of lysosomal, golgi or endosomal origin
4. to determine the contribution of drug or proton transporters in drug localization

2.0 MATERIALS AND METHODS

All general labware, eg. Tissue culture flasks, tissue culture plates, centrifuge tubes, and plastic pipettes were from Sarstedt (Montreal, QC) and Falcon.

2.1 Maintenance of Mammalian Tissue Culture

Human MCF-7 breast cancers cells were grown as a monolayer in Dulbecco's H21 medium (Princess Margaret Hospital, Toronto, ON) containing 10% fetal bovine serum (FBS, Hyclone, Logon, UT) and incubated at 37°C in a humidified 5% CO_2 atmosphere. For propagation of culture stocks, cells were grown in 50 ml tissue culture flasks, containing 11 mL of medium. Using a specific lot of the MCF-7 cell line provided by the American Tissue Culture Collection (ATCC, Manassas, VA), five cell lines were generated (Hembruff, S. 2005 unpublished data). One aliquot of cells was exposed to increasing concentrations (doses) of either paclitaxel (Taxol, Bristol-Myers-Squibb, Montreal, QC) (MCF-7_{TAX}), doxorubicin (Doxorubicin, PFS, USP, Mississauga, ON) (MCF-7_{DOX}), epirubicin (Pharmorubicin, PFS, Kirkland, QC) (MCF-7_{EPI}) or docetaxel (Taxotere, Sanofi-Aventis, Laval, QC) (MCF-7_{TXT}). A control cell line (MCF-7), which was "selected" in the absence of any drug served as the "co-cultured" control. The passaging of cells was accomplished by first washing the cells with 10 mL of phosphate buffered saline or PBS (PMH) to remove FBS followed by treatment with 3 ml of trypsin (0.25% EDTA in 500 mL trypsin) (Hyclone) to release cells from their flasks. Trypsinized cells were placed into a 15 mL centrifuge tube; 10 mL of media which was used to rinse the flasks was also added to their respective tubes. The cells were then spun at 10 000 rpm for 10 minutes to pellet them. All supernatant was discarded into a waste flask. Each cell pellet was re-suspended in 5 mL of the appropriate

medium, and then aliquoted into a new flask containing fresh Dulbecco's H21 media. For drug-resistant cells, cells were propagated at specific drug concentrations to maintain selective pressure (See Table 2.0).

Table 2.0 Concentrations used for selection of resistant MCF-7 cells.

Selection Dose	*Paclitaxel [M]*	*Docetaxel [M]*	*Doxorubicin [M]*	*Epirubicin [M]*
IC_{50}	5.56E-10	5.07E-10	8.90E-09	4.79E-09
1	5.56E-13	5.07E-10	8.91E-12	4.79E-12
2	1.67E-12	5.07E-13	2.67E-11	1.44E-11
3	5.01E-12	1.52E-12	8.01E-11	4.32E-11
4	1.50E-11	4.56E-12	2.40E-10	1.30E-10
5	4.50E-11	1.37E-11	7.20E-10	3.90E-10
6	1.35E-10	4.11E-11	2.16E-09	1.17E-09
7	4.05E-10	1.23E-10	6.48E-09	3.51E-09
8	1.22E-09	3.69E-10	1.94E-08	1.05E-08
9	3.66E-09	1.11E-09	2.91E-08†	3.15E-08
10	1.10E-08	3.33E-09†	4.36E-08†	9.45E-08
11	3.30E-08	5.00E-09	6.54E-08†	2.84E-07
12	9.90E-08	1.50E-08	9.81E-08†	8.52E-07

* Cells which were considered terminal but did not show slow growth.

† 1.5 fold increase was used instead of 3 fold.

2.2 Selection for Doxorubicin, Epirubicin, Taxol and Taxotere-resistant MCF-7 Cells

Previously, in our laboratory (Hembruff, S. Unpublished data 2005) MCF-7 cells, passaged as indicated above, were treated for two weeks, with each drug, beginning at a concentration equal to 1000-fold less than that required to inhibit the growth of 50% of the cells in a clonogenic assay (the IC_{50}). Every 3 to 4 days, dead and non-adherent cells were removed from the cultures and fresh drug-containing media was added. When confluency was reached, cells were removed from their flasks by treatment with trypsin, diluted 10-fold in PBS, and collected by centrifugation. Cells were then reintroduced into fresh media and aliquots were taken to allow for RNA and protein analysis, and for future propagation. A portion of these cells was then incubated with a 3-fold higher drug concentration than the previous dose. The selection process continued up to the maximally tolerated dose or until selection was stopped (see Table 2.0 for concentrations). During the drug selection process, the drug sensitive cell line was also propogated in a similar manner in the absence of drugs and served as the co-cultured control in order to ensure that changes observed in the resistant cell lines were not due to genetic drift as a result of long term culture.

2.3 Live Localization of Doxorubicin and Epirubicin in MCF-7 Human Breast Cancer Cells

A 40 mm glass (Bioptechs, Butler, PA) coverslip is placed in a 10 cm tissue culture plate and MCF-7 $_{WT}$, $_{EPI}$, $_{TAX}$, or $_{DOX}$ cells were grown on the coverslips for three days. Drug containing media was replaced with drug free media for 24 hours. Using the Focht Chamber System 2 (FCS2) system (Bioptechs), the glass coverslip is placed into a chamber flanked by

two gaskets and connected media perfusion tubes. The rubber perfusion tubes were connected to a 50 mL centrifuge tube through the lid. Drug containing media of the appropriate concentration was put in the tube. The FCS2 apparatus (Figure 2.0) allows for media exchange to buffer pH changes and allows for a constant concentration of drug to flow through the apparatus. Since epirubicin (Figure 1.2) is naturally fluorescent, its intracellular localization can be visualized via laser confocal microscopy (510 Meta, Zeiss, Toronto, ON). The same field of cells were monitored for 1, 4 and 8 hours and images were taken using the Argon laser excitation wavelength 488 nm and emission was collected at long pass filter 505 nm and HeNe laser excitation wavelength 543 nm with long pass filter 560 nm. For the purpose of determining the percentage of cells with nuclear fluorescence, 20 images were randomly captured at 30 min, 4 and 8 hours. In the determination of nuclear-cytoplasmic ratios (N/C ratios), 5 images were taken at 30 min, 4 and 8 hours. N/C ratios were acquired by quantifying the total fluorescence intensity via selection of the nuclear and cytoplasmic regions using the Zeiss 510 Meta software.

Alternatively, cells were grown on 1mm square Fisher glass coverslips and incubated in 2 μM epirubicin for 1, 4, 8 and 24 hours and placed on glass slides for visualization using the procedure mentioned above. All localization experiments were optimized to their corresponding co-cultured control MCF-7_{WT} cell line and were observed to compare drug uptake and localization over time.

2.4 Co-localization of Intracellular Organelles with Epirubicin

MCF-7_{WT} and MCF-7_{EPI} cells were grown in drug free media for 2-3 days prior to performing an experiment. All cells were plated on 40 mm circular glass coverslips in small

Figure 2.0: Schematic of FCS2 media flow system.

The FCS2 system (closed chamber system). Cells are grown on a 40mm glass coverslip which is placed cell side down towards the microaqueduct slide, with a rubber gasket in between acting as a spacer. Media flows in through the tubes one side of the chamber and over the cells via the channel in the microaqueduct slide and then out through the tube on the other end. An electrode (arrow no. 1) is attached to the chamber to maintain a temperature of 37°C (http://www.bioptechs.com/Products/FCS2/fcs2.html).

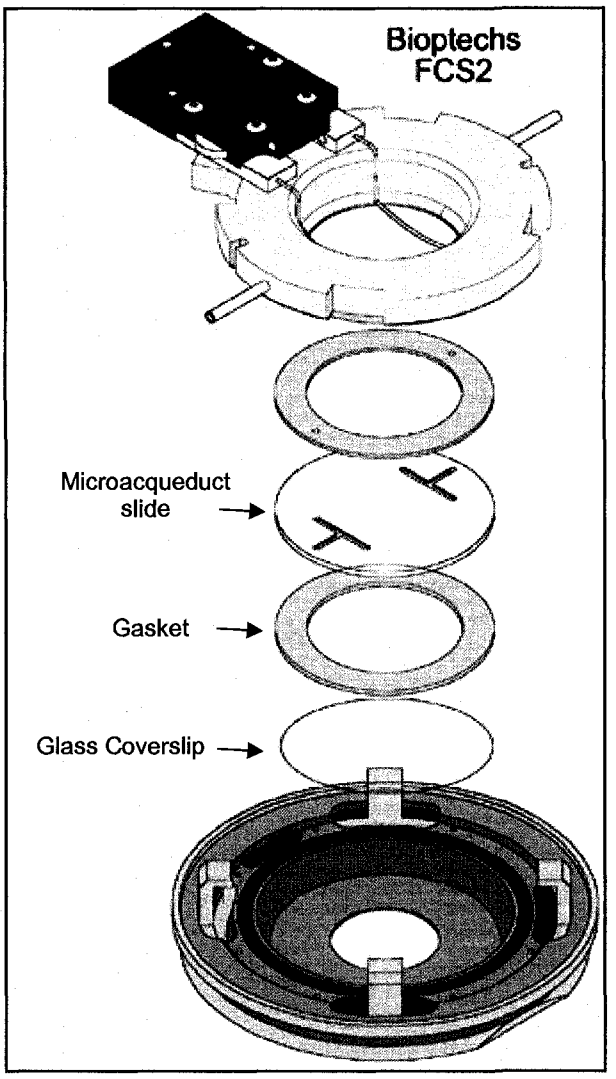
Bioptechs
FCS2
Microacqueduct
slide
Gasket
Glass Coverslip

tissue culture plates containing drug-free media. Following the protocol outlined in section 2.3, after 7 hours of incubation with epirubicin, fresh media containing the same concentration of epirubicin with either 100 nM Lysotracker, 50μg/mL Bodipy Transferrin, 100 nM NBD Ceramide, or 100 nM Bodipy Ceramide (Molecular Probes, Eugene, Oregon) (504 nm_{ex} and 511 nm_{em}, 505 nm_{ex} and 513 nm_{em}, 466 nm_{ex} and 536 nm_{em}, 505 nm_{ex} and 511 nm_{em} respectively) was circulated through the FCS2 system for 1 hour. All intracellular labels were excited using the Argon 488 nm laser, and emitted fluorescence was captured using band pass filter 505-530 nm. In order to prevent the overlapping of fluorescent signals epirubicin fluorescence was excited using the HeNe 543 nm laser and emission was collected using long pass filter 560 nm. $MCF\text{-}7_{WT}$ and $MCF\text{-}7_{EPI}$ cells were also incubated with the various intracellular markers in the absence of epirubicin to ensure that the differences observed were not induced by treatment with epirubucin.

2.5 Flow Cytometry and Epirubicin Drug Uptake

See section 2.1 in materials and methods for resuspension of MCF-7 cells. For each cell line suspension, 50 μL was pipetted into a 1.5 mL eppendorf tube and mixed with 100 μL of 0.1% Trypan Blue (Gibco BRL, Carlsbad, CA) in PBS. From this solution, 10 μL was injected between a glass coverslip and hemacytometer (Hausser Scientific, Horsham, PA) until the entire grid was filled. Under a light microscope, the number of cells was quantified in each of the four fields. To determine the concentration of cells in the suspension, the following calculation was performed:

(cells/mL) = [Average value of the 4 fields x 3(for the dilution factor)] x (10^4 volume factor of hemocytometer)

For this experiment, 400 000 cells were seeded for each 6 cm tissue culture plate containing 5 mL of drug free Dulbecco's H21 media and were grown for 24 hours. Four plates were seeded for each of the four cell lines in order to quantify and assess cells at 0, 1, 4 and 8 hours after the addition of epirubucin.

On the day of the drug uptake experiment, all plates were treated at the same time with 10 μM epirubicin. After specific time points, plates were removed from the incubator (37°C, 5% CO_2). Firstly, media was removed and each plate was rinsed with 5 mL of PBS. The cells were then released from the tissue culture plates by addition of 0.5 mL of trypsin for 5 min. Afterwards, 15 mL centrifuge tubes were prepared for each sample, containing 1 mL of Dulbecco's H21 media. The trypsinized cells were then added to appropriately labeled tubes, and any remaining cells in the tissue culture plates were washed again with 5 mL of PBS, and added to the centrifuge tubes. The cells were then harvested by centrifugation for 10 min. at 10 000 rpm, and re-suspended in tubes containing 700 μL of 1 mM EDTA (Sigma, Oakville, ON) in PBS for FACS analysis.

2.6 Drug Uptake Analysis

The flow Beckman Coulter Epics Elite flow cytometer (Coulter Electronics, FL), is capable of quantifying the level of fluorescence for each of 20 000 cells in a sample due to the inherent fluorescence of epirubicin. The wavelength used for excitation was 488 nm, which was achieved using an argon laser. The mean "ungated" fluorescence values associated with the 20 000 cells in a given sample could then be measured at specific time points. The value obtained for the 8 hour time point for the MCF-7 co-cultured control cells was designated as 100% epirubicin uptake, and all subsequent values in the experiment were

normalized to that value. The purpose of this experiment was to show that 10 μM epirubicin is not sufficient to overcome the differences observed in uptake. These experiments will be compared with those previously performed in our laboratory using only 2 μM epirubicin (see discussion).

2.7 Localization of ABCB1 (P-glycoprotein) in MCF-7_{EPI} cells

The primary antibody used for localization of ABCB1 in cells by immunofluorescence microscopy was a mouse antibody clone MM4.17 (Chemicon, Millipore, Temecula, CA). The secondary antibody used in ABCB1 localization experiments was a donkey-antimouse IgG antibody (Jackson ImmunoResearch, CedarLane Laboratories, Burlington, ON) conjugated to Fluorescein. MCF-7_{WT}, MCF-7_{EPI} and MCF-7_{DOX} cells were plated on 1 mm glass square coverslips (Fisher Scientific), in 6 well tissue culture plates containing drug free media for 2 days.

Each experiment was set up with MCF-7_{WT} or MCF-7_{DOX} as negative controls as they are known to express very low levels of ABCB1. Also for each experiment, the omission of the primary antibody was used as a control for secondary antibody specificity.

Firstly, all coverslips were removed from media using tweezers, rinsed once with Tris Buffered Saline (TBS) (Fisher Scientific), edge dried and promptly immersed in 4% paraformadehyde (Sigma Aldrich, Oakville, ON) at room temperature for 10 minutes. After fixation, all coverslips were washed with TBS, edge dried and the cells remaining on the coverslip were permeabilized using 0.2% Triton X-100 (BDH, VWR) for 5 minutes. At this point, coverslips were then washed in TBS. Cells were then treated with blocking buffer for 60 minutes and washed once with TBS.

The primary and secondary antibody dilutions were prepared just prior to use. The coverslips were then incubated with the MM4.17 anti-ABCB1 antibody for 60 minutes. Using three fresh TBS solutions, all coverslips were washed three times and edge dried. Lastly coverslips were treated with secondary antibody for 45 minutes in the dark. The coverslips were then washed again in TBS, and then placed cell side down on glass microscope slides (Fisher Scientific) in 90% glycerol (Sigma) in water, and sealed using nail enamel. The finished microscope slides were then left in the dark until the time of analysis. All analyses took place within 1-2 hours after preparation.

2.8 Localization of Acidified Vesicles by Acridine Orange Staining.

MCF-7_{WT} or MCF-7_{EPI} cells were grown for 48 hours on (1 mm thick) square glass coverslips (Fisher Scientific, Ottawa, ON) in drug free media. (It should be noted that drug-free media was used when these cells were subcultured.) The coverslips were removed from the media using tweezers, washed once with phosphate buffered saline (PBS, Princess Margaret Hospital, Toronto, ON), and stained with 35 μL of 5 μg/mL acridine orange for 5 minutes at 37°C. After incubation, the coverslip was gently washed with PBS, placed onto a glass microscope slide (Fisher), and sealed with wax or nail polish. At this point images were taken using a confocal microscope. Images were collected using the argon laser and an excitation wavelength of 488 nm to obtain a green signal (emission filter 505-530 nm) and the He/N laser with an excitation wavelength of 543 nm to obtain a red signal (emission filter >560 nm).

2.9 Inhibition of Cellular Transport mechanisms

2.9.1 Inhibition of the Transporter Protein ABCB1

PSC-833, also known as Valspodar (Novartis) was pre-incubated in the cell line of choice for 60 min. at a concentration of 2 μM prior to a localization experiment.

2.9.2 Inhibition of the ABC Transport Protein Family

Cell culture medium containing 1 μM of Cyclosporin A was incubated with the MCF-7_{EPI} cell lines for 60 min. prior to the addition of drug in localization experiment.

2.9.3 Inhibition of H^+ Vacuolar ATPase

Cell culture medium containing 500 nM Bafilomycin (Upstate, Millipore, Temecula, CA) was added to cells for 30 min. prior to a localization experiment (see section 2.3). A control experiment was conducted to determine the toxicity level of the solvent (ethanol) in which the agent was dissolved. Media was prepared with 3%, 1%, 0.5% and 0.25% ethanol. Cells were grown on tissue culture plates in 5% CO_2 at 37°C in medium containing the above respective concentrations of ethanol. At the same time the effects of 385 nM bafilomycin A1 on drug localization was also assessed using fluorescence confocal microscopy.

3.0 RESULTS

The majority of data represented in the following sections were derived from dose 10 in the drug selection protocol unless otherwise indicated. Due to the high concentration of anthracycline being used in the localization studies below, the cutoff time for analysis was left at 8 hours in an attempt to maintain consistency within experiments, as well as to maintain viability of the majority of drug-sensitive control cells during the experiment. In some cases, MCF-7_{WT} cells appear committed to death at 8 hours.

3.1 Localization of Doxorubicin

Doxorubicin localization was observed by monitoring its fluorescence in four cell lines: MCF-7_{WT}, MCF-7_{TAX}, MCF-7_{DOX} and MCF-7_{EPI}. Each of these cell lines was also examined to ensure that autofluorescence would not interfere with fluorescence caused by epirubicin. In each cell line, only low intensity fluorescence was detected in the cytosol of most cells. Differences in the amount and/or localization of doxorubicin were observed in each of the resistant cell lines. Fluorescence was also often observed within the plasma membrane and almost always on the nuclear envelope of all cell lines. Furthermore, examination of the images after 8 hours show that the cells have decreased in overall size compared to the 1 hour time point (Figure 3.0). It is important to note that in each cell line the localization of drug or the amount of drug uptake can vary due to the likelihood that each cell line contains more than one population. All data presented are representative of three independent trials for each cell line.

Figure 3.0: Localization of Doxorubicin in cells selected at dose 10.

These images represent MCF-7_{WT}, MCF-7_{TAX}, MCF-7_{DOX}, MCF-7_{EPI} cells grown on glass coverslips and incubated with circulating media containing 10 μM doxorubicin for 1, 4, and 8 hours. Images were collected (505 nm long pass filter) using confocal microscopy and laser excitation wavelength of 488 nm as described in Materials and Methods section. The red fluorescence observed is due to doxorubicin. As time progressed, more doxorubicin was found in the nucleus as shown by the increasing fluorescence compared after 1, 4 and 8 hours in MCF-7_{WT}, MCF-7_{TAX} and MCF-7_{DOX} cells. In the MCF-7_{EPI} there was a significant decrease in fluorescence, as well as a decrease of nuclear doxorubicin after 8 hours.

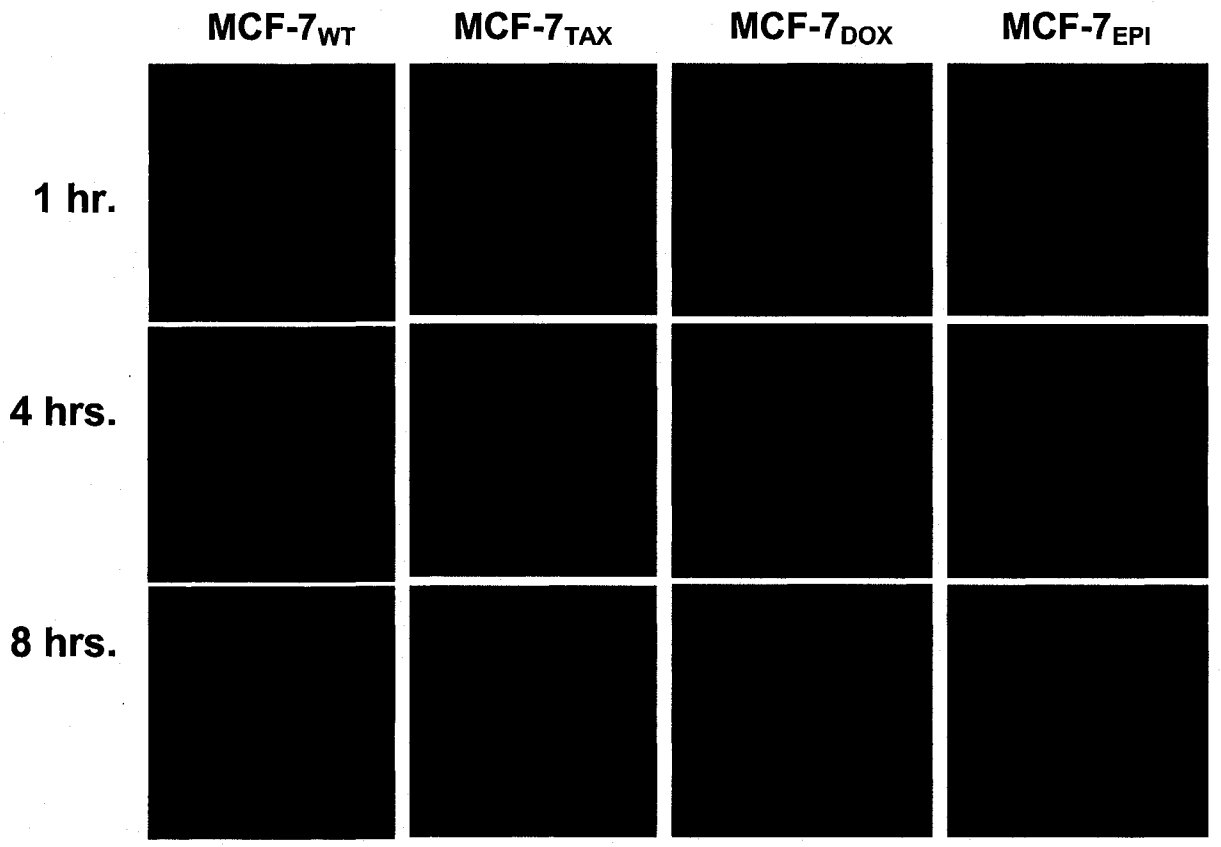
MCF-7WT
MCF-7TAX
MCF-7DOX
MCF-7EPI
1 hr.
4 hrs.
8 hrs.

3.1.1 Localization of Doxorubicin in MCF-7_{WT}

In MCF-7_{WT} cells, doxorubicin was observed predominantly in the nucleus. The fluorescence within the nucleus varied with the greatest intensity on the nuclear envelope and the least intensity in structures likely to be nucleoli, which are abundant in RNA (Figure 3.0). In addition to the nuclear localization of doxorubicin, some randomly distributed punctuate fluorescence was observed in the cytoplasm. Fluorescence increased in intensity over time reaching a maximum intensity at or greater than 8 hours of incubation with drug.

3.1.2 Localization of Doxorubicin in Resistant MCF-7 cells

In 2 of the 3 resistant cell lines (MCF-7_{TAX} and MCF-7_{DOX}), doxorubicin was found predominantly in the nuclei of cells in a pattern similar to that of MCF-7_{WT} cells. However, the fluorescence intensity within the nucleus was lower for each of the resistant cell lines compared to the wild type co-cultured control. Using the same laser and confocal microscope settings, the MCF-7_{TAX} and MCF-7_{DOX} cells had relatively similar doxorubicin fluorescence intensities (Figure 3.0). However, the MCF-7_{EPI} cells showed considerably lower levels of fluorescence in the cytoplasm and in the nucleus compared to the MCF-7_{TAX} and MCF-7_{DOX} cells. Although most MCF-7_{EPI} cells contained nuclear doxorubicin, these signals were significantly lower than previously observed in the other resistant cell lines. Furthermore, a sub-population of cells within the MCF-7_{EPI} cells showed even lower levels of fluorescence in the nucleus or absence of detectable fluorescence when compared to fluorescence observed in the cytoplasm or background signals. Moreover, in cells lacking nuclear drug, highly punctate cytoplasmic fluorescence was observed in the predominantly

perinuclear pattern. The MCF-7_{EPI} cells showed the least change in overall fluorescence intensity over the 8 hour time point experiments (Figure 3.0).

3.2 Localization of Epirubicin

Since no striking difference in localization was observed with the doxorubicin localization studies, epirubicin, another anthracycline, was also monitored to determine if the localization patterns would be identical to that of doxorubicin. Epirubicin, which also fluoresces within the same wavelength range as doxorubicin, was observed in four cell lines, MCF-7_{WT}, MCF-7_{TAX}, MCF-7_{DOX} and MCF-7_{EPI}. Only low intensity autofluorescence was detected in the cytosol of most cells for each of the above cell lines. In each of the resistant cell lines, differences in the amount and localization of epirubicin were observed (Figure 3.1). As seen with the doxorubicin localization experiments, fluorescence was also observed within the plasma membrane. Furthermore, examination of the cells at 8 hours show that the cells have decreased in overall size compared to the 1 hour time point. It is important to note that in each cell line the localization of drug or the amount of drug uptake can vary due to the likelihood that each cell line contains more than one population. All data presented are the representative of three independent trials for each cell line.

3.2.1 Localization of Epirubicin in MCF-7_{WT} Cells

In MCF-7_{WT} cells, epirubicin localization was identical to the doxorubicin localization (Figure 3.1).

3.2.2 Localization of Epirubicin in Resistant MCF-7 Cells

In MCF-7_{TAX} and MCF-7_{DOX} cells epirubicin was found to localize in the nuclei of the cells in a pattern similar to that observed in the MCF-7_{WT} cells. It was found that the MCF-7_{TAX} and MCF-7_{DOX} had similar levels of fluorescence intensity (Figure 3.1) in the nucleus but fluorescence intensity was lower in these cell lines compared to MCF-7_{WT} cells. The MCF-7_{EPI} cells however exhibited the lowest levels of fluorescence in both the cytoplasm and the nucleus (Figure 3.1). Most interesting is that unlike doxorubicin, epirubicin entry in the majority of cells in the MCF-7_{EPI} population was most reduced and resulted in even fewer cells with nuclear fluorescence. Moreover, many cells that had a lack of nuclear fluorescence also had cytoplasmic fluorescence that was arranged in a distinct perinuclear pattern (Figure 3.1-3.2). The MCF-7_{EPI} cells showed the least change in fluorescence intensity over the 8 hour time point experiments (Figure 3.1).

3.2.3 Drug Selection Dose and Localization of Epirubicin

When dose 8, 9 and 12 MCF-7_{WT} cells were treated with epirubicin, there was always nuclear fluorescence with no discernable changes with respect to its localization. Interestingly, when examining MCF-7_{EPI} cell lines selected from an earlier stage, dose 8, epirubicin fluorescence was observed in the nucleus, and its intensity was comparable to the co-cultured control. The MCF-7_{EPI} cells selected at dose 9 however showed a nuclear

Figure 3.1: Localization of Epirubicin in cells selected at dose 10.

These images represent MCF-7_{WT}, MCF-7_{TAX}, MCF-7_{DOX}, MCF-7_{EPI} cells grown on glass coverslips and incubated with circulating media containing 10 μM epirubicin for 1, 4, and 8 hours. Images were collected (505 nm long pass filter) using confocal microscopy and laser excitation wavelength of 488 nm as described in Materials and Methods section. The red fluorescence observed is due to epirubicin. As time progressed, more doxorubicin was found in the nucleus as shown by the increasing fluorescence compared after 1, 4 and 8 hours in MCF-7_{WT}, MCF-7_{TAX} and MCF-7_{DOX} cells. In the MCF-7_{EPI} there was a significant decrease in epirubicin uptake into the cells, as well as a decrease of nuclear epirubicin after 1, 4, and 8 hours.

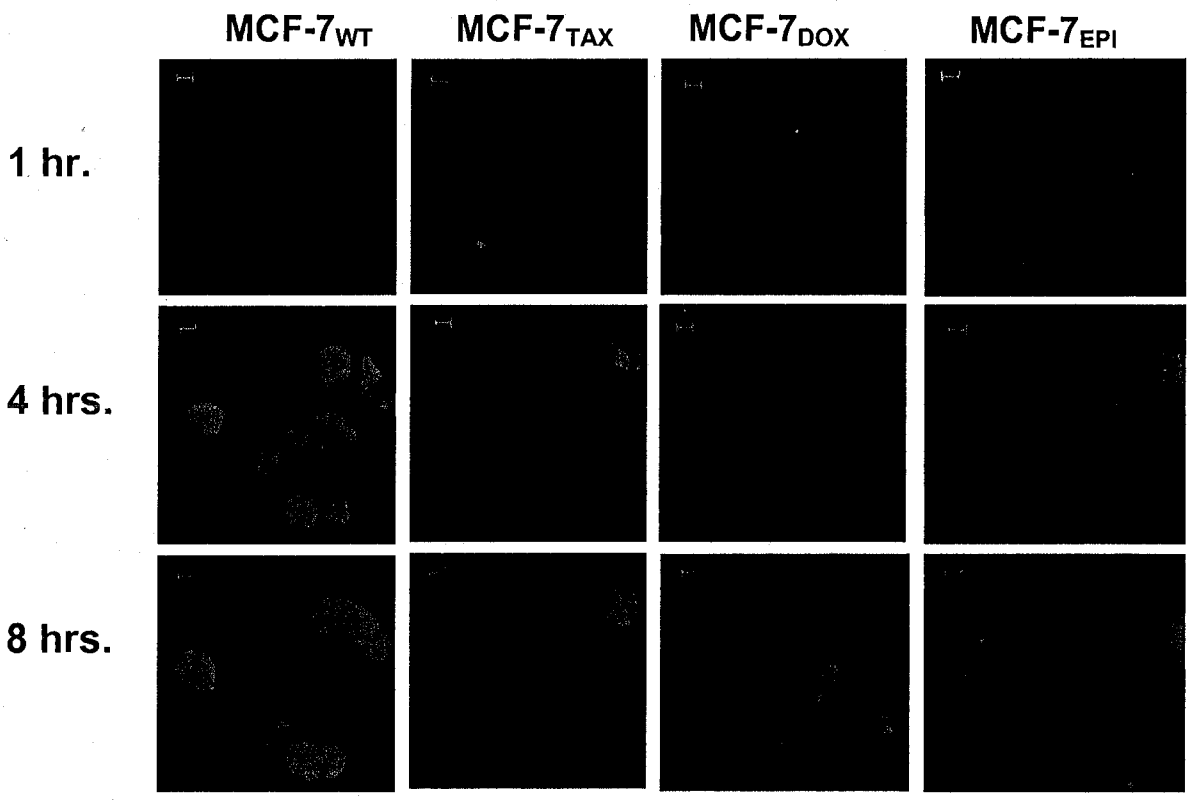
MCF-7WT
MCF-7TAX
MCF-7DOX
MCF-7EPI
1 hr.
4 hrs.
8 hrs.

Figure 3.2: Distinct perinuclear localization of epirubicin.

Images were taken of MCF-7_{EPI} cells after 8 hours of incubation in media containing 20 μM Epirubicin to improve visualization by confocal microscopy as described in the Materials and Methods section with readjusted laser settings for optimized visualization. The left column depict the distribution of epirubicin (red). The middle column shows the corresponding bright field images, and the final column of images on the right is the corresponding overlay, clearly showing a lack of nuclear fluorescence as well as the striking amount of perinuclear epirubicin.

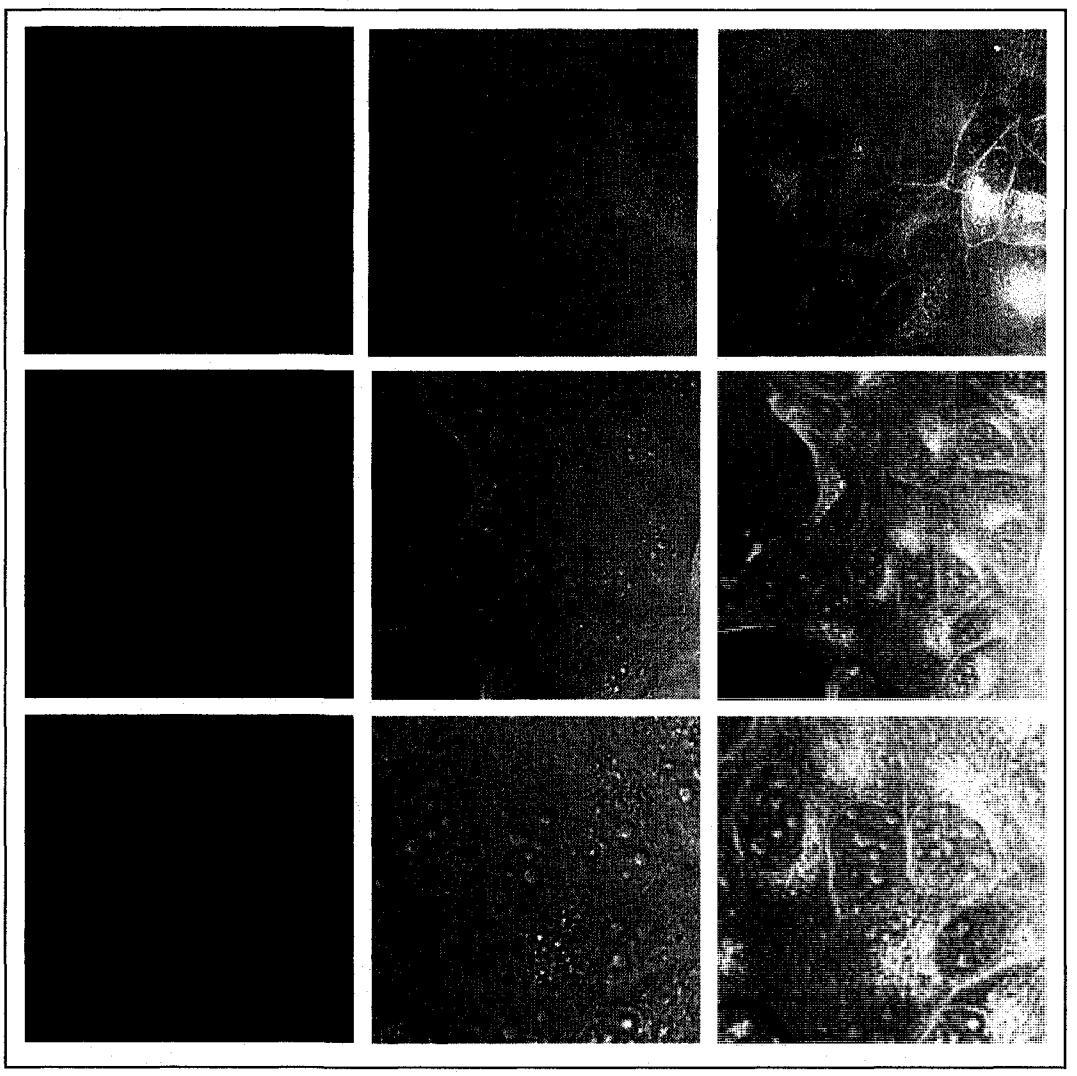

localization defect of epirubicin, which persisted even in cells selected at dose 12 (Figure 3.3-3.4).

3.2.4 Quantification of Nuclear Fluorescence in MCF-7_{WT}, MCF-7_{DOX}, MCF-7_{EPI}

In order to provide quantitative evidence for the apparent differences amongst the resistant cell lines in anthracycline localization, the above experiments were repeated to obtain a sufficient number of images in order to accurately quantify the percentage of cells with or without nuclear epirubicin. Table 3.0 and Figure 3.5 depict the cumulative data from three independent experiments for each cell line. Both the MCF-7_{WT} and MCF-7_{DOX} cell lines had the highest percentage of cells exhibiting nuclear localization of epirubicin, which peaked at 4 hours. The percent of cells at a given time point with nuclear epirubicin ranged from 95 to 99.7% for MCF-7_{WT} and MCF-7_{DOX} cell selected to dose 10. The MCF-7_{EPI} cells had a significantly lower percentage of cells with nuclear epirubicin ($p=0.005$). The percentages of cells with nuclear epirubicin were 62.8%, 52.1% and 37.1% at 1, 4 and 8 hours after the addition of drug respectively.

3.2.5 Comparison of Nuclear Cytoplasmic Ratios

We also assessed by confocal microscopy the ratio of epirubicin fluorescence distribution between the nucleus and cytoplasm of cells. The number of cells assessed in these experiments per time point ranged from 150 to 230. As shown in Figure 3.6, the nuclear cytoplasmic ratio for each of the cell lines was averaged for each time point. The nuclear cytoplasmic ratios for both the MCF-7_{WT} and MCF-7_{DOX} were both over 1.0. The average N/C ratios for the MCF-7_{WT} cells ranged 1.29 ± 0.01 to 2.02 ± 0.01, and the average

Figure 3.3: Epirubicin localization in dose 8, 9, 10 and 12 MCF-7_{WT} cells.

These images represent MCF-7_{WT} from selected doses 8, 9, 10 and 12 incubated with circulating media containing 10 μM epirubicin for 1, 4, and 8 hours. Images were collected using confocal microscopy as described in Materials and Methods section. The co-cultured control cell lines from each dose selection exhibited a predominatly nuclear localization of epirubicin with comparable total fluorescence intensities as seen after 4 and 8 hours. No apparent changes were observed between any of the MCF-7_{WT} from each dose.

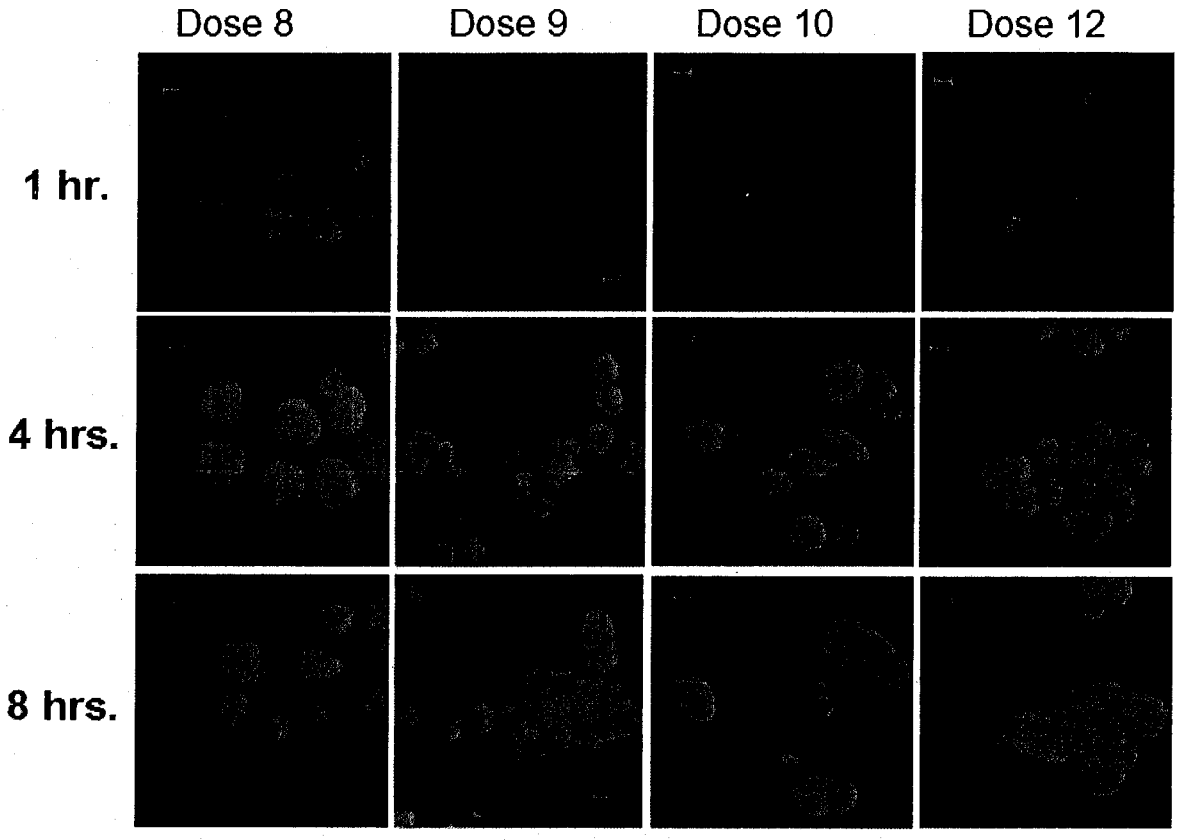
Dose 8
Dose 9
Dose 10
Dose 12
1 hr.
4 hrs.
8 hrs.

Figure 3.4: Epirubicin localization in dose 8, 9, 10 and 12 MCF-7_{EPI} cells.

These images represent MCF-7_{EPI} from selected doses 8, 9, 10 and 12 incubated with circulating media containing 10 μM (20 μM for localization in dose 12 cells) epirubicin for 1, 4, and 8 hours. Images were collected using confocal microscopy as described in Materials and Methods section. MCF-7_{EPI} cells selected at dose 8, show similar levels of fluorescence as observed in the co-cultured MCF-7_{WT}. However, the MCF-7_{EPI} cells selected at dose 9, also the threshold for resistance, show a decrease in epirubicin fluorescence as well as decreased nuclear epirubicin. The nuclear localization defect was also present in the cells selected at dose 10 (as previously described) and dose 12.

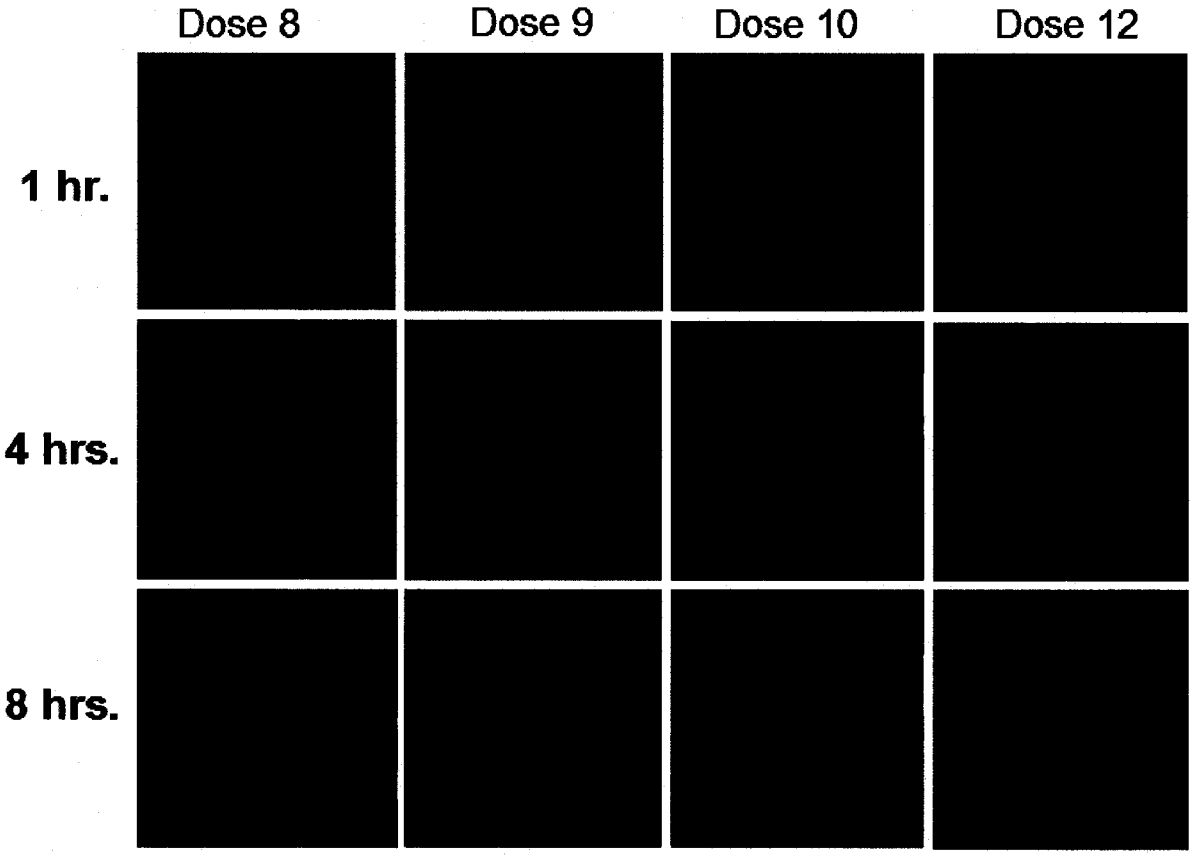
Dose 8
Dose 9
Dose 10
Dose 12
1 hr.
4 hrs.
8 hrs.

Table 3.0 Percentage of Cells with Nuclear Epirubicin

Cell Line or Inhibitor Used	*Duration (hrs.)*	*% of cells with nuclear epirubicin*			*Mean*	*Standard Error (±)*
		Trial 1	*Trial 2*	*Trial 3*		
$MCF\text{-}7_{WT}$	0.5	100	100	96.32	98.77	1.22
	4	100	98.41	100	99.47	0.53
	8	97.08	88.30	99.48	94.95	3.40
$MCF\text{-}7_{DOX}$	0.5	99.23	100	99.27	99.50	0.25
	4	98.85	99.75	99.57	99.39	0.28
	8	100	99.70	99.28	99.66	0.21
$MCF\text{-}7_{EPI}$	0.5	50.58	69.17	68.78	62.84	6.13
	4	36.65	54.38	65.24	52.09	8.33
	8	40.28	35.68	35.25	37.07	1.61
$MCF\text{-}7_{EPI}$ With 60min of Cyclosporin A (1uM)	0.5	86.9	79.9	77.9	81.6	2.73
	4	66.2	56.6	61.2	61.3	2.77
	8	49.2	47.6	44.3	47.0	1.44
$MCF\text{-}7_{EPI}$ With 60min of Cyclosporin A (5uM)	0.5	67.6	85.5	81.2	78.1	5.39
	4	54.5	64.5	64.7	61.2	3.36
	8	40.3	41.3	43.8	41.8	1.04
$MCF\text{-}7_{EPI}$ With 30min of Bafilomycin A1 (500nM)	0.5	73.6	83.7	81.4	79.6	3.06
	4	51.4	61.2	36.5	49.7	7.18
	8	33.1	31.9	16.8	27.7	5.24

Figure 3.5: Comparison of the percentage of cells with nuclear epirubicin.

The graph is a representation of 3 trials of 20 μM epirubicin localization experiments of MCF-7_{DOX}, MCF-7_{EPI} and MCF-7_{WT} selected to dose 10 by which 20 random images were taken at each time point using confocal microscopy and individually quantified for the percentage of cells with nuclear fluorescence. The MCF-7_{EPI} cells showed the lowest percentage of cells with nuclear fluorescence compared to MCF-7_{WT} and MCF-7_{DOX}. In addition, 1 and 5 μM concentrations of cyclosporin A as well as 500 nM of the vacuolar H^+ ATPase inhibitor, bafilomycin A1 were individually co-incubated with 20 μM epirubicin to determine their effects on the localization of epirubicin as described in Materials and Methods. Both inhibitors showed no significant effect on the percentage of MCF-7_{EPI} cells with nuclear epirubicin during the 8 hour time course.

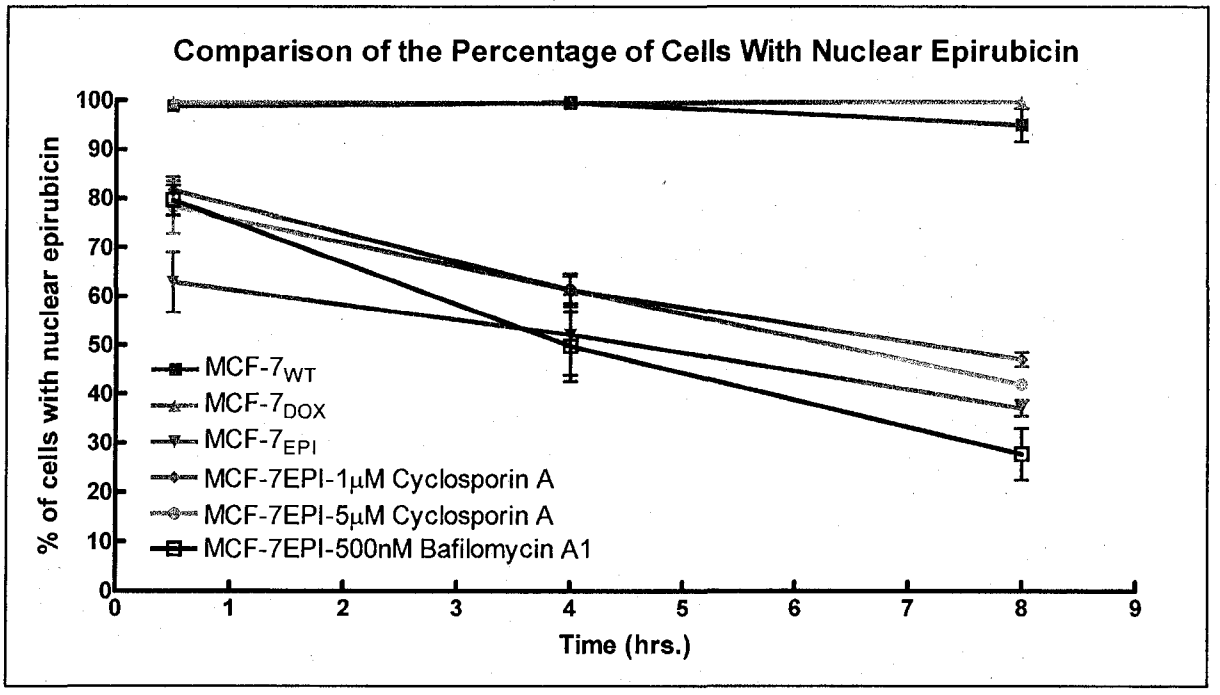
Comparison of the Percentage of Cells With Nuclear Epirubicin
% of cells with nuclear epirubicin
100
90
80
70
60
50
40
30
20
10
0
0
1
2
3
4
5
6
7
8
9
Time (hrs.)
MCF-7WT
MCF-7DOX
MCF-7EPI
MCF-7EPI-1μM Cyclosporin A
MCF-7EPI-5μM Cyclosporin A
MCF-7EPI-500nM Bafilomycin A1

Figure 3.6: Comparison of the nuclear cytoplasmic ratios of epirubicin localization in anthracycline resistant cell lines with MCF-7_{WT}.

These localization experiments were performed by optimizing the confocal settings for the 8 hour time point of each cell line MCF-7_{DOX}, MCF-7_{EPI} and MCF-7_{WT}, in order to properly assess the change in the nuclear cytoplasmic ratio of epirubicin distribution over an 8 hour time period. All cells were incubated with media containing 20 μM epirubicin. At each time point, 5 random images were taken using confocal microscopy as described in Materials and Methods. Ratios were determined using the 510 Meta confocal imaging program. The graph clearly displays the decreased nuclear cytoplasmic ratio of epirubicin distribution in the MCF-7_{EPI} cells compared the MCF-7_{DOX} and MCF-7_{WT}. The image on the right displays how each individual cell in a field was quantified for the total fluorescence in the nucleus, compared to the total fluorescence in the cytoplasm.

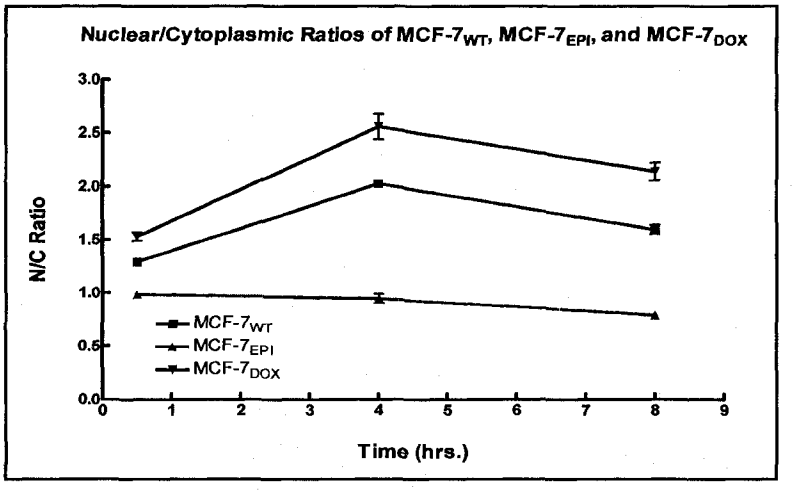
Nuclear/Cytoplasmic Ratios of MCF-7WT, MCF-7EPI, and MCF-7DOX
N/C Ratio
3.0
2.5
2.0
1.5
1.0
0.5
0.0
0
1
2
3
4
5
6
7
8
9
MCF-7WT
MCF-7EPI
MCF-7DOX
Time (hrs.)

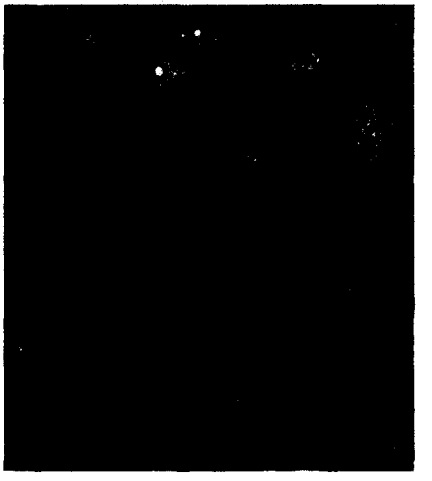

N/C ratios for the MCF-7_{DOX} cells ranged from 1.53 ± 0.07 to 2.56 ± 0.21. In contrast, the MCF-7_{EPI} cells had average N/C ratios which ranged from 0.79 ± 0.03 to 0.94 ± 0.07 (Table 3.1). The scattergraph (Figure 3.7) displays the entire data set, and depicts that the population of MCF-7_{EPI} cells generally has lower N/C ratios (significantly lower, p=0.001), while the MCF-7_{DOX} and MCF-7_{WT} cells both have a large number of their populations in the same higher range of N/C ratios.

Figure 3.7: Comparison of the population distribution of nuclear cytoplasmic ratios of epirubicin localization in anthracycline resistant cell lines with MCF-7_{WT}.

The following series of graphs were generated using the same data set used to produce Figure 3.6. However, instead of showing the mean N/C ratio at each time point for each cell line, this figure depicts the entire population distribution for each of the three cell lines. The population shifted to lower N/C ratios when comparing the MCF-7_{EPI} cells to the MCF-7_{DOX} and MCF-7_{WT}.

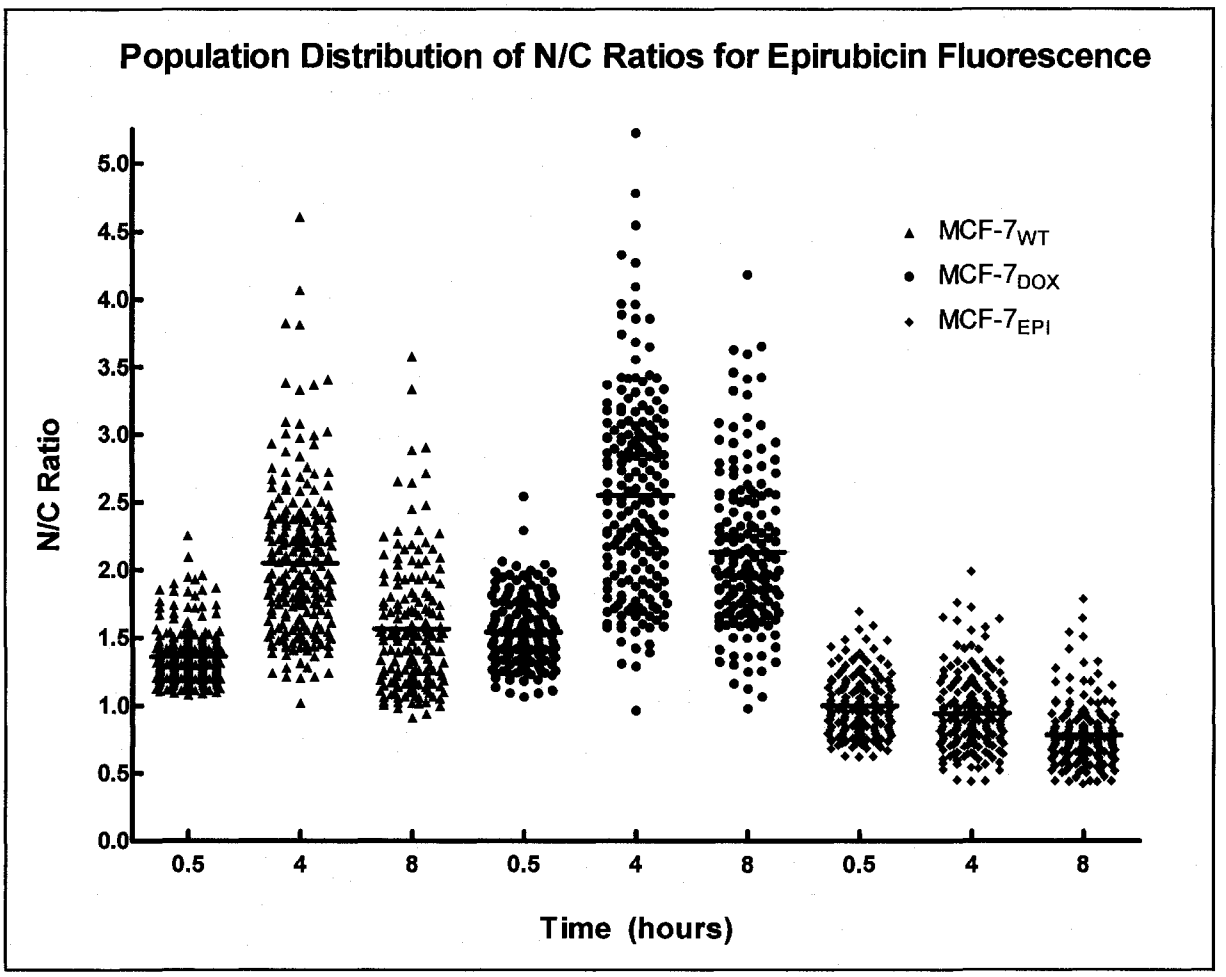
Population Distribution of N/C Ratios for Epirubicin Fluorescence
N/C Ratio
5.0
4.5
4.0
3.5
3.0
2.5
2.0
1.5
1.0
0.5
0.0
0.5
4
8
0.5
4
8
0.5
4
8
Time (hours)
MCF-7WT
MCF-7DOX
MCF-7EPI

Table 3.1 Nuclear/Cytoplasmic Ratios of Epirubicin Distribution

Cell Line	Duration (hrs.)	N/C Ratio of epirubicin distribution			Mean	Standard Error (±)
		Trial 1	Trial 2	Trial 3		
$MCF\text{-}7_{WT}$	0.5	1.273	1.301	1.296	1.290	0.009
	4	2.014	2.032	2.025	2.024	0.005
	8	1.640	1.510	1.636	1.595	0.043
$MCF\text{-}7_{DOX}$	0.5	1.449	1.595	1.551	1.532	0.043
	4	2.336	2.742	2.590	2.556	0.118
	8	2.300	2.090	2.026	2.139	0.083
$MCF\text{-}7_{EPI}$	0.5	0.942	1.055	0.955	0.984	0.036
	4	0.924	0.884	1.028	0.945	0.043
	8	0.761	0.821	0.791	0.791	0.017

3.3 Co-localization of Cellular Organelles with Epirubicin

To determine the cellular location of epirubicin, several organelle-specific strains were added to cells along with epirubicin.

3.3.1 Co-localization of Epirubicin with Lysosomes

When comparing $MCF\text{-}7_{EPI}$ cells with co-cultured control $MCF\text{-}7_{WT}$ cells after staining with lysotracker, it was observed that lysosomes concentrated in the perinuclear region compared to the more randomly distributed packets of fluorescence in the cytoplasm of the $MCF\text{-}7_{WT}$ cells (Figure 3.8). It is important to note that this difference in lysosome organization is present prior to incubation with epirubicin. Furthermore, when $MCF\text{-}7_{EPI}$ cells were incubated with both epirubicin and lysotracker, the green fluorescence from

3.8: Co-localization of lysosomes and epirubicin.

The first column of images on the left was the result of 100 nM lysotracker incubation in MCF-7_{WT} and MCF-7_{EPI} cells in the absence of epirubicin . The lysosomes of the MCF-7_{WT} cells were more randomly distributed compared to the perinuclear accumulation of lysosomes within the cytoplasm of the MCF-7_{EPI} cells (represented by green fluorescence). MCF-7_{WT} and MCF-7_{EPI} cells treated with 20 μM epirubicin for 7 hours and co-incubated with 100 nM lysotracker for 1 hour using the FCS2 system and images were acquired using the confocal microscope as described in Materials and Methods. The lysosomes observed in green, co-localize with the red fluorescence from epirubicin in the MCF-7_{EPI} cells to produce a yellow signal (see arrows). There was no significant co-localization observed in the MCF-7_{WT} cells.

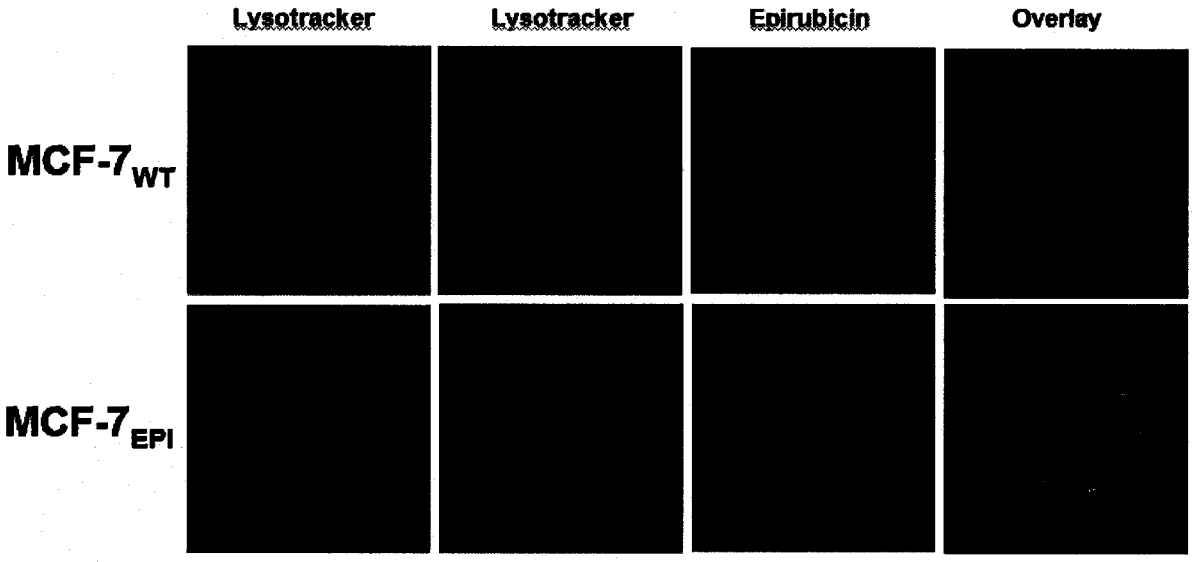
Lysotracker
Lysotracker
Epirubicin
Overlay
MCF-7WT
MCF-7EPI

Lysotracker and the red fluorescence from epirubicin localized in the same intracellular region to produce a yellow signal indicative of co-localization. It is important to note that only a fraction of the lysosomes co-localized with the epirubicin (Figure 3.8).

3.3.2 Lack of Co-localization of Epirubicin with Recycling Endosomes

Bodipy Transferrin labeling of the recycling endosomes showed diffuse plasma membrane and cytoplasmic green fluorescence in both MCF-7_{EPI} and MCF-7_{WT}. There was no co-localization between the recycling endosomes and epirubicin. Moreover, both the MCF-7_{WT} and MCF-7_{EPI} cells have similar localization patterns for the recycling endosomes. The majority of the fluorescence was found in proximity to the plasma membrane (Figure 3.9).

3.3.3 Lack of Co-localization of Epirubicin with Trans-golgi Network

NBD Ceramide, which also fluoresces green, was also observed in the perinuclear region of both MCF-7_{EPI} and MCF-7_{WT} dose 10 cells. In general, both epirubicin and the trans-golgi network had signals in the same region of the cells; however, regions of drug did not exhibit a yellow colour when both the red- and green-fluorescing images were merged, suggesting a lack of colocalization of epirubicin with a trans-golgi specific protein (Figure 3.10).

3.3.4 Lack of Co-localization of Epirubicin with Golgi Bodies

Similar to the NBD ceramide labeling, the golgi bodies were labeled with bodipy ceramide and were located in the perinuclear region. When both MCF-7_{EPI} and MCF-7_{WT} were labeled with only bodipy ceramide, the labeling pattern was identical. Although

Figure 3.9: Lack of co-localization of recycling endosomes and epirubicin.

The first column of images on the left was the result of 50 μg/mL bodipy transferrin incubation in MCF-7_{WT} and MCF-7_{EPI} cells in the absence of epirubicin. Recycling endosome localization were similar in both cell lines. MCF-7_{WT} and MCF-7_{EPI} (row A and B respectively) cells treated with 20 μM epirubicin for 7 hours and co-incubated with 50 μg/mL bodipy transferrin for 1 hour. The recycling endosomes were randomly distributed in proximity to the plasma membrane and did not co-localize with epirubicin (red) in both cell lines as the green and red signals to not appear to overlap in the same cellular regions.

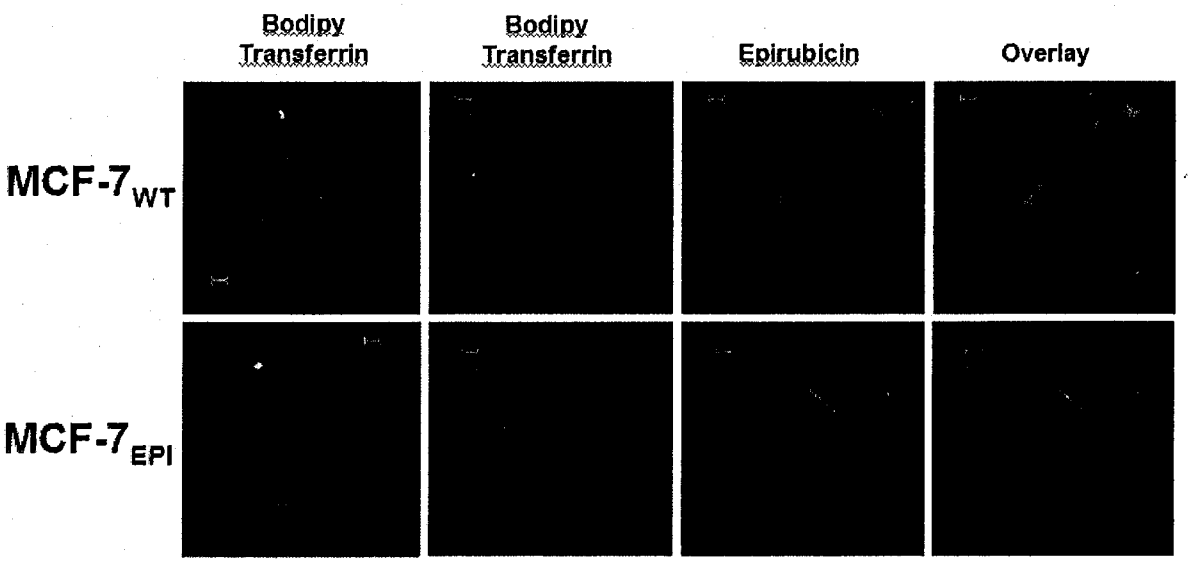
Bodipy Transferrin
Bodipy Transferrin
Epirubicin
Overlay
MCF-7WT
MCF-7EPI

Figure 3.10: Lack of co-localization of TGN and epirubicin.

$MCF\text{-}7_{WT}$ and $MCF\text{-}7_{EPI}$ (row A and B respectively) cells treated with 20 μM epirubicin for 7 hours and co-incubated with 100 nM NBD ceramide an additional hour. The trans-golgi network (green) was randomly distributed in the perinuclear region in both cell lines. Epirubicin did not localize with the trans-golgi network in the co-cultured control $MCF\text{-}7_{WT}$, whereas, in the $MCF\text{-}7_{EPI}$ cells, although the signals appear in approximately the same area of the cells, there is no discernable yellow co-localization signal produced.

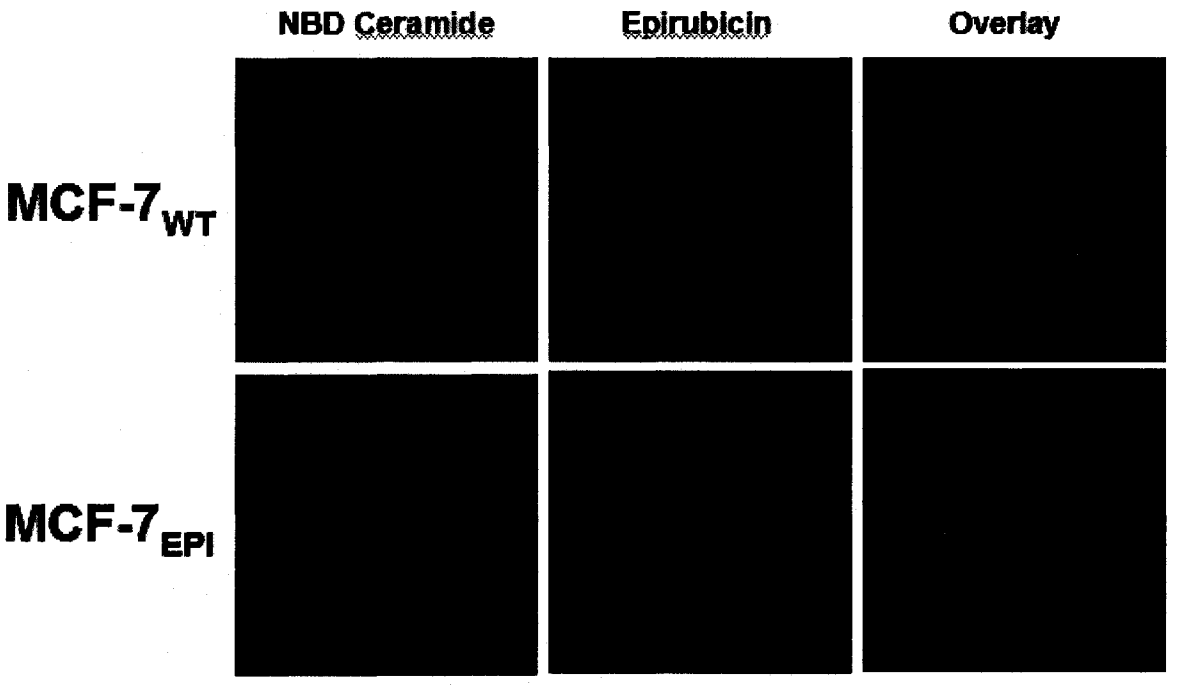
NBD Ceramide
Epirubicin
Overlay
MCF-7WT
MCF-7EPI

epirubicin fluorescence was still located in a perinuclear region similar to that of the bodipy ceramide, there was no apparent co-localization of the two fluorescent signals (Figure 3.11).

3.4 Localization of ABCB1 in MCF-7_{EPI} cells

Previous studies have shown that ABCB1 can be localized to acidic vesicles where it may play a role in drug transport into these vesicles (Rajagopal and Simon, 2003). To determine the location of ABCB1 in cells immunofluorescence microscopy was performed using antibodies specific for ABCB1. The co-cultured MCF-7_{WT} cells showed some minor expression of ABCB1 (Figure 3.12 B). A second negative control, MCF-7_{DOX} (Figure 3.12 C), also showed similar levels of ABCB1 expression as the co-cultured control. The ABCB1 antibody was found to localize and concentrate near or within the plasma membrane of MCF-7_{EPI} cells (Figure 3.12 D-F) with the greatest fluorescence intensity compared to the MCF-7_{WT} and MCF-7_{DOX} cells (Figure 3.12). Furthermore, in the MCF-7_{EPI} cells, in addition to the diffuse cytoplasmic distribution of the ABCB1 antibody, the perinuclear region of many cells consisted of concentrations of ABCB1. Although these pools of green fluorescence had a weaker signal than that of the plasma membrane staining, the fluorescence intensity was far greater than the rest of the cytoplasm and background fluorescence (Figure 3.12 E-F).

3.5. Inhibition of Cellular Transport Mechanisms

All data presented are the cumulative results of three independent trials for each cell line.

Figure 3.11: Lack of co-localization of golgi and epirubicin.

The first column of images on the left was the result of 100 nM bodipy ceramide incubation in MCF-7_{WT} and MCF-7_{EPI} cells in the absence of epirubicin showing perinuclear localization of the golgi bodies. MCF-7_{EPI} and MCF-7_{WT} cells treated with epirubicin for 7 hours and co-incubated with 100 nM bodipy ceramide for an additional hour. Epirubicin did not localize with the golgi apparatus in the co-cultured control MCF-7_{WT} (top panel of images), whereas, in the MCF-7_{EPI} cells, although the signals appear in approximately the same area of the cells, there is no discernable yellow co-localization signal produced (overlay image).

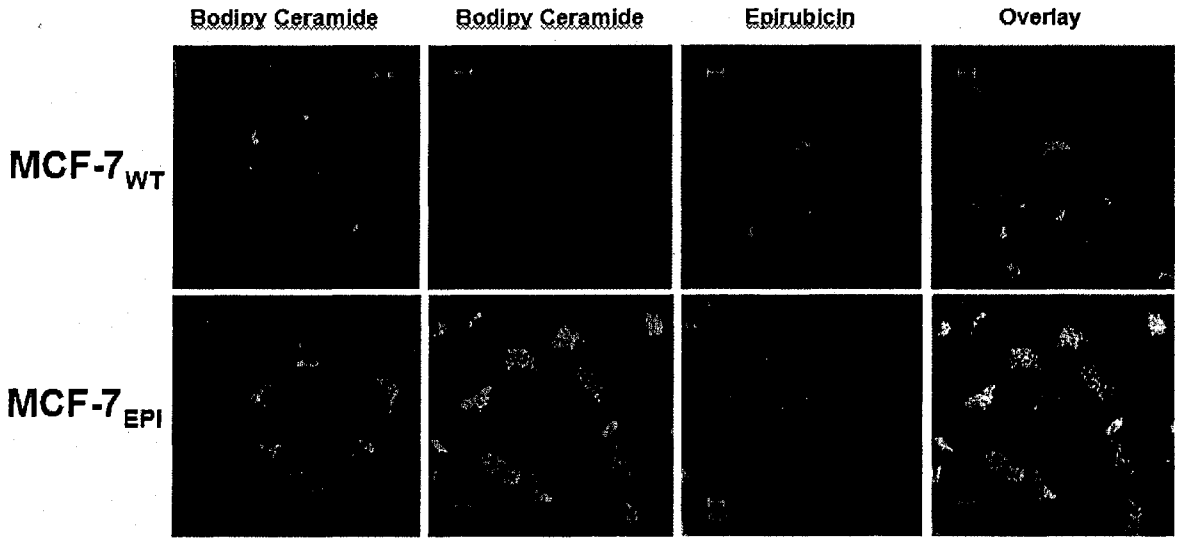
Bodipy Ceramide
Bodipy Ceramide
Epirubicin
Overlay
MCF-7WT
MCF-7EPI

Figure 3.12: MM4.17 clone ABCB1 antibody staining.

MCF-7_{EPI} cells are grown on glass coverslips and permeabilized using Triton X-100 prior to treating cells with antibody as described in Materials and Methods. Localization of the ABCB1 transporter was achieved using an ABCB1 primary antibody and FITC secondary antibody staining in MCF-7_{WT}, MCF-7_{DOX}, and MCF-7_{EPI} (panels b-d respectively). The co-cultured control and MCF-7_{DOX} show similar levels of ABCB1 expression, whereas the MCF-7_{EPI} showed intense amounts of fluorescence suggesting the presence of ABCB1 in the plasma membrane, in addition, some perinuclear ABCB1 can be observed (panels e-f). Interestingly, no nuclear envelope ABCB1 was observed in any of these cell lines. (a) Primary antibody omission control.

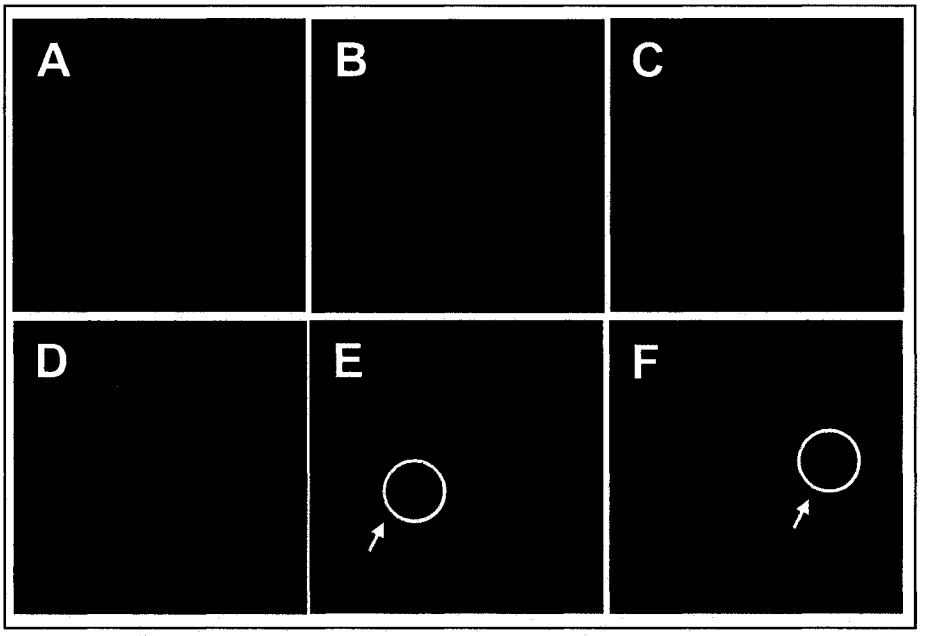
A
B
C
D
E
F

3.5.1 Effect of Valspodar on Epirubicin Localization

Past studies have shown possible links between intracellular p-glycoprotein and sequestration into vesicles (Rajagopal and Simon, 2003). There did not appear to be any change in the localization of 20 μM epirubicin at 1, 4 and 8 hours when MCF-7_{EPI} cells were pre-incubated with 2 μM Valspodar for 1 hour (ABCB1 inhibitor). The same settings that were used for the 20 μM epirubicin localization experiments were applied. The total cellular fluorescence of these cells was comparable to cell treated with only epirubicin (Figure 3.13).

3.5.2 Effect of Cyclosporin A on Epirubicin Localization

Evidence in the literature suggests other ABC drug transporters may play a role in the localization of anthracyclines by transporting them outside of the nucleus or by sequestration by pumping them into vesicles (Rajagopal and Simon, 2003). We thus examine the effect of a pan ABC drug transport inhibitor (also known to inhibit LRP), Cyclosporin A (Qadir *et al.*, 2005) on the localization of epirubicin in cells. When MCF-7_{EPI} cells selected to dose 10 were pre-incubated with 1 μM or 5 μM Cyclosporin A (Figure 3.13), no apparent changes occurred in the localization of epirubicin. These results were further confirmed quantitively by computing the percentage of cells with nuclear epirubicin in both MCF-7_{WT} and MCF-7_{EPI} cells selected to dose 10. There were no statistically significant differences in the localization of epirubicin in either cell line in the absence or presence of Cyclosporin A (p values comparing with no inhibitors vs. with cyclosporin A was p=0.14).

Figure 3.13: The effect of ABC transport inhibitors on the localization of epirubicin.

Cells were grown on glass coverslips and localization was monitored using confocal microscopy as described in Materials and Methods. The localization of 20 μM of epirubicin was observed over 8 hours in MCF-7_{EPI} cells selected to dose 10 pre-incubated with either the 2 μM valspodar (an inhibitor of ABCB1) or cyclsoporin A (a pan ABC transporter inhibitor and also inhibits the major vault protein, LRP (Qadir, M. 2005) (1 and 5 μM concentrations). No distinct differences were observed in the localization of epirubicin upon the addition of either inhibitor.

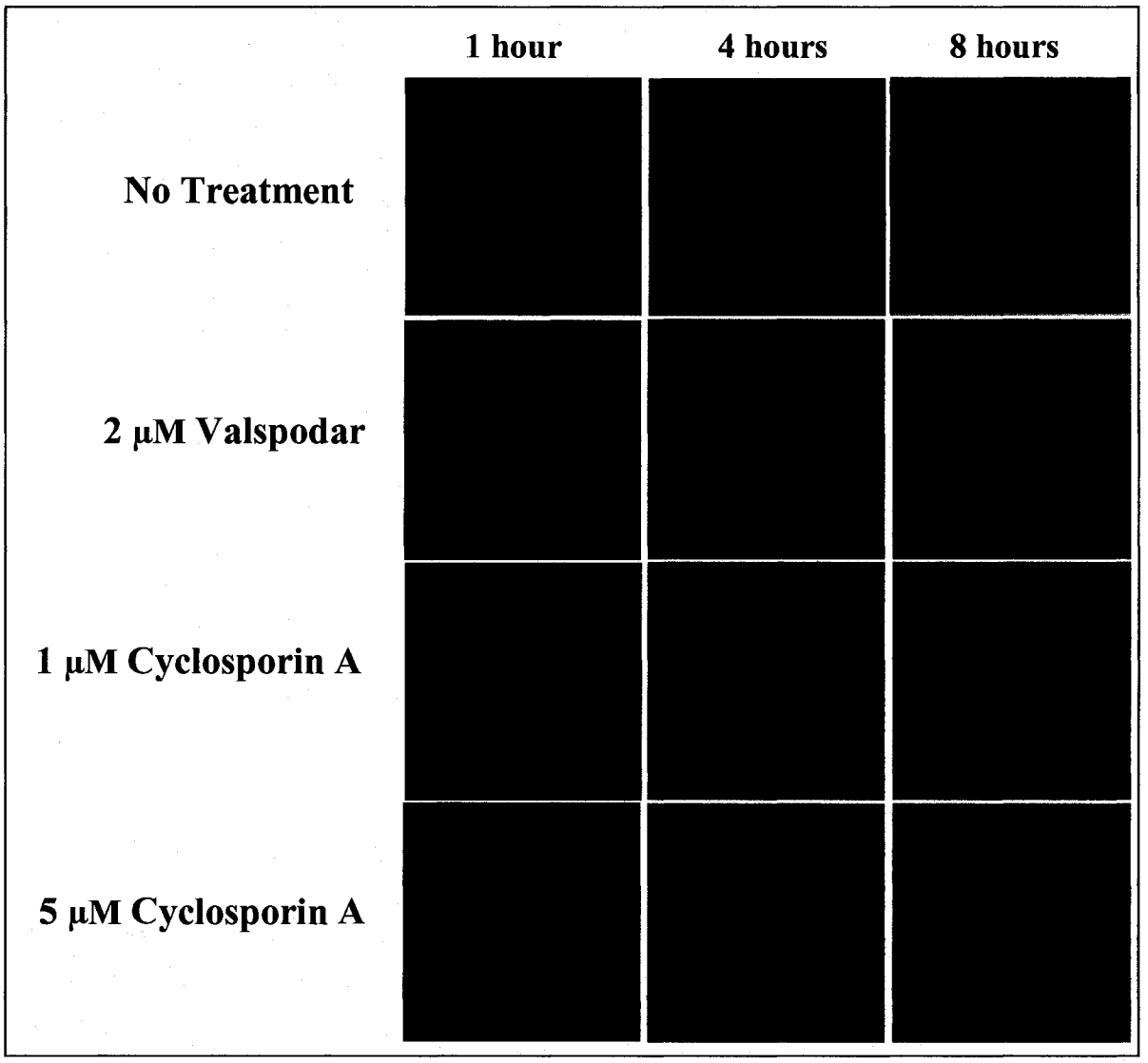
1 hour
4 hours
8 hours
No Treatment
2 μM Valspodar
1 μM Cyclosporin A
5 μM Cyclosporin A

3.6 Identification of Acidified Vesicles

Acridine orange is known to bind to DNA and RNA as well as other cellular constituents. Its fluorescence changes from green to red in acidic environments (Altan *et al.*, 1998). This stain can thus be used to identify the presence of acidic vesicles which have been proposed to play a role in drug resistance by permitting anthracyclines to be "locked" in these vesicles where they no longer can bind to nuclear DNA. As shown in Figure 3.14, acridine orange stained the entire cell for both MCF-7_{WT} and MCF-7_{EPI} cells selected to dose 10. The co-cultured cell line MCF-7_{WT} served as a control to identify the location of acidic vesicles in a drug sensitive cell line. Acridine orange stained the nucleus and other subcellular structures with a green colour. However, both the drug sensitive and drug-resistant cells showed punctuate red fluorescence within the cytoplasm indicative of acidic vesicles. The percentage of cells that had acidified staining was not statistically different ($p=0.49$) between the two cell lines (MCF-7_{WT} 56.1 ± 8.0 % and MCF-7_{EPI} 47.2 ± 18.8 % (Table 3.2). Moreover, when comparing the MCF-7_{EPI} cells with the co-cultured control MCF-7_{WT} cells, the pattern of red fluorescence when cells were stained with acridine orange was also quite similar.

Table 3.2: Comparison of organelle acidification in MCF-7_{WT} and MCF-7_{EPI}

Cell Line	% of cells with acidic vesicles			Mean	Standard Error
	Trial 1	Trial 2	Trial 3		
MCF-7_{WT}	57.6	58.4	25.5	47.2	10.8
MCF-7_{EPI}	48.2	64.2	55.9	56.1	4.6

Figure 3.14: Comparison of acridine orange staining in MCF-7_{WT} and MCF-7_{EPI} with or without treatment of inhibitor, Bafilomycin A1.

MCF-7_{EPI} cells grown on square coverslips were washed with PBS, stained with 5 μg/mL acridine orange for 5 minutes, placed on microscope slides, sealed and visualized using excitation wavelength 488 nm and 543 nm as described in Materials and Methods. Both the epirubicin resistant cell line and the co-cultured drug-sensitive control showed similar amounts and distribution of acidified vesicles seen represented by orange fluorescence. Green fluorescence indicates where acridine orange has stained DNA, RNA and other cell cellular constituents. Upon preincubation of MCF-7_{EPI} cells with 500 nM of Bafilomycin A1 for 30 minutes, the prescence of acidified vesicles was abolished in both cell lines as seen with the lack of distinguishable orange fluorescence.

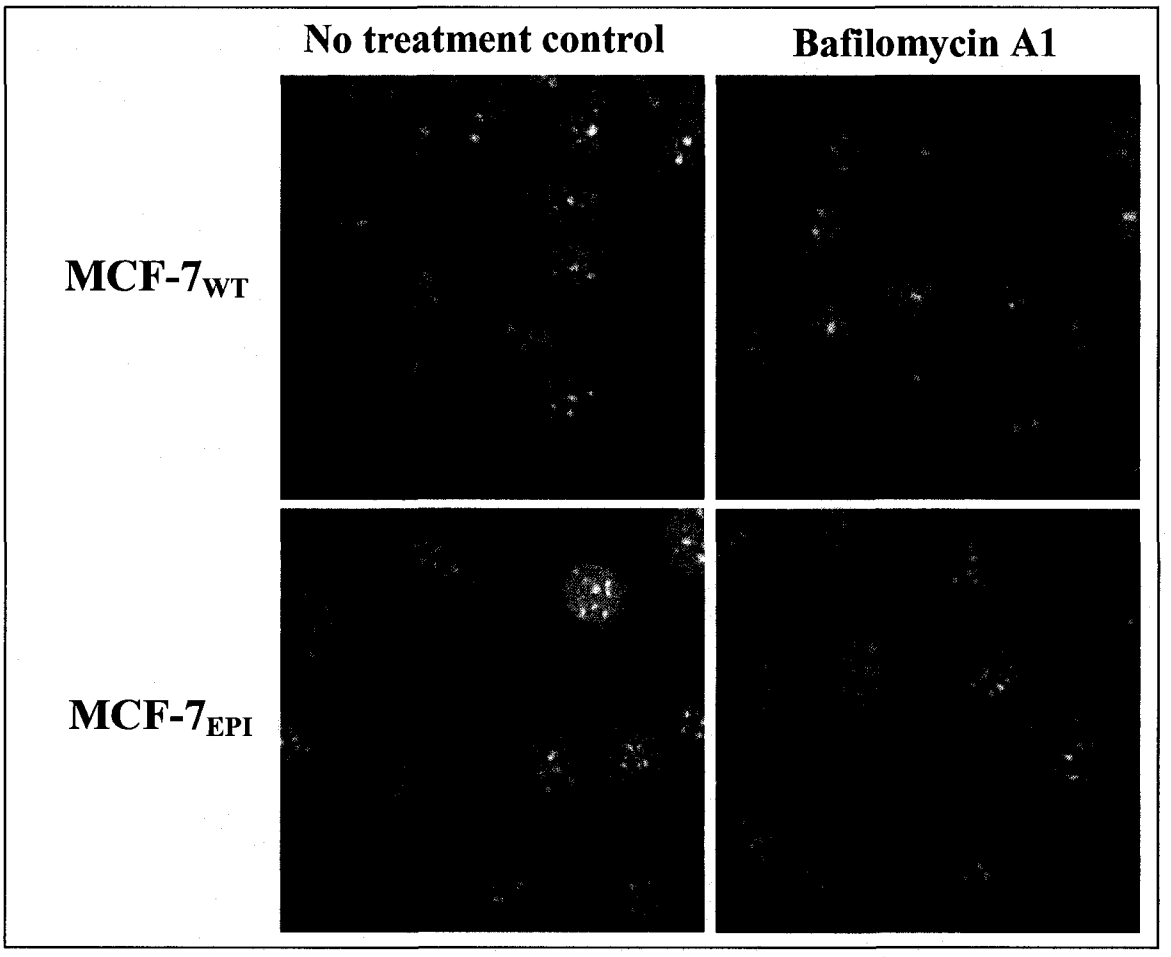
No treatment control
Bafilomycin A1
MCF-7WT
MCF-7EPI

3.6.1 Effect of Bafilomycin A1 on Acridine Orange Staining

Should the red-staining vesicles identified by the addition of acridine orange be acidic vesicles, then the addition of bafilomycin (an inhibitor of vacuolar H+ATPase, thus inhibiting vesicle acidification (Paglin *et al.*, 2001) should eliminate the presence of punctuate red cytoplasmic staining. The 30 minute pre-incubation of both MCF-7_{WT} and MCF-7_{EPI} cell lines yielded a substantial and in most cells a complete loss of red acridine orange staining (Figure 3.14). Within this experiment, the negative control (vehicle without agent) had no effect on the punctuate red cytoplasmic staining observed in MCF-7_{WT} and MCF-7_{EPI} cells.

3.6.2 Effect of Bafilomycin A1 on the Localization of Epirubicin

Since the MCF-7_{EPI} cells were positive for acidified vesicles, bafilomycin was pre-incubated with cells in order to assess whether neutralization of vesicles restores epirubicin localization to the nucleus. MCF-7_{EPI} cells pre-incubated for 30 minutes with 500 nM Bafilomycin A1 did not exhibit a change in the localization of 20 μM Epirubicin (Figure 3.15). The total cellular fluorescence also remained unchanged compared to MCF-7_{EPI} cells incubated with epirubicin only, suggesting that total uptake of epirubicin into MCF-7_{EPI} cells was also unchanged and that there was no redistribution of the perinuclear punctuate fluorescence observed.

Previous experiments required the application of bafilomycin treatment controls since some of the earlier localization experiments using bafilomycin pre-incubation showed an abundance dead cells occurring at 4 and 8 hours such that cell counts for nuclear fluorescence could not be accurately performed. A titration experiment was conducted with

Figure 3.15: Effect of bafilomycin A1 on the epirubicin localization in MCF-7_{EPI}.

The localization of 20 μM of epirubicin was observed over 8 hours in MCF-7_{EPI} cells selected to dose 10 that were pre-incubated with 500 nM bafilomycin A1 for 30 minutes. Compared to MCF-7EPI cells incubated with only 20 μM epirubicin, bafilomycin did not appear to cause any noticeable changes in localization. Although the localization of epirubicin was not restored to the nucleus when incubated with an inhibitor of vesicle acidification, it appears that the cytoplasmic fluorescence is more diffuse in the perinuclear region, compared to the intense punctuate fluorescence observed in cells treated without bafilomycin.

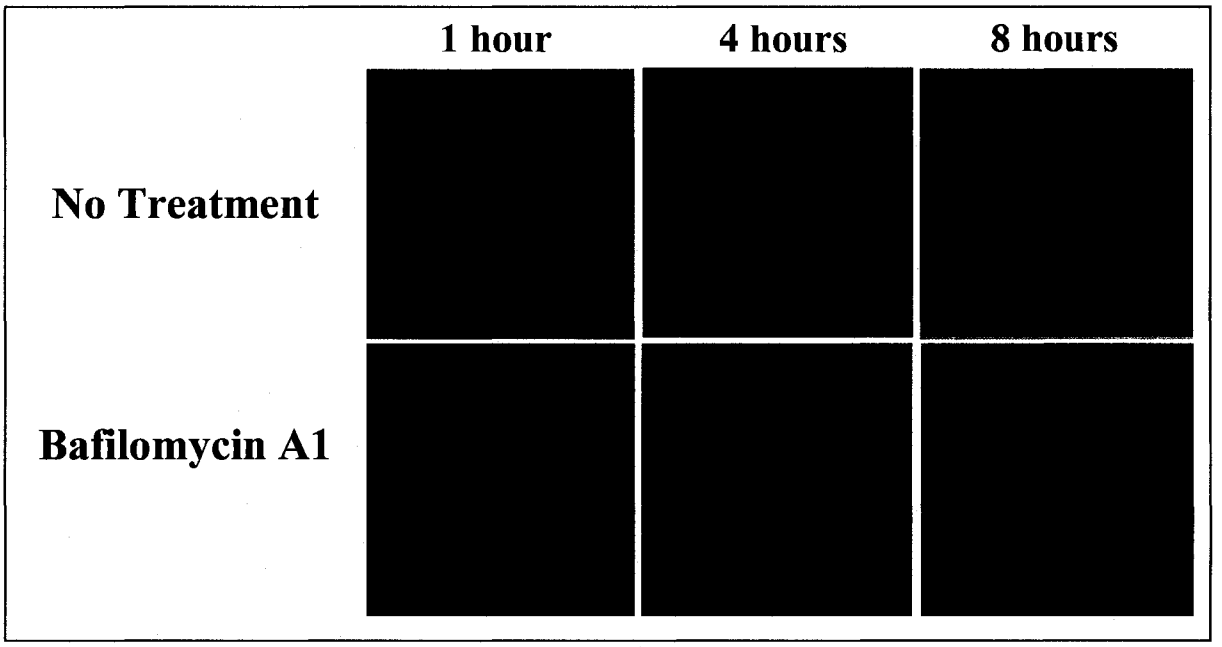
1 hour
4 hours
8 hours
No Treatment
Bafilomycin A1

the diluent, (ethanol) and it was found that 3% ethanol in media was sufficient to cause considerable cell death when incubated with MCF-7_{EPI} cells for 8 hours. In medium containing 1% ethanol, cells appeared of normal fibroblastic and flat morphology. Similarly, 0.5% and 0.25% ethanol in the culture medium did not appear to cause any cell morphology changes compared to untreated controls incubated with media alone (Figure 3.16). When MCF-7_{EPI} cells were incubated (in a tissue culture plate) with 385 nM bafilomycin A1 (in 0.37% ethanol) for 8 hours, no noticeable change in cell morphology was observed. Unfortunately, such experiments indicated that cells (grown on glass coverslips) in medium containing 0.37% ethanol had morphological changes and some cell toxicity.

3.7 Epirubicin Uptake in Dose 10 MCF-7 Cell Lines

As a control for the 10 μM epirubicin localization studies comparing overall fluorescent intensity of epirubicin in each cell line, the amount of epirubicin uptake was observed in dose 10 MCF-7_{WT}, MCF-7_{TAX}, MCF-7_{DOX}, and MCF-7_{EPI}. In order of decreasing epirubicin uptake, MCF-7_{WT}, MCF-7_{DOX}, MCF-7_{TAX} and MCF-7_{EPI} cells also showed a similar trend when comparing the fluorescence profiles with their corresponding confocal microscope images (Figure 3.17). Moreover, these experiments reproduced the same trends observed when only examining the uptake of 2μM epirubicin (see discussion).

Figure 3.16: MCF-7_{EPI} cells incubated with media containing ethanol.

MCF-7_{EPI} cells were grown in 10 cm tissue culture plates. Media was exchanged with media containing 3.3%, 1%, 0.5% and 0.25% ethanol (clockwise A to D respectively) and cells were incubated for 8 hours and examined under a light microscope to visually determine general cell viability to determine the optimal volume of ethanol to prepare a primary stock solution of bafilomycin A1. These results demonstrate that cells incubated for 8 hours with media containing less than 1% ethanol appear to be fibroblastic in nature and there did not appear to be any signs of major cell death. Cells incubated with 3.3% ethanol showed lack of adherence to the tissue culture plates and shrinkage of cells and were likely committed to death.

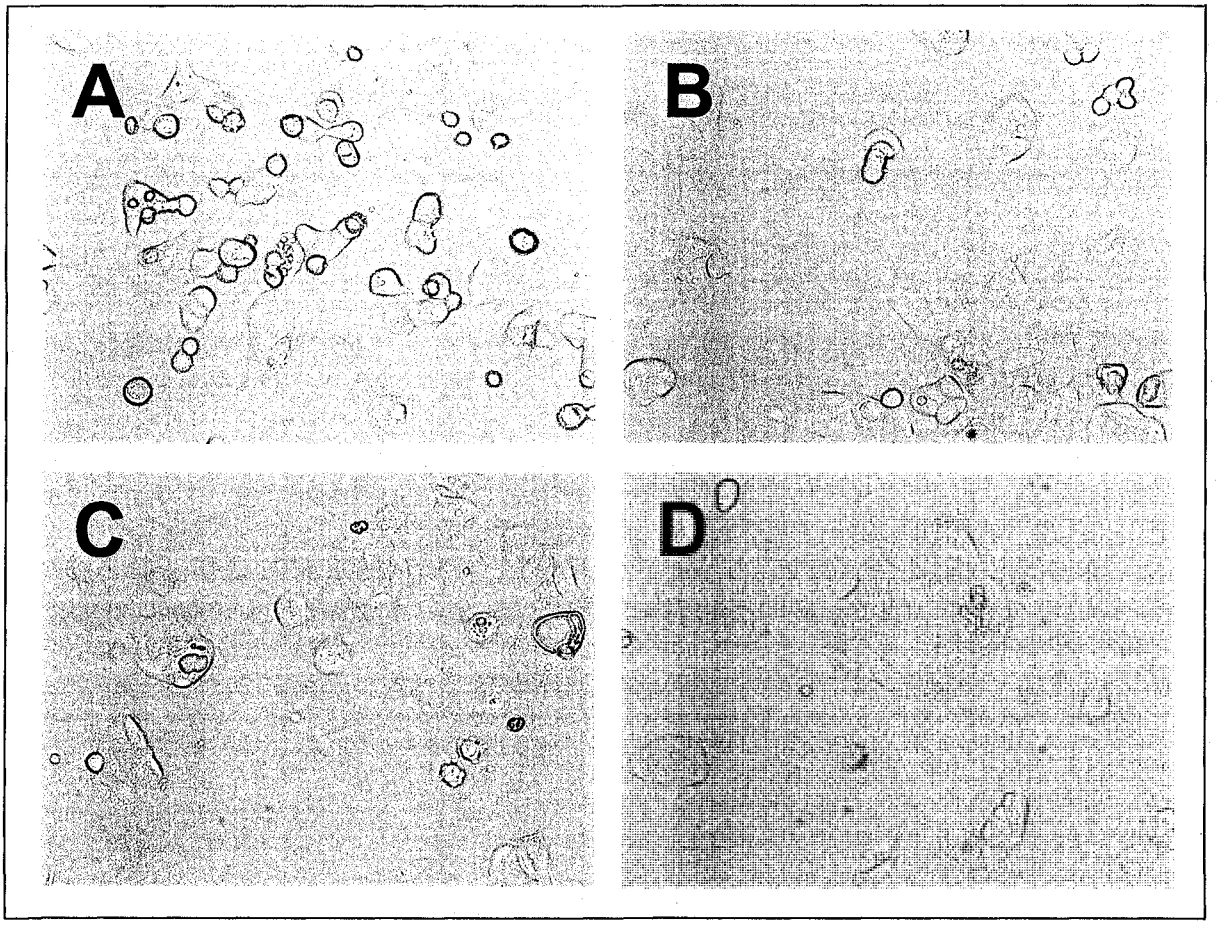
A
B
C
D

Figure 3.17: Comparison of 10uM epirubicin uptake in MCF-7_{WT}, MCF-7_{EPI}, MCF-7_{DOX} and MCF-7_{TAX}.

Cells were grown on 5 cm tissue culture plates for 24 hours, and then incubated with 10 μM epirubicin for 1, 4 and 8 hours. These cells were then trypsinized and analyzed for epirubicin uptake using flow cytometry. The relative uptake of epirubicin in each of the resistant cell lines selected to dose 10 was compared to the MCF-7_{WT} co-cultured control. As seen with the epirubicin localization data, the MCF-7_{EPI} cell line showed the lowest amount of epirubicin uptake.

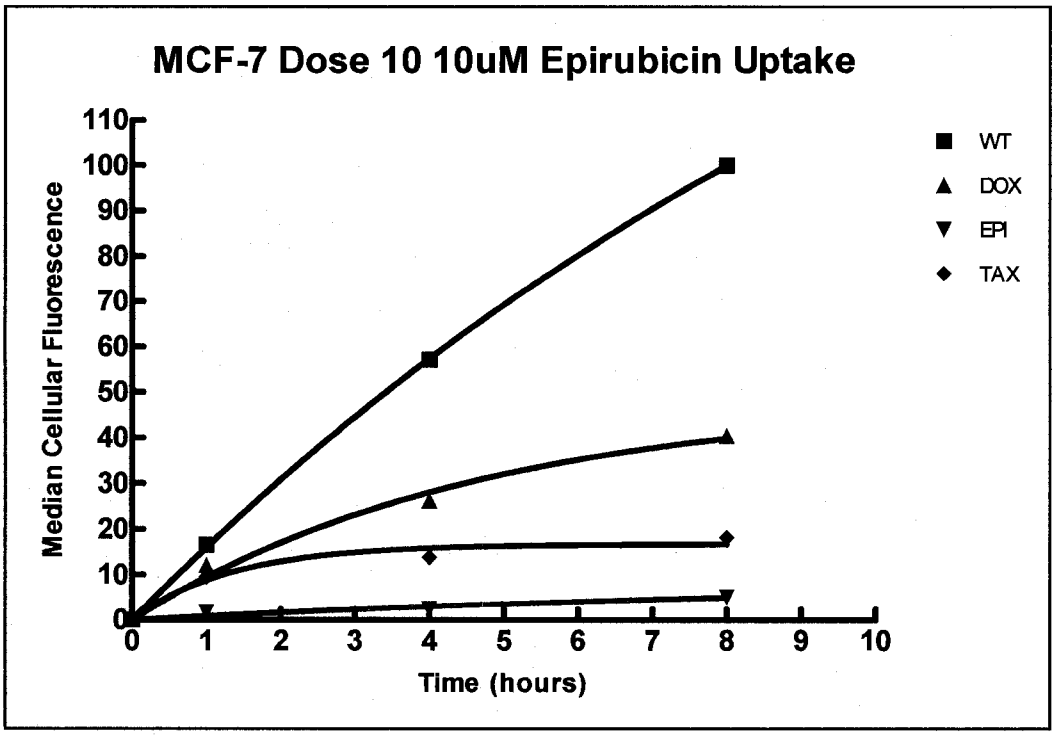
MCF-7 Dose 10 10uM Epirubicin Uptake
Median Cellular Fluorescence
110
100
90
80
70
60
50
40
30
20
10
0
0
1
2
3
4
5
6
7
8
9
10
Time (hours)
WT
DOX
EPI
TAX

4.0 DISCUSSION

Past studies suggest that anthracycline resistance in tumours may stem from reductions in the amount of drug associated with the nucleus (Altan *et al.*, 1998;Featherstone *et al.*, 2005). Studies further suggest that anthracylines in drug-resistant cells are sequestered into acidic vesicles and/or that drug transporters may help facilitate the transport of drugs into acidic or non-acidic vesicles, where they can be excreted by cells through exocytosis. However, there are a number of questions that remain to be addressed with regards to these hypotheses: the study by Altan et. Al. (Altan *et al.*, 1998) compared wild type MCF-7 breast tumour cells to adriamycin-resistant MCF-7 cells, which are now known to be unrelated to MCF-7 and are actually of ovarian origin; it is unclear whether the changes in anthracycline localization can be temporally correlated with the acquisition of anthracycline resistance (relative to other potential mechanisms); it is also not known whether vesicle acidification is critical to drug sequestration and resistance and/or whether drug transporters such as ABCB1 play a role in the transport of drugs into vesicles.

This study addressed these issues and provided significant insight into the role of drug sequestration in anthracycline resistance. In this study we used newly established cell lines consisting of a co-cultured control and four drug resistant cell lines. Furthermore, these resistant cell lines have been proven to be $\geq$ 98.4% isogenicity (Veitch and Parissenti, 2007), thus providing a good model to compare drug-sensitive and drug-resistant cells. Morever, since these cell lines were selected at increasing concentrations of chemotherapeutics, it was possible to determine a temporal relationship between the role of vesicle acidification and establishment of drug resistance. Data from this study suggest that only the epirubicin resistant cell line, MCF-7_{EPI} displayed the most dramatic change in the localization in

anthracyclines, doxorubicin and epirubicin. Moreover, it was determined that as MCF-7 cells acquire resistance to epirubicin between the 8^{th} and 9^{th} selection (Figure 1.4) (Veitch and Parissenti, 2007), they also acquire a change in the localization of epirubicin. Furthermore, uptake studies also show a temporal correlation between the onset of epirubicin resistance and decreased drug uptake into cells (Figure 4.0) (Laberge, M., unpublished observations 2007). It is also important to note that cells were selected for resistance at concentrations that are clinically relevant (Veitch and Parissenti, 2007), supporting that the localization defect could be mechanism present in patient tumours resistant to epirubicin.

The localization of anthracyclines in the perinuclear region is consistent with many of the studies conducted in literature (Altan *et al.*, 1998;Bour-Dill *et al.*, 2000;Sognier *et al.*, 1994). Fluorescence localization studies have indicated that anthracyclines sequester to specific organelles including lysosomes, recycling endosome, and trans-golgi network (Altan *et al.*, 1998;Belhoussine *et al.*, 1998). The above organelles are all known to be slightly acidic in nature (Altan *et al.*, 1998). Weak base chemotherapeutics like the anthracyclines, upon entry into an acidic compartment become protonated, and then become membrane impermeable preventing anthracyclines from associating with the nucleus (Weisz, 2003). Although the co-localization studies confirmed that the epirubicin perinuclear fluorescence observed in MCF-7_{EPI} cells was occurring in the lysosomes, epirubicin was not found to be localized in the trans-golgi network and the recycling endosomes as reported for doxorubicin localization by Altan and colleagues. Although these studies also confirm the presence of acidified vesicles in the MCF-7_{EPI} cell line, the co-cultured control MCF-7_{WT} cells were also positive for acidified vesicles. Furthermore, inhibition of vesicle acidification by bafilomycin A1 did not restore the localization of epirubicin to the nucleus, suggesting that

Figure 4.0: Comparison of 2 μM Epirubicin uptake during selection of resistance.

Cells were grown on 5 cm tissue culture plates for 24 hours, and then incubated with 2 μM epirubicin. These cells were then trypsinized and analyzed for epirubicin uptake using flow cytometry over 16 hours. The relative uptake of epirubicin in each of the resistant cell lines was compared to the MCF-7_{WT} co-cultured control. The divergence of the resistant cell lines from the co-cultured control becomes evident at dose 9 in terms of uptake. The uptake deficiency also continues with the cell lines selected at later doses (eg. Selection dose 10 and 12), with the MCF-7_{EPI} cell line having the lowest amount of epirubicin uptake (Laberge, M. 2006, Unpublished data).

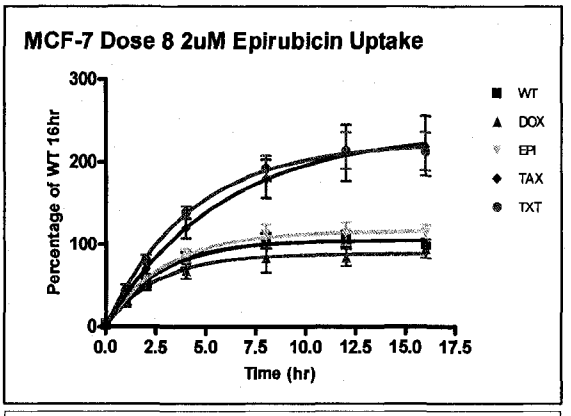
MCF-7 Dose 8 2uM Epirubicin Uptake
Percentage of WT 16hr
Time (hr)
WT
DOX
EPI
TAX
TXT

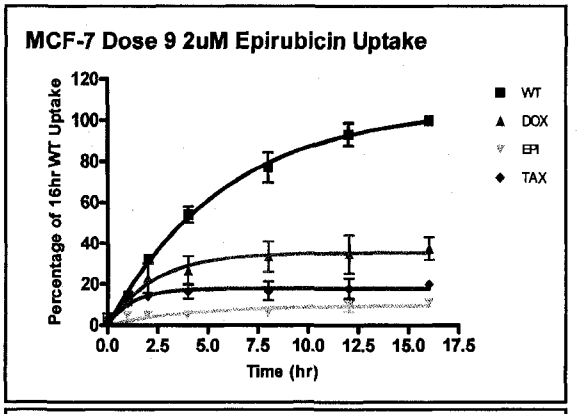
MCF-7 Dose 9 2uM Epirubicin Uptake
Percentage of 16hr WT Uptake
Time (hr)
WT
DOX
EPI
TAX

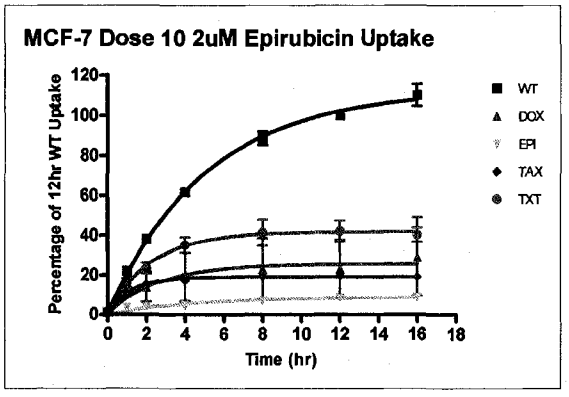
MCF-7 Dose 10 2uM Epirubicin Uptake
Percentage of 12hr WT Uptake
Time (hr)
WT
DOX
EPI
TAX
TXT

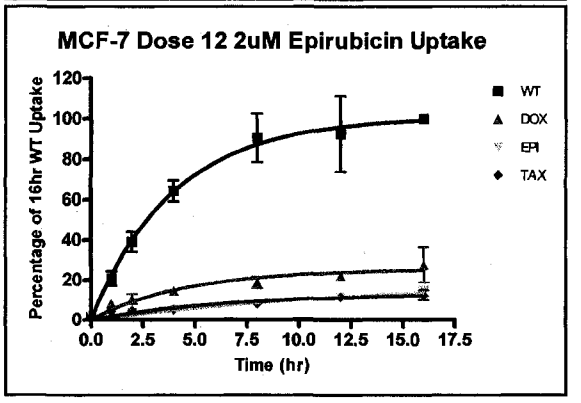
MCF-7 Dose 12 2uM Epirubicin Uptake
Percentage of 16hr WT Uptake
Time (hr)
WT
DOX
EPI
TAX

acidification of intracellular vesicles may also not be a significant contributor in the localization defect observed in MCF-7_{EPI}.

Also consistent with literature, was the observation that the nuclear cytoplasmic ratio was lower in epirubicin resistant cells than in epirubicin sensitive cells (Schuurhuis *et al.*, 1993). It is important to note here that the doxorubicin resistant cell line MCF-7_{DOX} cell line appeared to have a higher N/C ratio than the co-cultured control; this may be explained as an artifact, as the settings for the confocal microscope were not set the same across cell lines for this experiment, but were rather all optimized to the 8 hour time point for each cell line.

The role of ABCB1 and other ABC transporters in anthracycline sequestration were also investigated. Although Q-PCR results (M. Laberge, unpublished observations, 2007) and immunohistochemistry confirmed the increased expression of the multidrug transporter ABCB1 (Figure 1.5), the role of the ABCB1 and other ABC transporters were likely minimal in the localization defect observed in MCF-7_{EPI} cells since inhibition via both Cyclosporin A and Valspodar proved unable to restore the localization of epirubicin to the nuclei. It is interesting to note however, that despite the lack of nuclear membrane ABCB1, there appeared to be pools of ABCB1 shown in the perinuclear region. It is possible that intracellular ABCB1 could be playing a role in drug sequestration by pumping drug from the cytoplasm into vesicles. In this case, valspodar may have failed to inhibit intracellular ABCB1 due to the overwhelming amount of plasma membrane ABCB1. The concentration of valspodar was not increased during these experiments due to concerns of cellular toxicity. In a separate study, the concentration of valspodar and cyclosporin A was, however, sufficient to restore uptake of taxol in MCF-7_{TAX} cells which also highly express ABCB1 (Hembruff, S., unpublished observations, 2007).

Unfortunately, the mechanism by which this defect in localization occurs remains unclear. Also of note, the major vault protein, LRP, in this study did not appear to play a significant role in the localization defect, as both Q-PCR (Figure 1.4) and microarray data (Veitch and Parissenti, 2007) suggest that this gene is not significantly upregulated at dose 10 compared the co-cultured MCF-7_{EPI} cells. Moreover, elevated LRP activity in MCF-7_{EPI} cells was unlikely since cyclosporin A, the pan ABC transporter inhibitor, is also known to inhibit LRP (Qadir, M., 2005) was unable to restore epirubicin uptake.

Although imaging of cells was conducted after placement of cells in drug-free medium for 24 hours, it remains possible that drug previously given to the cells remains in the nucleus that may potentially prevent new drug from entering resulting in the discussed phenotype. However, several observations argue against this:

1) The doxorubicin resistant cell line (doxorubicin being structurally very similar to epirubicin) did not show the same phenotype.
2) There was no evidence of epirubicin in the MCF-7_{EPI} cells prior to drug administration that was detectable by confocal microscopy, though some have metabolized to a non-fluorescent form that remains in the nucleus.
3) The intensity of staining in the nucleus of MCF-7_{EPI} cells appears to be highest after 30 minutes and falls significantly over time (8 hours), suggesting active extrusion of drug out of the nucleus.

Results from these studies indicate that there is a significant nuclear localization defect present in epirubicin resistant MCF-7_{EPI} cell lines. However, the MCF-7_{TAX}, MCF-7_{DOX}, MCF-7_{TXT} dose 10 resistant cell lines did not exhibit any significant nuclear localization defect within the 8 hour time point experiment. It should also be noted that an

additional experiment consisting of one trial each, the MCF-7_{TXT} cells (selected to dose 10) were examined for the localization of both doxorubicin and epirubicin. Interestingly, the MCF-7_{DOX} cell lines have shown infrequent and limited nuclear localization defects at 8 hours. Furthermore, during an incubation of 2 μM epirubicin for 24 hours, the MCF-7_{DOX} dose 10 cell line did show a majority of cells exhibiting the nuclear localization defect within the population. These results suggest that these anthracycline resistant cell lines behave distinctly with respect to the localization of epirubicin from the taxane resistant cell lines. Moreover, even within the same class of drugs, the anthracycline resistant cell lines did not behave identically.

It should be noted that though these anthracyclines are enantiomers and consequently share almost the same structure which generated the MCF-7_{DOX} and MCF-7_{EPI} cell lines, the resistant cell lines appear to have distinct mechanisms of resistance, as seen with the differences in anthracycline localization and drug transporter gene expression (Figure 1.4) (Laberge, M., unpublished observations, 2007). These cell lines have also shown other dissimilarities when treated with various chemotherapeutic agents. One example in which differences were observed between these two cell lines was drug sensitivity. Clonogenic assays performed within our lab demonstrated that the MCF-7_{EPI} cell line was the most resistant to all four chemotherapeutic agents tested, whereas the MCF-7_{DOX} cell line was the least resistant to the same agents (Figure 1.3). Also of note, is that during the generation of the anthracycline resistant cell lines, the MCF-7_{DOX} dose 10 (3 fold increase of drug from dose 9) selection did not survive, and as such, underwent a selection using a lower fold increase in the concentration of doxorubicin approximately 1.5 fold. Flow cytometry experiments measuring epirubicin and doxorubicin uptake compliment the localization

results, and clearly demonstrated a significant difference in uptake between dose 10 MCF-7_{EPI} and MCF-7_{DOX} (Figure 1.4). These uptake studies also showed that the MCF-7_{EPI} cells contained the least amount of epirubicin. Due to these notable differences, it is not surprising that the localization of epirubicin and doxorubicin were not identical in the MCF-7_{EPI} cells selected to dose 10.

Of particular interest in this study was the finding that the MCF-7_{DOX} cell line and the MCF-7_{EPI} cell line did not show the nuclear localization defect to the same extent. One can examine the microarray profiles for these two cell lines and observe significant differences in gene expression suggesting that resistance in MCF-7_{DOX} may occur largely by an alternate mechanism. For example, the MCF-$_{7DOX}$ cell line has very little ABCB1 expression, comparable to that of the co-cultured control. Most interestingly however, is that the MCF-7_{DOX} cell line exhibited elevated expression of a particular gene known as AKR1C2. The gene AKR1C2 encodes for an aldoketoreductase, which may be responsible for metabolizing doxorubicin, consequently rendering doxorubicin less active. Clonogenic assays performed within our laboratory using an AKR1C2 inhibitor, beta-cholanic acid, restored a significant amount of sensitivity to doxorubicin in the MCF-7_{DOX} cells (Figure 4.1). Since this gene was found to be highly expressed in MCF-7_{DOX} and not in MCF-7_{EPI} dose 10 cells, it may explain why the MCF-7_{DOX} does not show a significant nuclear localization defect at the 8 hour time point. In this case, the longer time points do show that MCF-7_{DOX} has a nuclear localization (of epirubicin) defect, which suggested that there are multiple mechanisms of drug resistance present.

Figure 4.1: Effect of beta cholanic acid.

Clonogenic survival assay depicting reversal of resistance in MCF-7_{DOX} cells using 5-beta-cholanic-3-alpha-7-alpha-diol. The MCF-7_{DOX} and MCF-7_{EPI} cells selected to dose 12 were examined. Treatment of the MCF-7_{DOX} cells resulted in a reversion of resistance. Symbols for each cell line with or without beta cholanic acid are as follows: doxorubicin resistant (MCF-7_{DOX} [ ]), epirubicin resistant (MCF-7_{EPI} [ ]) cell lines and the MCF-7 co-cultured control cell line (MCF-7_{CC} [■]), in the presence (---) or absence (—) of 200 μM 5β-cholanic acid with continuous doxorubicin drug exposure (representative of two trials). (Veitch, Z, 2007, Unpublished data).

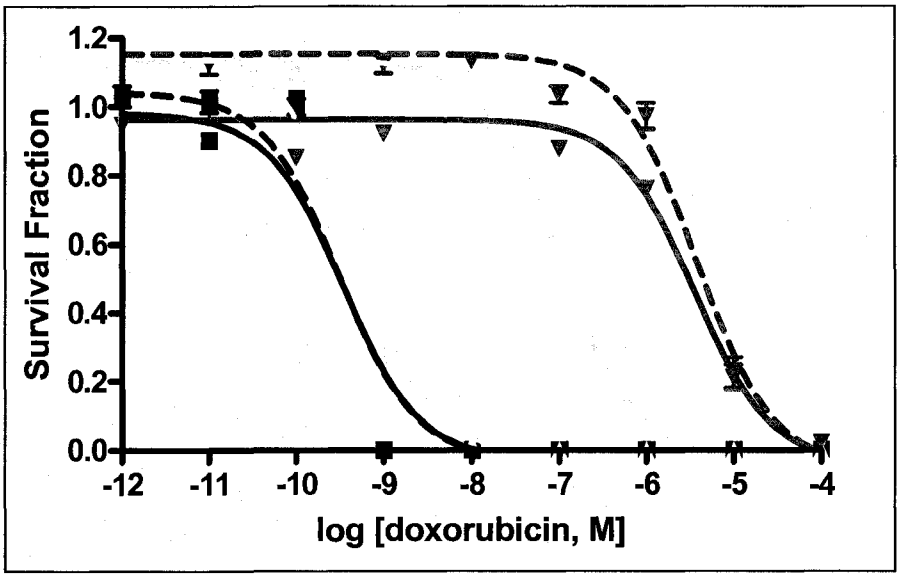
Survival Fraction
1.2
1.0
0.8
0.6
0.4
0.2
0.0
-12
-11
-10
-9
-8
-7
-6
-5
-4
log [doxorubicin, M]

As a whole, these studies provide insight into the mechanism(s) by which drug sequestration may play a role in anthracycline resistance. It would appear that anthracyclines are sequestered into lysosomes, which need not be acidic, nor do they appear to require the activity of drug transporters. These vesicles may be part of the exosome pathway, which enables cells to excrete agents via exocytosis. Furthermore, as epirubicin was found to be co-localized with lysosomes which originate from endosomes in the MCF-7_{EPI} cells (Weisz, 2003), it is possible that nuclear localization could be restored using chloroquine, an inhibitor which disrupts the formation of endosomes (Jones *et al.*, 2004). Past studies have shown that chloroquine was able to restore the localization of anthracyclines to the nucleus as well as restore sensitivity (Hurwitz *et al.*, 1997).

Future studies can be performed in order to examine the contribution of the exosome pathway in sequestration and exocytosis of anthracyclines. A protein known as VPS4A, is known to play an important role in the exosome pathway and has been found to be expressed in intracellular vesicular membranes. Its increased expression has been linked with decreased sensitivity to doxorubicin (Chen *et al.*, 2006). Interestingly, a large microarray data set has shown the upregulation of this gene in MCF-7_{EPI} dose 9. Q-PCR analysis can be performed on this particular gene in order to confirm its increased expression. Also there are inhibitors and siRNAs for VPS4A readily available to perform inhibition experiments to determine whether the exosome pathway is involved in the nuclear localization defect.

5.0 CONCLUSION AND CLOSING REMARKS

The results of this investigation confirmed that the localization of anthracyclines is reduced in the nucleus of MCF-7_{EPI} cells, more specifically epirubicin. Furthermore, there was a reduction in the N/C ratio in the epirubicin resistant cell line compared to the epirubicin sensitive cell line, and that the cytoplasmic localization of epirubicin primarily occurs within the lysosomes. Despite these findings, the mechanism by which the nuclear localization defect occurs is still under investigation, as the typically reported mechanisms fail to answer this question. Thus in conclusion, other mechanisms should be explored in order to determine a method of reversing the localization defect. If this mechanism can be elucidated, it would contribute greatly in developing combination treatments involving anthracyclines in the treatment of breast cancer.

6.0 REFERENCES

Altan, N., Chen, Y., Schindler, M., and Simon, S. M. (1998) Defective acidification in human breast tumor cells and implications for chemotherapy. *J Exp Med* **187:** 1583-1598.

Arcamone, F., Cassinelli, G., Fantini, G., Grein, A., Orezzi, P., Pol, C. *et al.* (2000) Adriamycin, 14-hydroxydaunomycin, a new antitumor antibiotic from S. peucetius var. caesius. Reprinted from Biotechnology and Bioengineering, Vol. XI, Issue 6, Pages 1101-1110 (1969). *Biotechnol Bioeng* **67:** 704-713.

Arcamone, F., Penco, S., Vigevani, A., Redaelli, S., Franchi, G., DiMarco, A. *et al.* (1975) Synthesis and antitumor properties of new glycosides of daunomycinone and adriamycinone. *J Med Chem* **18:** 703-707.

Ax, W., Soldan, M., Koch, L., and Maser, E. (2000) Development of daunorubicin resistance in tumour cells by induction of carbonyl reduction. *Biochem Pharmacol* **59:** 293-300.

Bachur, N. R. and Huffman, D. H. (1971) Daunorubicin metabolism: estimation of daunorubicin reductase. *Br J Pharmacol* **43:** 828-833.

Bakos, E. and Homolya, L. (2007) Portrait of multifaceted transporter, the multidrug resistance-associated protein 1 (MRP1/ABCC1). *Pflugers Arch* **453:** 621-641.

Belhoussine, R., Morjani, H., Millot, J. M., Sharonov, S., and Manfait, M. (1998) Confocal scanning microspectrofluorometry reveals specific anthracyline accumulation in cytoplasmic organelles of multidrug-resistant cancer cells. *J Histochem Cytochem* **46:** 1369-1376.

Biedler, J. L. (1992) Genetic aspects of multidrug resistance. *Cancer* **70:** 1799-1809.

Blagosklonny, M. V. and Fojo, T. (1999) Molecular effects of paclitaxel: myths and reality (a critical review). *Int J Cancer* **83:** 151-156.

Bobichon, H., Colin, M., Depierreux, C., Liautaud-Roger, F., and Jardillier, J. C. (1996) Ultrastructural changes related to multidrug resistance in CEM cells: role of cytoplasmic vesicles in drug exclusion. *J Exp Ther Oncol* **1:** 49-61.

Bonneterre, J., Roche, H., Kerbrat, P., Bremond, A., Fumoleau, P., Namer, M. *et al.* (2005) Epirubicin increases long-term survival in adjuvant chemotherapy of patients with poor-prognosis, node-positive, early breast cancer: 10-year follow-up results of the French Adjuvant Study Group 05 randomized trial. *J Clin Oncol* **23:** 2686-2693.

Borst, P., Evers, R., Kool, M., and Wijnholds, J. (2000) A family of drug transporters: the multidrug resistance-associated proteins. *J Natl Cancer Inst* **92:** 1295-1302.

Bour-Dill, C., Gramain, M. P., Merlin, J. L., Marchal, S., and Guillemin, F. (2000) Determination of intracellular organelles implicated in daunorubicin cytoplasmic

sequestration in multidrug-resistant MCF-7 cells using fluorescence microscopy image analysis. *Cytometry* **39:** 16-25.

Brenner, D. E., Galloway, S., Cooper, J., Noone, R., and Hande, K. R. (1985) Improved high-performance liquid chromatography assay of doxorubicin: detection of circulating aglycones in human plasma and comparison with thin-layer chromatography. *Cancer Chemother Pharmacol* **14:** 139-145.

Broxterman, H. J., Pinedo, H. M., Schuurhuis, G. J., and Lankelma, J. (1990) Cyclosporin A and verapamil have different effects on energy metabolism in multidrug-resistant tumour cells. *Br J Cancer* **62:** 85-88.

Burczynski, M. E., Harvey, R. G., and Penning, T. M. (1998) Expression and characterization of four recombinant human dihydrodiol dehydrogenase isoforms: oxidation of trans-7, 8-dihydroxy-7,8-dihydrobenzo[a]pyrene to the activated o-quinone metabolite benzo[a]pyrene-7,8-dione. *Biochemistry* **37:** 6781-6790.

Calcabrini, A., Meschini, S., Stringaro, A., Cianfriglia, M., Arancia, G., and Molinari, A. (2000) Detection of P-glycoprotein in the nuclear envelope of multidrug resistant cells. *Histochem J* **32:** 599-606.

Canadian Cancer Society, National Cancer Institute of Canada, Statistics Canada, Provincial/Territorial Cancer Registries, and Public Health Agency of Canada. Canadian Cancer Statistics 2007. 2007. 2007.
Ref Type: Pamphlet

Centonze, V. and Pawley, J. (1995) Tutorial on Practical Confocal Microscopy and use of the Confocal Test Specimen. In *Handbook of Biological Confocal Microscopy*. New York: Plenum Press, pp. 549-570.

Chen, V. Y., Posada, M. M., Blazer, L. L., Zhao, T., and Rosania, G. R. (2006) The role of the VPS4A-exosome pathway in the intrinsic egress route of a DNA-binding anticancer drug. *Pharm Res* **23:** 1687-1695.

Conchello, J.-A., Cogswell, C. G., Wilson, T., Carlsson, K., Kino, G. S., Lerner, J. M. *et al.* (2005) *Three-Dimensional and Multidimensional Microscopy: Image Acquisition and Processing*. Bellingham: SPIE International Society for Optical Engineering.

Cullinane, C., Cutts, S. M., Panousis, C., and Phillips, D. R. (2000) Interstrand cross-linking by adriamycin in nuclear and mitochondrial DNA of MCF-7 cells. *Nucleic Acids Res* **28:** 1019-1025.

Das, G. C., Holiday, D., Gallardo, R., and Haas, C. Taxol-induced cell cycle arrest and apoptosis: dose-response relationship in lung cancer cells of different wild-type p53 status and under isogenic condition. Cancer Letters 165, 147-153. 2000.
Ref Type: Journal (Full)

Deng, H. B., Parekh, H. K., Chow, K. C., and Simpkins, H. (2002) Increased expression of dihydrodiol dehydrogenase induces resistance to cisplatin in human ovarian carcinoma cells. *J Biol Chem* **277:** 15035-15043.

DeVita, V. T., Hellman, S., and Rosenburg, S. A. (1993) *Cancer Principles and Practice in Oncology*. Philadelphia: J.B. Lippincott.

Endicott, J. A. and Ling, V. (1989) The biochemistry of P-glycoprotein-mediated multidrug resistance. *Annu Rev Biochem* **58:** 137-171.

Featherstone, J. M., Speers, A. G., Lwaleed, B. A., Hayes, M. C., Cooper, A. J., and Birch, B. R. (2005) The nuclear membrane in multidrug resistance: microinjection of epirubicin into bladder cancer cell lines. *BJU Int* **95:** 1091-1098.

Felsted, R. L. and Bachur, N. R. (1982) Human liver daunorubicin reductases. *Prog Clin Biol Res* **114:** 291-305.

Fumoleau, P., Roche, H., Kerbrat, P., Bonneterre, J., Romestaing, P., Fargeot, P. *et al.* (2006) Long-term cardiac toxicity after adjuvant epirubicin-based chemotherapy in early breast cancer: French Adjuvant Study Group results. *Ann Oncol* **17:** 85-92.

Ganasia-Leymarie, V., Bischoff, P., Bergerat, J. P., and Holl, V. Signal transduction pathways of taxane-induced apoptosis. Curr Med Chem Anticancer Agents 3, 291-306. 2003. Ref Type: Journal (Full)

Gaudiano, G., Koch, T. H., Lo, B. M., Nuccetelli, M., Ravagnan, G., Serafino, A. *et al.* (2000) Lack of glutathione conjugation to adriamycin in human breast cancer MCF-7/DOX cells. Inhibition of glutathione S-transferase p1-1 by glutathione conjugates from anthracyclines. *Biochem Pharmacol* **60:** 1915-1923.

Gewirtz, D. A. (1999) A critical evaluation of the mechanisms of action proposed for the antitumor effects of the anthracycline antibiotics adriamycin and daunorubicin. *Biochem Pharmacol* **57:** 727-741.

Gottesman, M. M., Ludwig, J., Xia, D., and Szakacs, G. (2006) Defeating drug resistance in cancer. *Discov Med* **6:** 18-23.

Greene, R. F., Collins, J. M., Jenkins, J. F., Speyer, J. L., and Myers, C. E. (1983) Plasma pharmacokinetics of adriamycin and adriamycinol: implications for the design of in vitro experiments and treatment protocols. *Cancer Res* **43:** 3417-3421.

Horenstein, M. S., Vander Heide, R. S., and L'Ecuyer, T. J. (2000) Molecular basis of anthracycline-induced cardiotoxicity and its prevention. *Mol Genet Metab* **71:** 436-444.

Hsu, N. Y., Ho, H. C., Chow, K. C., Lin, T. Y., Shih, C. S., Wang, L. S. *et al.* (2001) Overexpression of dihydrodiol dehydrogenase as a prognostic marker of non-small cell lung cancer. *Cancer Res* **61:** 2727-2731.

Hudis, C. A. (2003) Current status and future directions in breast cancer therapy. *Clin Breast Cancer* **4 Suppl 2:** S70-S75.

Hurwitz, S. J., Terashima, M., Mizunuma, N., and Slapak, C. A. (1997) Vesicular anthracycline accumulation in doxorubicin-selected U-937 cells: participation of lysosomes. *Blood* **89:** 3745-3754.

Jain, R. K. (1990) Vascular and interstitial barriers to delivery of therapeutic agents in tumors. *Cancer Metastasis Rev* **9:** 253-266.

Jain, R. K. (1997) Delivery of molecular and cellular medicine to solid tumors. *Adv Drug Deliv Rev* **26:** 71-90.

Janicke, R. U., Sprengart, M. L., Wati, M. R., and Porter, A. G. (1998) Caspase-3 is required for DNA fragmentation and morphological changes associated with apoptosis. *J Biol Chem* **273:** 9357-9360.

Jones, H. M., Hamilton, K. L., Papworth, G. D., Syme, C. A., Watkins, S. C., Bradbury, N. A. *et al.* (2004) Role of the NH2 terminus in the assembly and trafficking of the intermediate conductance Ca2+-activated K+ channel hIK1. *J Biol Chem* **279:** 15531-15540.

Keizer, H. G., Schuurhuis, G. J., Broxterman, H. J., Lankelma, J., Schoonen, W. G., Van, R. J. *et al.* (1989) Correlation of multidrug resistance with decreased drug accumulation, altered subcellular drug distribution, and increased P-glycoprotein expression in cultured SW-1573 human lung tumor cells. *Cancer Res* **49:** 2988-2993.

Kitazono, M., Sumizawa, T., Takebayashi, Y., Chen, Z. S., Furukawa, T., Nagayama, S. *et al.* (1999) Multidrug resistance and the lung resistance-related protein in human colon carcinoma SW-620 cells. *J Natl Cancer Inst* **91:** 1647-1653.

Kiyomiya, K., Matsuo, S., and Kurebe, M. (2001a) Differences in intracellular sites of action of Adriamycin in neoplastic and normal differentiated cells. *Cancer Chemother Pharmacol* **47:** 51-56.

Kiyomiya, K., Matsuo, S., and Kurebe, M. (2001b) Mechanism of specific nuclear transport of adriamycin: the mode of nuclear translocation of adriamycin-proteasome complex. *Cancer Res* **61:** 2467-2471.

Klug, W. S. and Cummings, M. R. (2002) *Essentials of Genetics*.

Kondo, M., Oshita, F., Kato, Y., Yamada, K., Nomura, I., and Noda, K. (1999) Early monocytopenia after chemotherapy as a risk factor for neutropenia. *Am J Clin Oncol* **22:** 103-105.

Kool, M., de, H. M., Scheffer, G. L., Scheper, R. J., van Eijk, M. J., Juijn, J. A. *et al.* (1997) Analysis of expression of cMOAT (MRP2), MRP3, MRP4, and MRP5, homologues of the multidrug resistance-associated protein gene (MRP1), in human cancer cell lines. *Cancer Res* **57:** 3537-3547.

Lacroix, M. and Leclercq, G. (2004) Relevance of breast cancer cell lines as models for breast tumours: an update. *Breast Cancer Res Treat* **83:** 249-289.

Lichtmann, J. W. (1994) Confocal Microscopy. *Scientific American* 40-45.

Lindley, C., McCune, J. S., Thomason, T. E., Lauder, D., Sauls, A., Adkins, S. *et al.* (1999) Perception of chemotherapy side effects cancer versus noncancer patients. *Cancer Pract* **7:** 59-65.

List, A. F., Spier, C. S., Grogan, T. M., Johnson, C., Roe, D. J., Greer, J. P. *et al.* (1996) Overexpression of the major vault transporter protein lung-resistance protein predicts treatment outcome in acute myeloid leukemia. *Blood* **87:** 2464-2469.

Longley, D. B. and Johnston, P. G. (2005) Molecular mechanisms of drug resistance. *J Pathol* **205:** 275-292.

Manfredi, J. J., Parness, J., and Horwitz, S. B. (1982) Taxol binds to cellular microtubules. *J Cell Biol* **94:** 688-696.

Mayer, L. D. (1998) Future developments in the selectivity of anticancer agents: drug delivery and molecular target strategies. *Cancer Metastasis Rev* **17:** 211-218.

Minotti, G., Cairo, G., and Monti, E. (1999) Role of iron in anthracycline cardiotoxicity: new tunes for an old song? *FASEB J* **13:** 199-212.

Minotti, G., Menna, P., Salvatorelli, E., Cairo, G., and Gianni, L. (2004) Anthracyclines: molecular advances and pharmacologic developments in antitumor activity and cardiotoxicity. *Pharmacol Rev* **56:** 185-229.

Minsky, M. (1988) Memoir on Inventing the Confocal Scanning Microscopy. *Scanning* **10:** 128-138.

Molinari, A., Calcabrini, A., Meschini, S., Stringaro, A., Crateri, P., Toccacieli, L. *et al.* (2002) Subcellular detection and localization of the drug transporter P-glycoprotein in cultured tumor cells. *Curr Protein Pept Sci* **3:** 653-670.

Nooter, K., Brutel de la, R. G., Look, M. P., van Wingerden, K. E., Henzen-Logmans, S. C., Scheper, R. J. *et al.* (1997) The prognostic significance of expression of the multidrug resistance-associated protein (MRP) in primary breast cancer. *Br J Cancer* **76:** 486-493.

Paglin, S., Hollister, T., Delohery, T., Hackett, N., McMahill, M., Sphicas, E. *et al.* (2001) A novel response of cancer cells to radiation involves autophagy and formation of acidic vesicles. *Cancer Res* **61:** 439-444.

Parissenti, A. M., Hembruff, S. L., Villeneuve, D. J., Veitch, Z., Guo, B., and Eng, J. (2007) Gene expression profiles as biomarkers for the prediction of chemotherapy drug response in human tumour cells. *Anticancer Drugs* **18:** 499-523.

Parness, J. and Horwitz, S. B. (1981) Taxol binds to polymerized tubulin in vitro. *J Cell Biol* **91:** 479-487.

Paus, R. and Cotsarelis, G. (1999) The biology of hair follicles. *N Engl J Med* **341:** 491-497.

Pivot, X., Asmar, L., and Hortobagyi, G. N. (1999) The efficacy of chemotherapy with docetaxel and paclitaxel in anthracycline-resistant breast cancer (Review). *Int J Oncol* **15:** 381-386.

Pohl, G., Filipits, M., Suchomel, R. W., Stranzl, T., Depisch, D., and Pirker, R. (1999) Expression of the lung resistance protein (LRP) in primary breast cancer. *Anticancer Res* **19:** 5051-5055.

Qadir, M., O'Loughlin, K. L., Fricke, S. M., Williamson, N. A., Greco, W. R., Minderman, H. *et al.* (2005) Cyclosporin A Is a Broad-Spectrum Multidrug Resistance Modulator. *Clinical Cancer Research* **11:** 2320-2326.

Rajagopal, A. and Simon, S. M. (2003) Subcellular localization and activity of multidrug resistance proteins. *Mol Biol Cell* **14:** 3389-3399.

Rao, S., Krauss, N. E., Heerding, J. M., Swindell, C. S., Ringel, I., Orr, G. A. *et al.* (1994) 3'-(p-azidobenzamido)taxol photolabels the N-terminal 31 amino acids of beta-tubulin. *J Biol Chem* **269:** 3132-3134.

Richert, N. D., Aldwin, L., Nitecki, D., Gottesman, M. M., and Pastan, I. (1988) Stability and covalent modification of P-glycoprotein in multidrug-resistant KB cells. *Biochemistry* **27:** 7607-7613.

Sandison, D. and Webb, W. (1994) Backround Rejection and Signal-to-Noise Optimization in the Confocal and Alternative Fluorescence Microscopes. *Applied Optics* 603-610.

Scheffer, G. L., Schroeijers, A. B., Izquierdo, M. A., Wiemer, E. A., and Scheper, R. J. (2000) Lung resistance-related protein/major vault protein and vaults in multidrug-resistant cancer. *Curr Opin Oncol* **12:** 550-556.

Schiff, P. B., Fant, J., and Horwitz, S. B. (1979) Promotion of microtubule assembly in vitro by taxol. *Nature* **277:** 665-667.

Schindler, M., Grabski, S., Hoff, E., and Simon, S. M. (1996) Defective pH regulation of acidic compartments in human breast cancer cells (MCF-7) is normalized in adriamycin-resistant cells (MCF-7adr). *Biochemistry* **35:** 2811-2817.

Schuurhuis, G. J., Broxterman, H. J., de Lange, J. H., Pinedo, H. M., van Heijningen, T. H., Kuiper, C. M. *et al.* (1991) Early multidrug resistance, defined by changes in intracellular doxorubicin distribution, independent of P-glycoprotein. *Br J Cancer* **64:** 857-861.

Schuurhuis, G. J., van Heijningen, T. H., Cervantes, A., Pinedo, H. M., de Lange, J. H., Keizer, H. G. *et al.* (1993) Changes in subcellular doxorubicin distribution and cellular

accumulation alone can largely account for doxorubicin resistance in SW-1573 lung cancer and MCF-7 breast cancer multidrug resistant tumour cells. *Br J Cancer* **68:** 898-908.

Scudiero, D. A., Monks, A., and Sausville, E. A. (1998) Cell line designation change: multidrug-resistant cell line in the NCI anticancer screen. *J Natl Cancer Inst* **90:** 862.

Seksek, O., Biwersi, J., and Verkman, A. S. (1995) Direct measurement of trans-Golgi pH in living cells and regulation by second messengers. *J Biol Chem* **270:** 4967-4970.

Serafino, A., Sinibaldi-Vallebona, P., Gaudiano, G., Koch, T. H., Rasi, G., Garaci, E. *et al.* (1998) Cytoplasmic localization of anthracycline antitumor drugs conjugated with reduced glutathione: a possible correlation with multidrug resistance mechanisms. *Anticancer Res* **18:** 1159-1166.

Siegfried, J. M., Tritton, T. R., and Sartorelli, A. C. (1983) Comparison of anthracycline concentrations in S180 cell lines of varying sensitivity. *Eur J Cancer Clin Oncol* **19:** 1133-1141.

Singal, P. K. and Pierce, G. N. (1986) Adriamycin stimulates low-affinity Ca2+ binding and lipid peroxidation but depresses myocardial function. *Am J Physiol* **250:** H419-H425.

Snyder, J. P., Nettles, J. H., Cornett, B., Downing, K. H., and Nogales, E. (2001) The binding conformation of Taxol in beta-tubulin: a model based on electron crystallographic density. *Proc Natl Acad Sci U S A* **98:** 5312-5316.

Sognier, M. A., Zhang, Y., Eberle, R. L., Sweet, K. M., Altenberg, G. A., and Belli, J. A. (1994) Sequestration of doxorubicin in vesicles in a multidrug-resistant cell line (LZ-100). *Biochem Pharmacol* **48:** 391-401.

Sonee, M., Barron, E., Yarber, F. A., and Hamm-Alvarez, S. F. (1998) Taxol inhibits endosomal-lysosomal membrane trafficking at two distinct steps in CV-1 cells. *Am J Physiol* **275:** C1630-C1639.

Soule, H. D., Vazguez, J., Long, A., Albert, S., and Brennan, M. (1973) A human cell line from a pleural effusion derived from a breast carcinoma. *J Natl Cancer Inst* **51:** 1409-1416.

Stelzer, E. H. K. (2000) Practical Limits to Resolution in Fluorescence Light Microscopy. In *Imaging Neurons: A Laboratory Manual.* Yuste, R., Lanni, F., and Konnerth, A. (ed.) New York: Cold Spring Harbor Press, pp. 12.1-12.9.

Swedlow, J. R., Hu, K., Andrews, P. D., Roos, D. S., and Murray, J. M. (2002) Measuring Tubulin Content in Taxoplasma gondii: A Comparison of Laser-Scanning Confocal and Wide-Field Fluorescence Microscopy. *Proc Natl Acad Sci* 2014-2019.

Takanashi, S. and Bachur, N. R. (1975) Daunorubicin metabolites in human urine. *J Pharmacol Exp Ther* **195:** 41-49.

Tewey, K. M., Rowe, T. C., Yang, L., Halligan, B. D., and Liu, L. F. (1984) Adriamycin-induced DNA damage mediated by mammalian DNA topoisomerase II. *Science* **226:** 466-468.

Thiebaut, F., Currier, S. J., Whitaker, J., Haugland, R. P., Gottesman, M. M., Pastan, I. *et al.* (1990) Activity of the multidrug transporter results in alkalinization of the cytosol: measurement of cytosolic pH by microinjection of a pH-sensitive dye. *J Histochem Cytochem* **38:** 685-690.

Trudeau, M., Sinclair, S. E., and Clemons, M. (2005) Neoadjuvant taxanes in the treatment of non-metastatic breast cancer: a systematic review. *Cancer Treat Rev* **31:** 283-302.

Ueda, K., Cornwell, M. M., Gottesman, M. M., Pastan, I., Roninson, I. B., Ling, V. *et al.* (1986) The mdr1 gene, responsible for multidrug-resistance, codes for P-glycoprotein. *Biochem Biophys Res Commun* **141:** 956-962.

Vasquez-Vivar, J., Martasek, P., Hogg, N., Masters, B. S., Pritchard, K. A., Jr., and Kalyanaraman, B. (1997) Endothelial nitric oxide synthase-dependent superoxide generation from adriamycin. *Biochemistry* **36:** 11293-11297.

Veitch, Z. and Parissenti, A. s. The Pharmacogenomic Response of MCF-7 breast cancer cells to taxane and anthracycline based chemotherapy regimens. 2007. Biology Department, Laurentian University.
Ref Type: Thesis/Dissertation

Wang, J., He, F. T., Tzang, C. H., Fong, W. F., Xiao, P. G., Han, R. *et al.* (2005) Differential gene expression profiles in paclitaxel-induced cell cycle arrest and apoptosis in human breast cancer MCF-7 cells. *Yao Xue Xue Bao* **40:** 1099-1104.

Wani, M. C., Taylor, H. L., Wall, M. E., Coggon, P., and McPhail, A. T. (1971) Plant antitumor agents. VI. The isolation and structure of taxol, a novel antileukemic and antitumor agent from Taxus brevifolia. *J Am Chem Soc* **93:** 2325-2327.

WARBURG, O. (1956) On the origin of cancer cells. *Science* **123:** 309-314.

Weisz, O. A. (2003) Organelle acidification and disease. *Traffic* **4:** 57-64.

White, J. G., Amos, W. B., and Fordham, M. (1987) An Evaluation of Confocal versus Conventional Imaging of Biological Structures By Fluorescence Microscopy. *Journal of Cell Biology* 41-48.

Willingham, M. C., Cornwell, M. M., Cardarelli, C. O., Gottesman, M. M., and Pastan, I. (1986) Single cell analysis of daunomycin uptake and efflux in multidrug-resistant and -sensitive KB cells: effects of verapamil and other drugs. *Cancer Res* **46:** 5941-5946.

Wilson, T. (1989) Optical Sectioning in Confocal Fluorescence Microscopes. *Journal of Microscopy* 143-156.

Wright, S. J. and Wright, D. J. (2002) Introduction to Confocal Microscopy in B. Matsumoto (ed). *Methods in Cell Biology* 1-85.

Wu, X. X., Mizutani, Y., Kakehi, Y., Yoshida, O., and Ogawa, O. (2000) Enhancement of Fas-mediated apoptosis in renal cell carcinoma cells by adriamycin. *Cancer Res* **60:** 2912-2918.

Zhou, S., Palmeira, C. M., and Wallace, K. B. (2001) Doxorubicin-induced persistent oxidative stress to cardiac myocytes. *Toxicol Lett* **121:** 151-157.

Zhu, B. T. (1999) A novel hypothesis for the mechanism of action of P-glycoprotein as a multidrug transporter. *Mol Carcinog* **25:** 1-13.

APPENDIX

Eng, Jamei

From: Zachary Veitch
Sent: September 4, 2007 2:01 PM
To: Eng, Jamei
Subject: RE: Permission for use of data in Jamei Eng's Thesis

This e-mail shall be taken as full permission to use the requested data, figures, and/or information cited below. I here by release such scientific data generated at the Northeastern Ontario Regional Cancer Centre to Mrs. Jamei Eng for use in her thesis and/or publications.

Sincerely,

Zachary Veitch B.A., H.B.Sc., M.Sc.

From: ,
To: ;
Subject: Permission for use of data in Jamei Eng's Thesis
Date: Tue, 4 Sep 2007 13:57:26 -0400

Mr. Zachary Veitch,
I wish to request your permission for use of the following data, as it appears in my thesis discussion.
1) Clongenic data including images for comparison of epirubicin sensitivity across all 5 cell lines for dose 8, 9, 10 and 12
2) Data on reversion of doxorubicin resistance using B-cholanic acid - consisting of an image for a clonogenic experiment performed on dose 12 MCF-7WT, MCF-7DOX and MCF-7EPI
3) Discussion of microarray results such as isogenicity among cell lines as well as the mention of specific genes found during these array studies such as AKRs and ABC transporters.
Your cooperation is greatly appreciated.
Jamei Eng
M.Sc. Candidate
University of Ottawa

Eng, Jamei

From: Monique Laberge [
Sent: September 5, 2007 6:52 AM
To: Eng, Jamei
Subject: Re: Permission for data used in Jamei Eng's Masters Thesis

Ms. Jamei Eng:

I give you, Jamei Eng, permission to use the data mentioned below as part of the discussion in your thesis.

Good luck.

Sincerely,

Monique Laberge

>>> "Eng, Jamei" <jeng@hrsrh.on.ca> 09/04/07 2:02 PM >>>
Ms. Monique Laberge:

I would like to request permission from you to use the following as it appears in my thesis discussion.

1) Q-PCR data on the ABC transporters including LRP, analyses spanning over selection doses 8-12 for all 4 cell lines compared to MCF-7WT.

2) Flow Cytometry data, comparing the amount of 2uM epirubicin uptake in all 4 cell lines compared to MCF-7WT, analyses from selection doses 8, 9, 10, and 12.

Your cooperation is greatly appreciated.

Jamei Eng
M.Sc. Candidate
University of Ottawa

PS: your reply and this email will be appended to my thesis.

Eng, Jamei

From: Hembruff, Stacey
Sent: September 5, 2007 10:39 AM
To: Eng, Jamei
Subject: RE: Permissions for use of data in Jamei Eng's Thesis - updated

Jamei,
I grant you the permission to use the data listed below as part of the materials and methods and discussion sections of your thesis.
Stacey Hembruff
Research Technician
Sudbury Regional Hospital

From: Eng, Jamei
Sent: September 5, 2007 10:38 AM
To: Hembruff, Stacey
Subject: Permissions for use of data in Jamei Eng's Thesis - updated

Ms. Stacey Hembruff:

I would like to request official permission to refer to data that you produced in the materials and methods and discussion section of my thesis:

1) Generation of 4 drug resistant MCF-7 cell lines (resistance to epirubicin, doxorubicin, paclitaxel and taxotere)

2) Radiolabelled paclitaxel uptake data involving the restoration of uptake using *valspodar or cyclosporin A.*

Please note that this email and your response will be appended to my masters thesis.

Your cooperation is appreciated.

Jamei Eng
M.Sc. Candidate
University of Ottawa

CURRICULUM VITAE

Jamei Raena Eng

Education

2001-Present **M.Sc. Biochemistry (candidate)**
Department of Biochemistry, Microbiology, and Immunology
University of Ottawa, Ottawa, Ontario
Thesis title – **Localization of Anthracyclines in Drug Resistant Human MCF-7 Breast Cancer Cells**

1997-2001 **B.Sc. Honours – Biochemistry**
Department of Chemistry and Biochemistry
Laurentian University, Sudbury, Ontario
Thesis title – **The Pharmacogenomics of Paclitaxel and Doxorubicin Resistance in Human MCF-7 Breast Cancer Cell Lines**

Honours and Distinctions

2005-2006	Ontario Graduate Scholarship
2005	University of Ottawa Excellence Scholarship
2004	University of Ottawa Entrance Scholarship
2000-2004	Laurentian University Academic Bursaries
2003	Ontario Genomics Institute Student Fellowship
2000	Laurentian University Entrance Scholarship
2000	Herbert H. Carnegie Citizenship Award
2000	Regional Cablesystems Scholarship

University activities

01/2005-04/2005 Teaching assistant for Biochemistry course for Dr. Rodriguez
Department of Biochemistry, University of Ottawa

05/2002-08/2003	Student research assistant for Dr. Amadeo Parissenti Department of Biochemistry Laurentian University
09/2002-04/2003	Member of the Laurentian University Pre-Med Society

Publications in refereed journals

Parissenti, A. M., Hembruff, S. L., Villeneuve, D. J., Veitch, Z., Guo, B., and **Eng, J.** (2007). Gene expression profiles as biomarkers for the prediction of chemotherapy drug response in human tumour cells. Anticancer Drugs 18: 499-523.

Publications in preparation/submitted

Veitch, Z. W., Hembruff, S., Villeneuve, D., Shuart, M., **Eng, J. R.**, Laberge, M., and Parissenti, A. (2007). Induction of Aldoketoreductase 1C2 and Other Dose-dependent Genes Upon Acquisition of Anthracycline Resistance in MCF-7 Breast Tumour Cells. Submitted to Breast Cancer Research and Treatment.

Published conference abstracts

Eng, J. R. and Parissenti, A. and Kosarova, A. (2005). Novel Regions in PKC-alpha regulatory domain that are responsible for PKC autoinhibition. Department of Biochemistry, Microbiology and Immunology Graduate Students 2005 Poster Competition, University of Ottawa, Ottawa.

Eng, J. R. and Parissenti, A. (2003). The Pharmacogenomics of Paclitaxel and Doxorubicin Resistance in Human MCF-7 Breast Cancer Cell Lines. Ontario Genomics Insitute Student Fellowship Conference. Toronto, Ontario. August, 2003.